A prototype RF power source for JLC at X-band
(1 Tev. Ecm)

(Results and perspectives, 1988-1994 R&D in KEK)

RF-94, Montauk.N.Y, 1994.Oct.2-7th

KEK, H.Mizuno

JLC parameters(Ecm=1Tev)

Beam energy	500Gev	
RF frequency	11.424ghz	
No.of particles per bunch	6.9x10e9	
Nr of bunches per pulse	85	(120nsec train)
Bunch spacing	1.40nsec	
Repetition rate	150Hz	
Luminosity	10e34	
Nominal accelerating gradient	76.1MeV/m	
Effective gradient in cavities	57.1MeV/m	
Length of a cavity unit	1300mm	(8413m per beam)
Nr of cavity units(per beam)	6423	
a/L	0.1576	
Filling time(Tf)	120nsec	
Attenuation parameter	0.648	
Vg/c	3.64%	
Rf input per a cavity unit	130MW	(240nsec)
Efficiency(wallplug to RF)	30%	
Total AC power(RF)	194MW(and some more)	

Problem-1) Find differences between this Table and Yokoya Parameters presented this morning.

The prototype RF power source for JLC(Ec=1Tev)

(1)Klystron(XB72k)

RF out	130MW	97MW
Pulse width	500ns	
Efficiency	42%	36%(50MW)
Focusing	Super cond. Mag.	(unit test OK)

(2)x2 or x3 RF pulse compression system

RF input	500ns 130MW	(Design stage)
RF out	240ns 250MW	
Efficiency	>96%	

(3)Blumlein modulator

Output pulse	600kV 500ns(flat top)	500kV 700ns
Effiency	75%	
Pulse trans.	1:5	1:7 was tested
Rise &Fall time	150ns 200ns	250ns(rise)

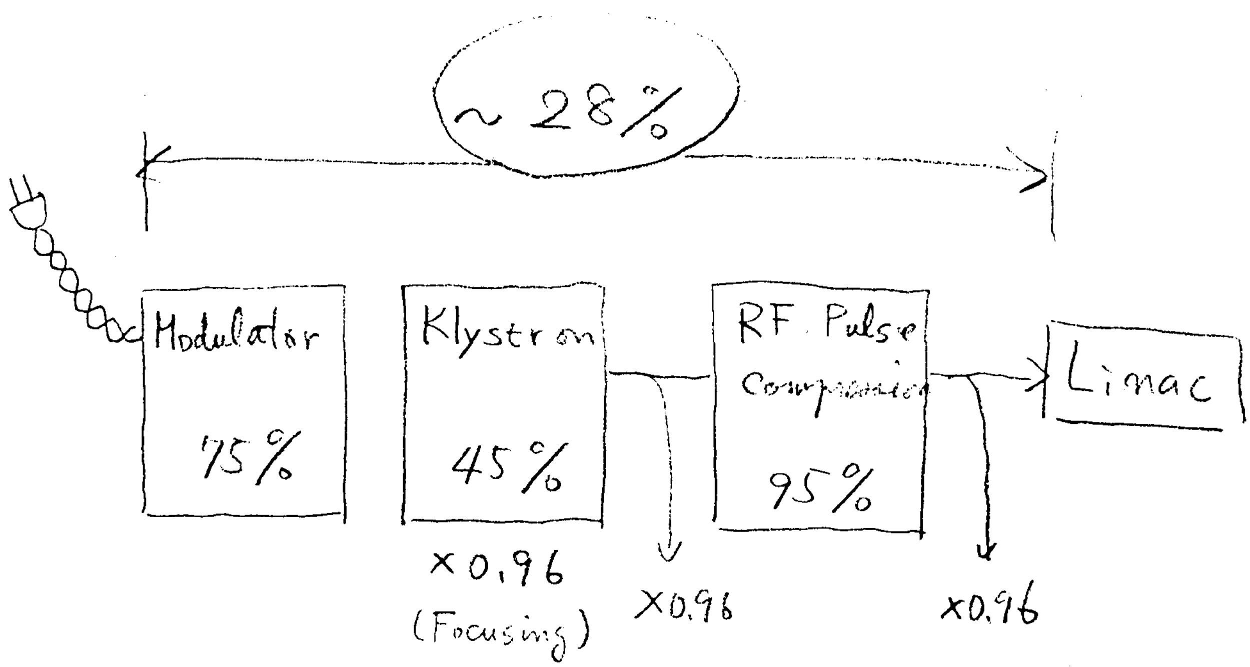

Table-1)XB-72 Parameters

Beam voltage	550kV
Beam current	490A
Max. surface field	273kV/cm
Beam areal compression	110-1
Cathode diameter	72 mm
Current density(Max.)	17A/cm2
Focusin field(Max.)	6.5kG
Number of cavities	5
Frequency	11.424GHz
RF power	120MW
Efficiency	47%
Max. surface Grad. (Output gap)	720kV
Gain	53-56dB

OK?	• Beam Voltage	620 kV	
	• Beam Current	550 A	
	• Beam Power	340 MW	Diode is OK.
Problems	• Efficiency	35%	
	• Output Cavity	Damaged. (Discharge)	Need Multi Gap
	• Peak RF Power	95 MW (26%)	
OK(?)	• Window	TE_{11} ½ λ_g	600ns 70MW
	• Focusing Solenoid	under Test	B_z ok.
		to be measured in SLAC (94 · Dec)	

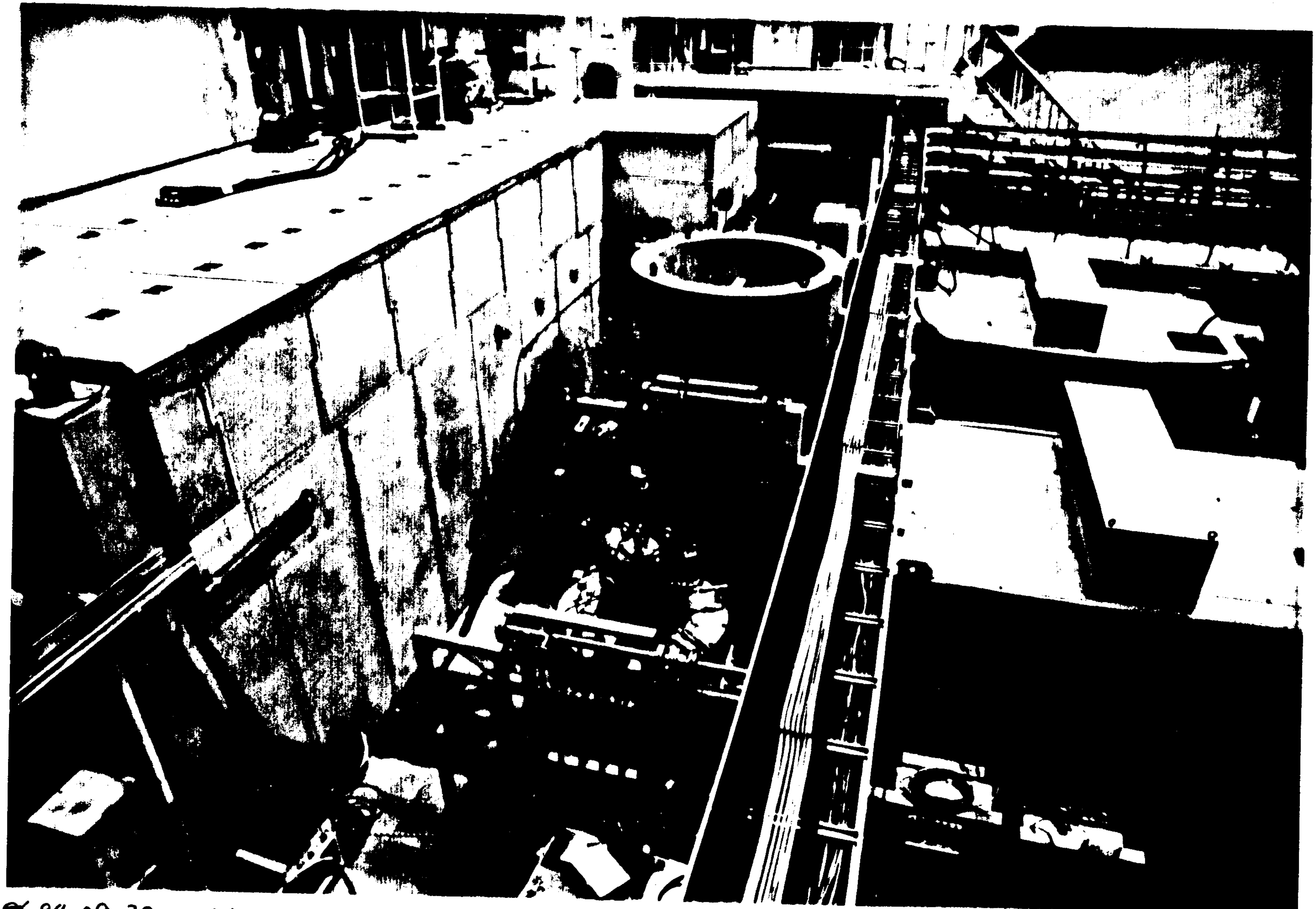

94-08-30 No1 & No2 XB72k RF Station for H.G テスト用

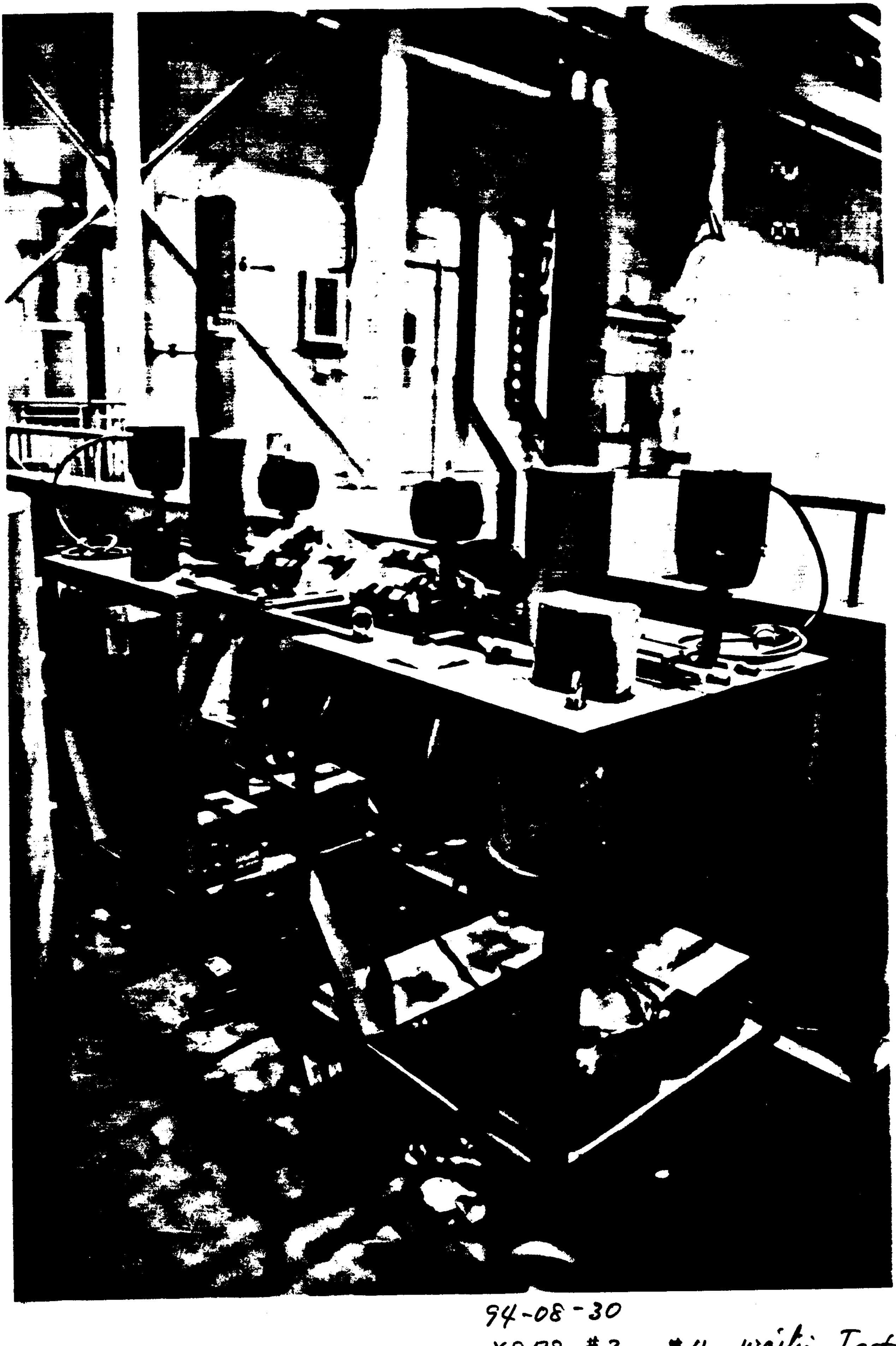

94-08-30
XB72K#3, #4 waiting Tests.

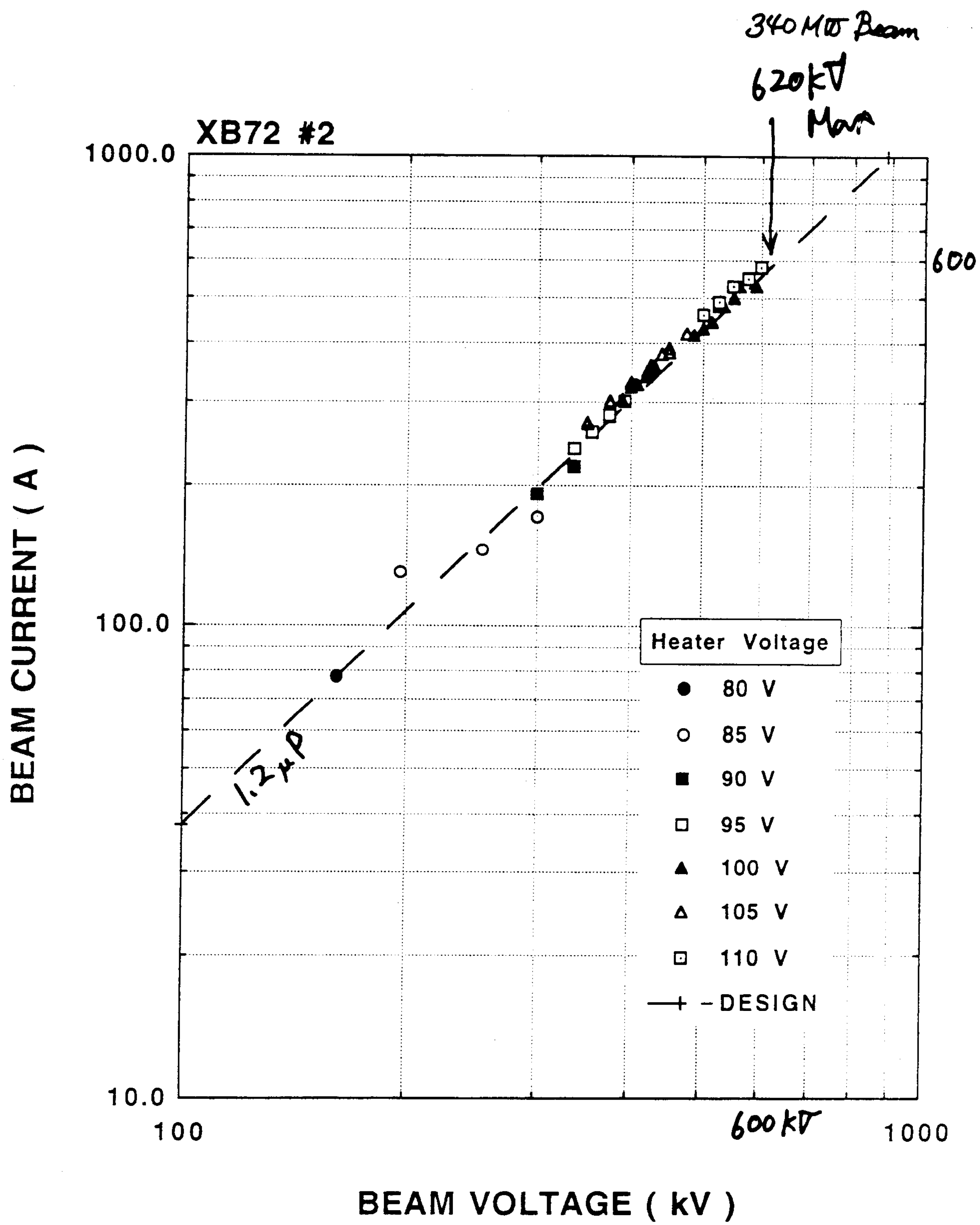
340 MW Beam
620 kV
Max
XB72 #2
1000.0
100.0
10.0
600
1.2 μP
Heater Voltage
80 V
85 V
90 V
95 V
100 V
105 V
110 V
-DESIGN
BEAM CURRENT (A)
100
600 kV
1000
BEAM VOLTAGE (kV)

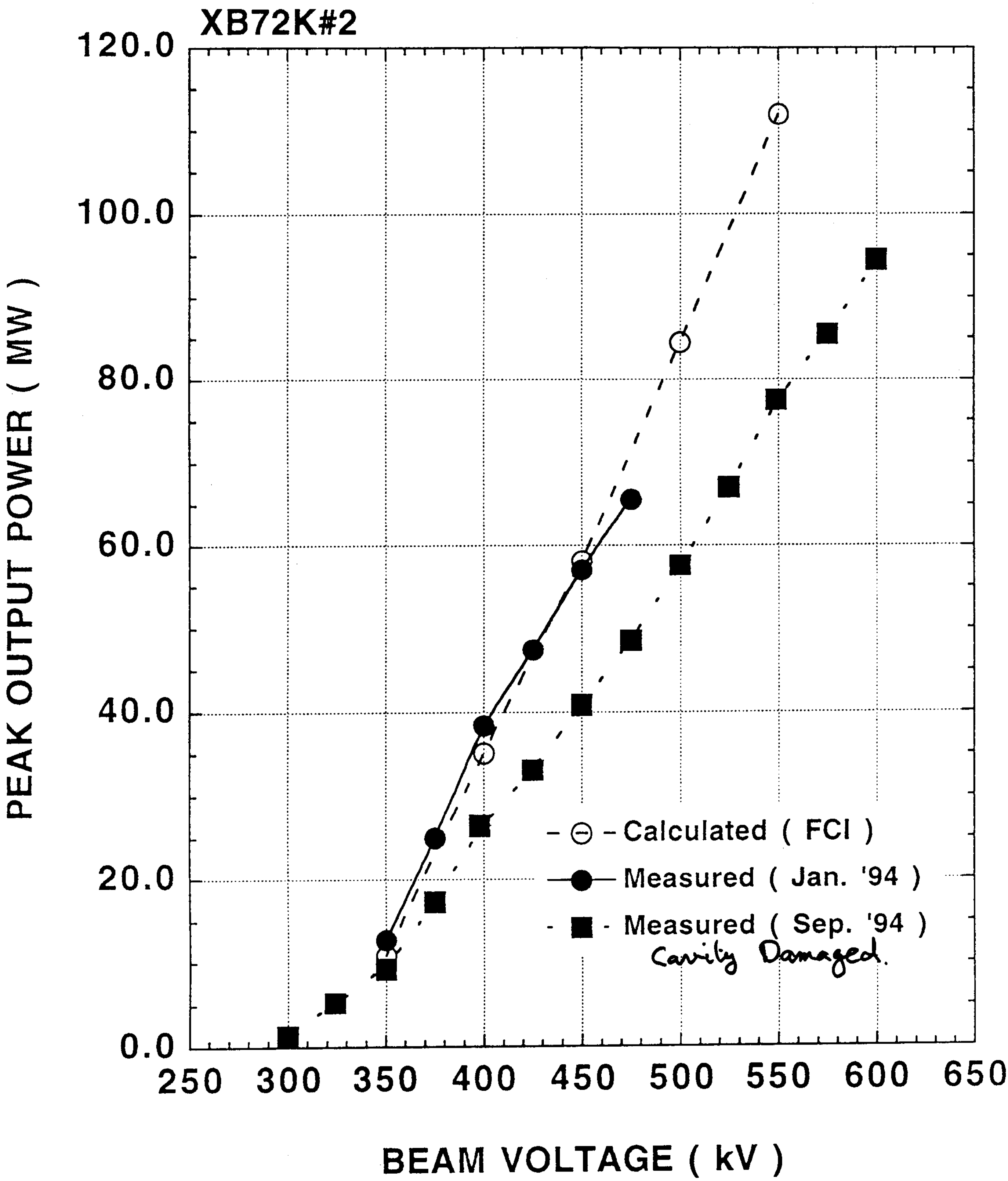
XB72K#2
120.0
100.0
80.0
60.0
40.0
20.0
0.0
PEAK OUTPUT POWER (MW)
250
300
350
400
450
500
550
600
650
BEAM VOLTAGE (kV)
Calculated (FCI)
Measured (Jan. '94)
Measured (Sep. '94)
Cavity Damaged.

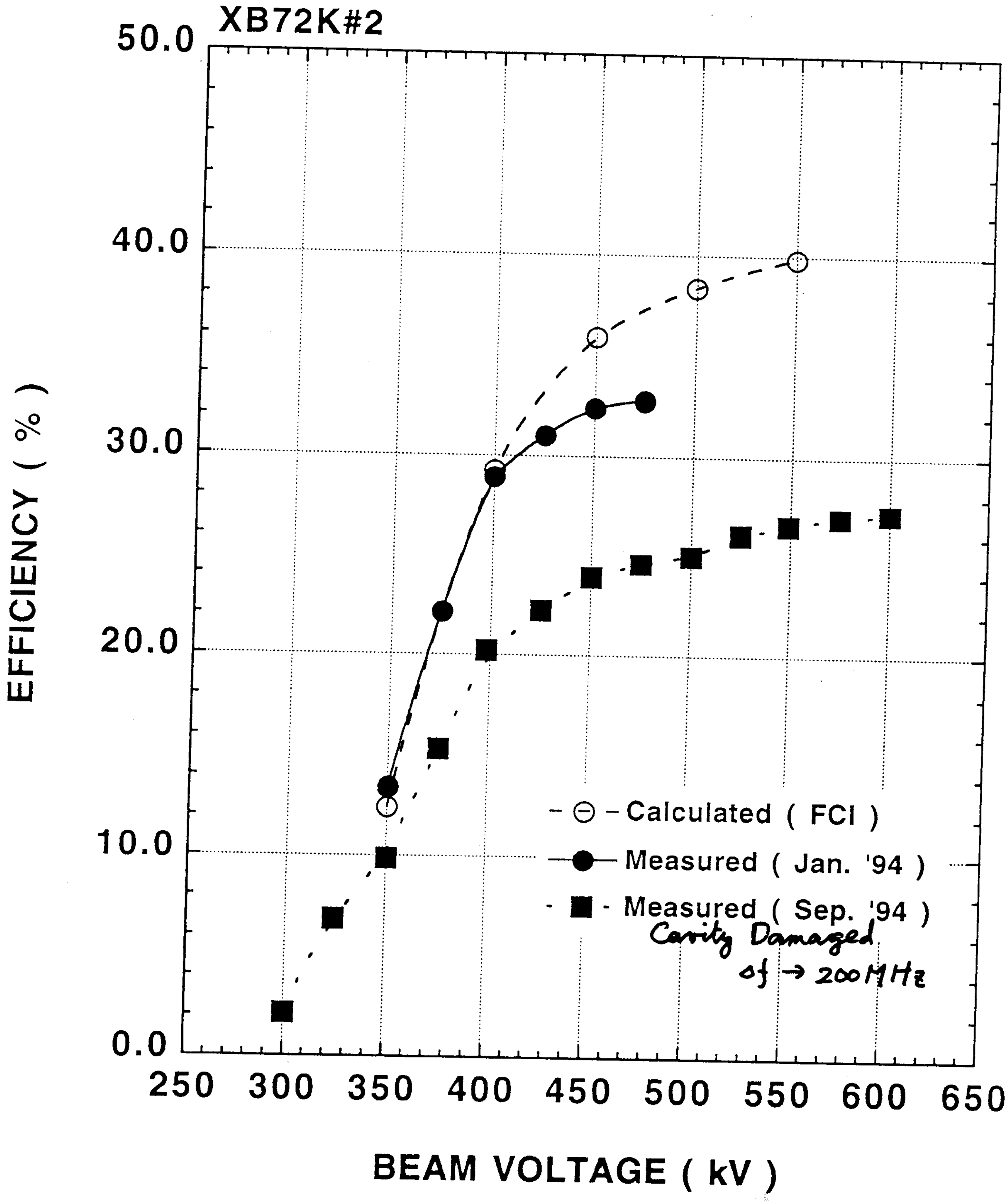
XB72K#2
EFFICIENCY (%)
50.0
40.0
30.0
20.0
10.0
0.0
250
300
350
400
450
500
550
600
650
BEAM VOLTAGE (kV)
Calculated (FCI)
Measured (Jan. '94)
Measured (Sep. '94)
Cavity Damaged
of → 200MHz

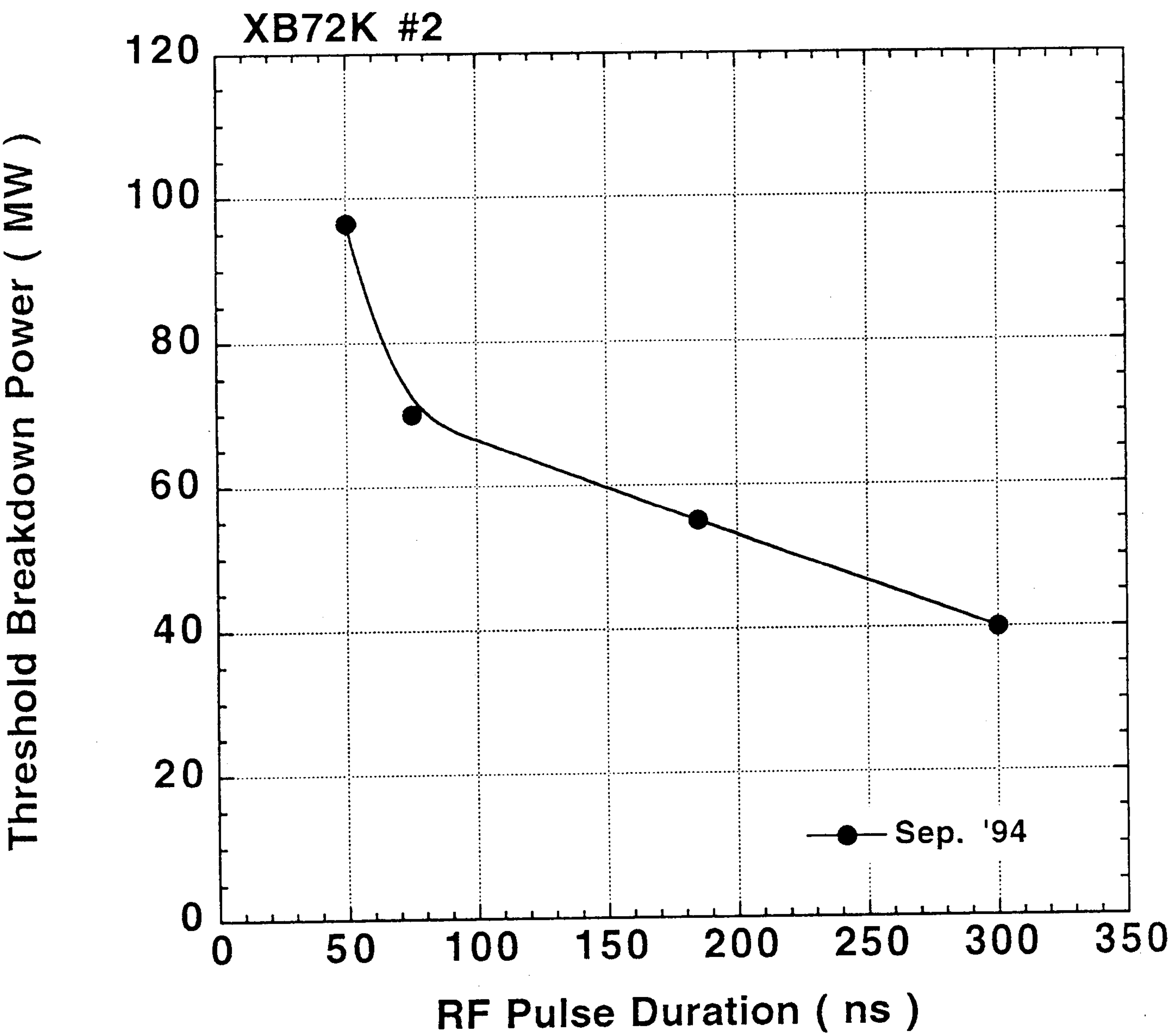
XB72K #2
Threshold Breakdown Power (MW)
120
100
80
60
40
20
0
0
50
100
150
200
250
300
350
RF Pulse Duration (ns)
Sep. '94

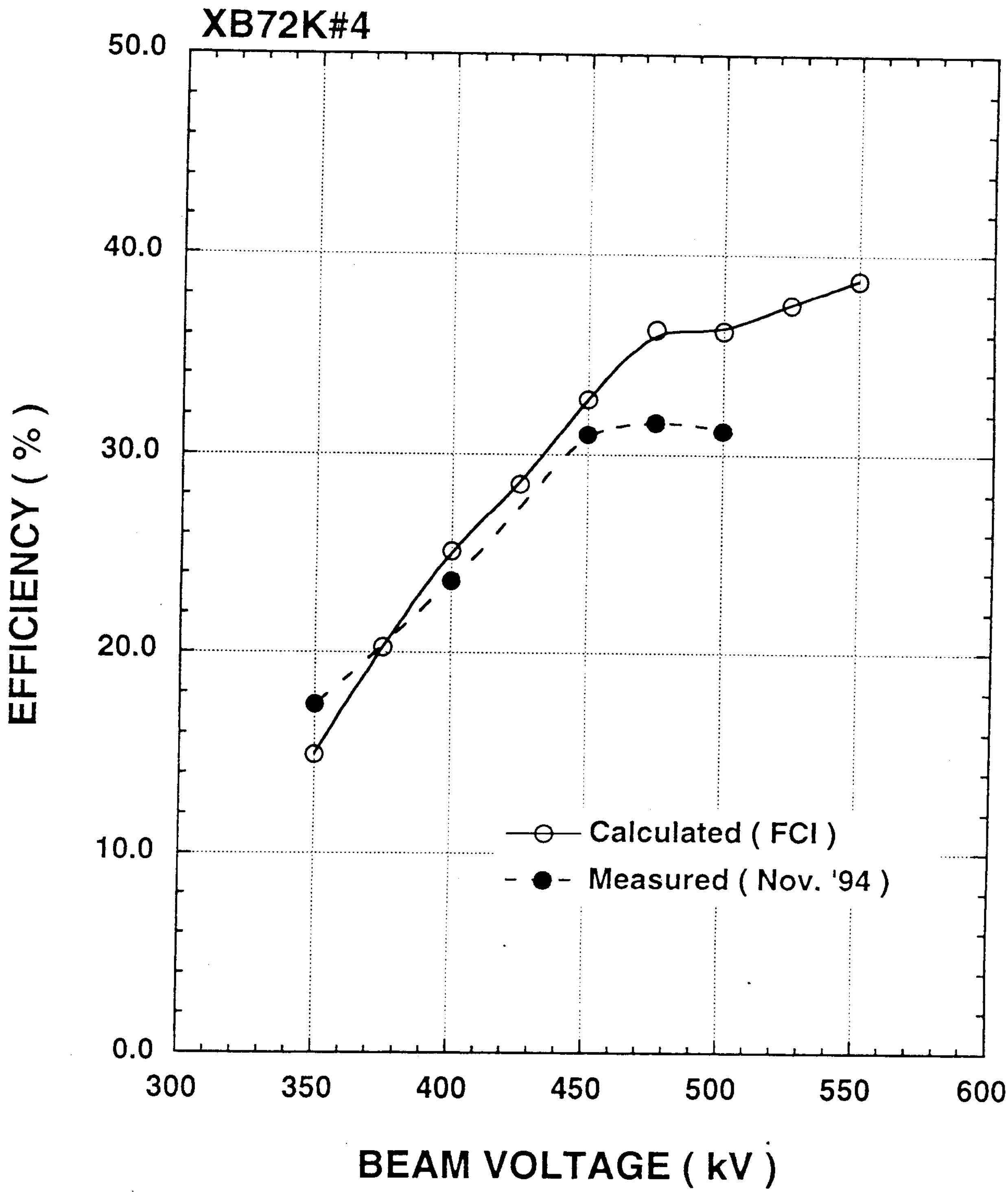
XB72K#4
EFFICIENCY (%)
50.0
40.0
30.0
20.0
10.0
0.0
300
350
400
450
500
550
600
BEAM VOLTAGE (kV)
Calculated (FCI)
Measured (Nov. '94)

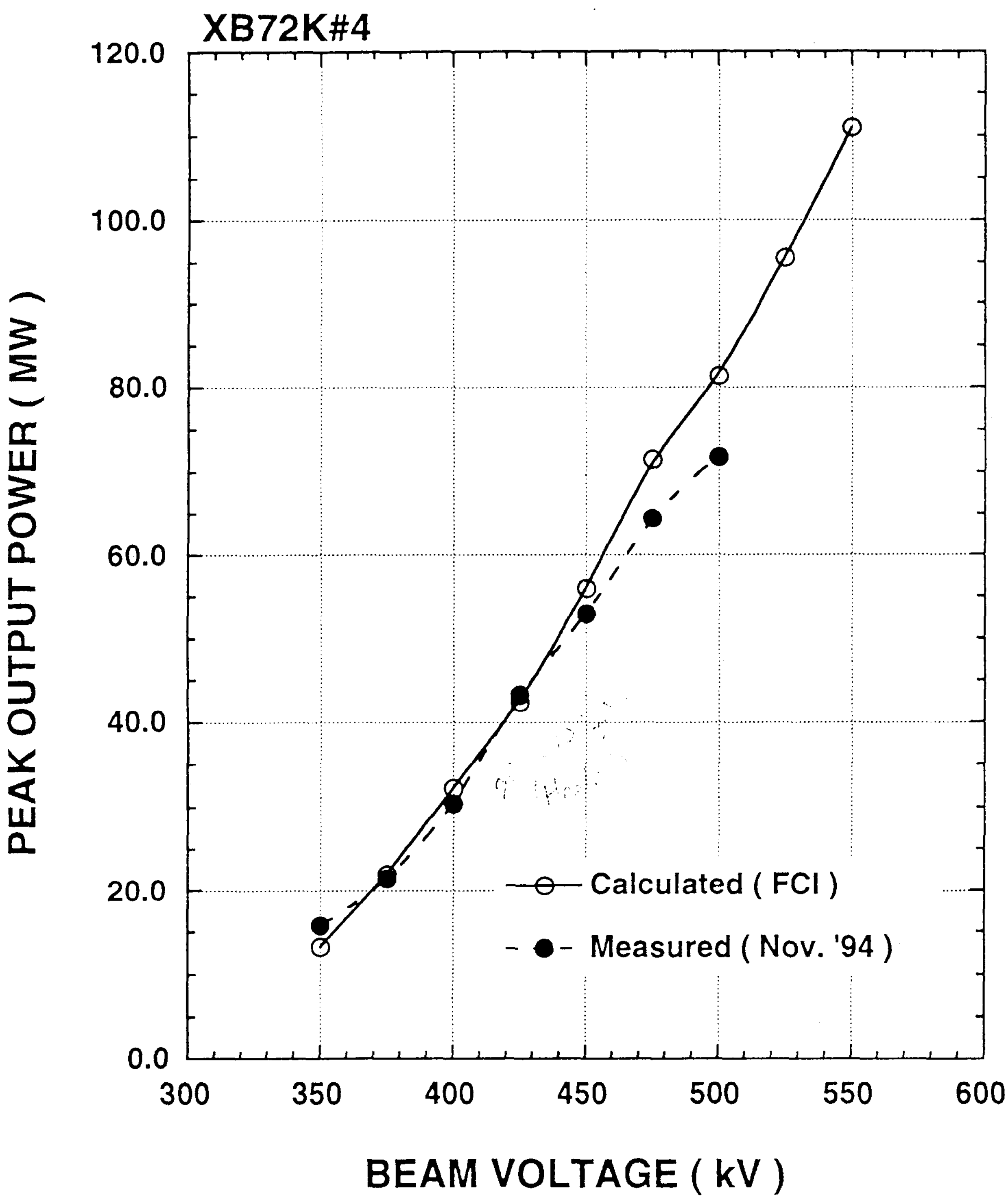
XB72K#4
PEAK OUTPUT POWER (MW)
120.0
100.0
80.0
60.0
40.0
20.0
0.0
300
350
400
450
500
550
600
BEAM VOLTAGE (kV)
Calculated (FCI)
Measured (Nov. '94)

994-09-20
XB72k#2
620kV 後.
アノード付近
のべ~200 hours.

157

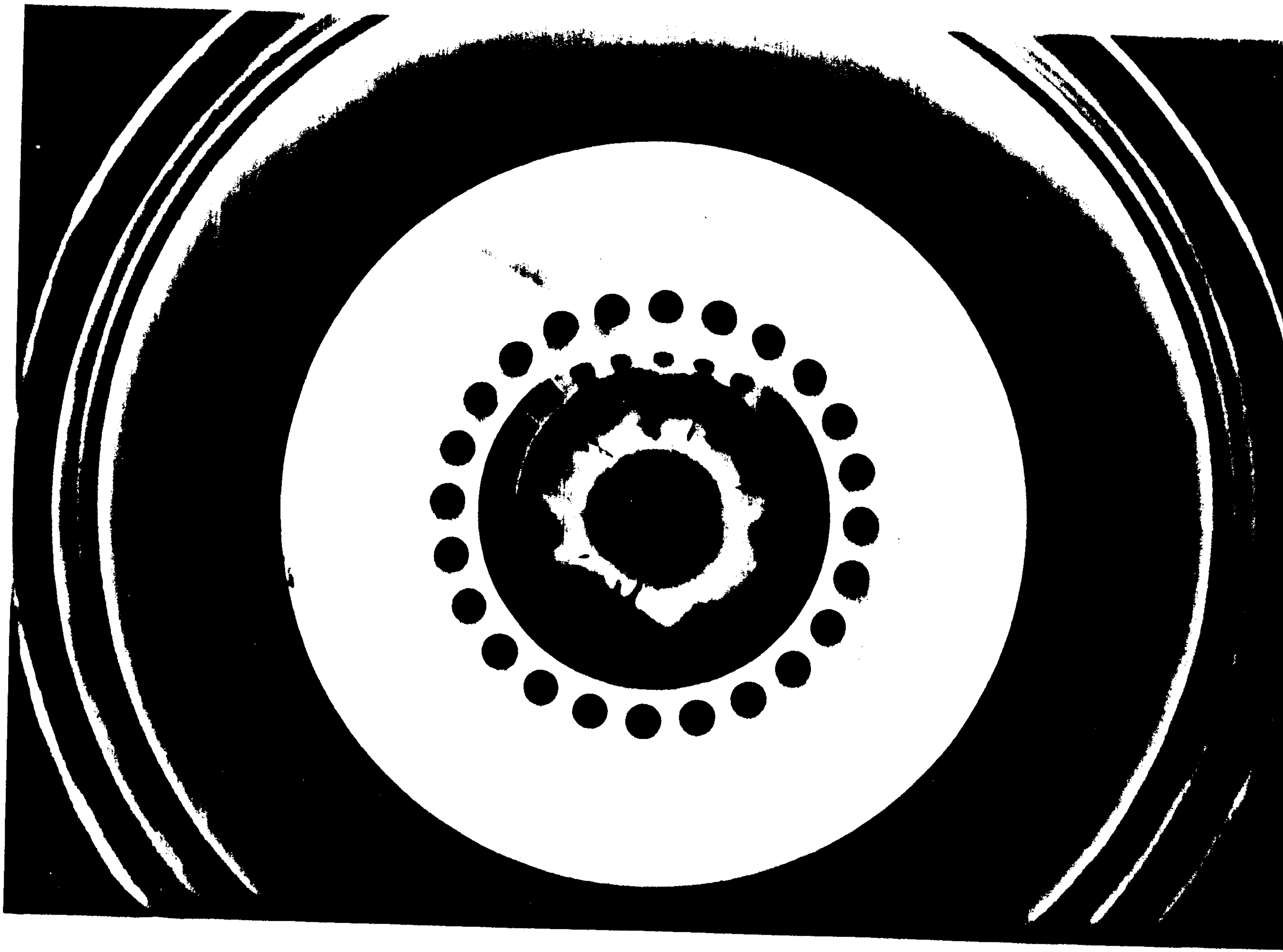

1994-09-20
XB72K #2
カソード付近
620kV 後
ウェーネルト 放電
セラミック内面
カラーリング.

計
~200 hours ?

The Field Strength on the Ceramic Surface

Type	Es *	Band Width	Peak RF (100ms)
Pill Box **	0.87	500 MHz	~30 MW damaged
TE11 (short) ***	0.42	250 MHz	~100 MW OK
TE11 (long)	~~~0.3~~ ~0.4	~300 MHz	?

* Normalized to the WR-90 Rect. W.G.

** Equipped on XB72K #1 → #4

*** Tested in the Res. Ring up to 100 MW
XB72K #5 will be equipped with this Type.

Ceramic Windows.

TE_{11} Window ($\frac{1}{2}\lambda_g$ Type 11.424 GHz)
51φ ceramic — Y. Otake.
X-Band Tested 100 MW peak.

T, Wave Window X, S band
S. Kazakov (Russia)
S-band 400 MW Tested.
X-Band finished, waiting RF Test.
28φ ceramics

Designe Principle (
~8 kV/mm on the Ceramic Surface
↑ (Y. Saito (KEK))
S-band Experiments

XB72k #1 → #4 — X-Band Pill Box ×2

XB72k #5 and after — TE_{11} Window ×2

½λg TE11 High Power Model #1 Completed
waiting Res. Ring Test (94-02-21)

93-10-06
Y. Otake 図面

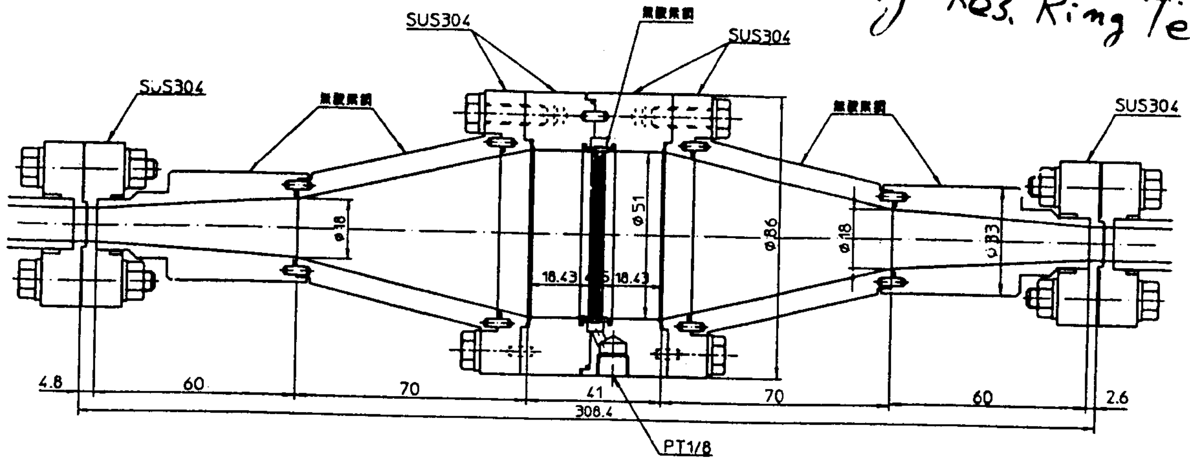

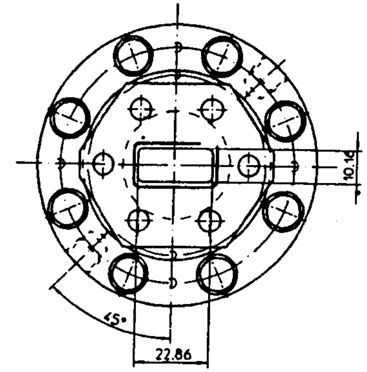

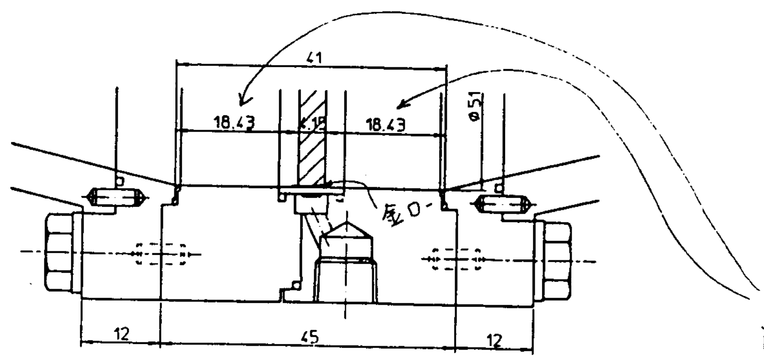

Al_2O_3 と OFHC リング は 金ロー付

この寸法は VSWR テストしながら
削ってゆき 最終(13.83 mm ?)寸法
決定する.

形式	WPW-108V1	名称	Xバンド真空窓
承認	鈴木久	図番	2-018981-
		日本高周波株式会社	0
第三角法			

TE11 ½λg High Power Model

X-Band window Hi-Power Model 測定

No. 1.

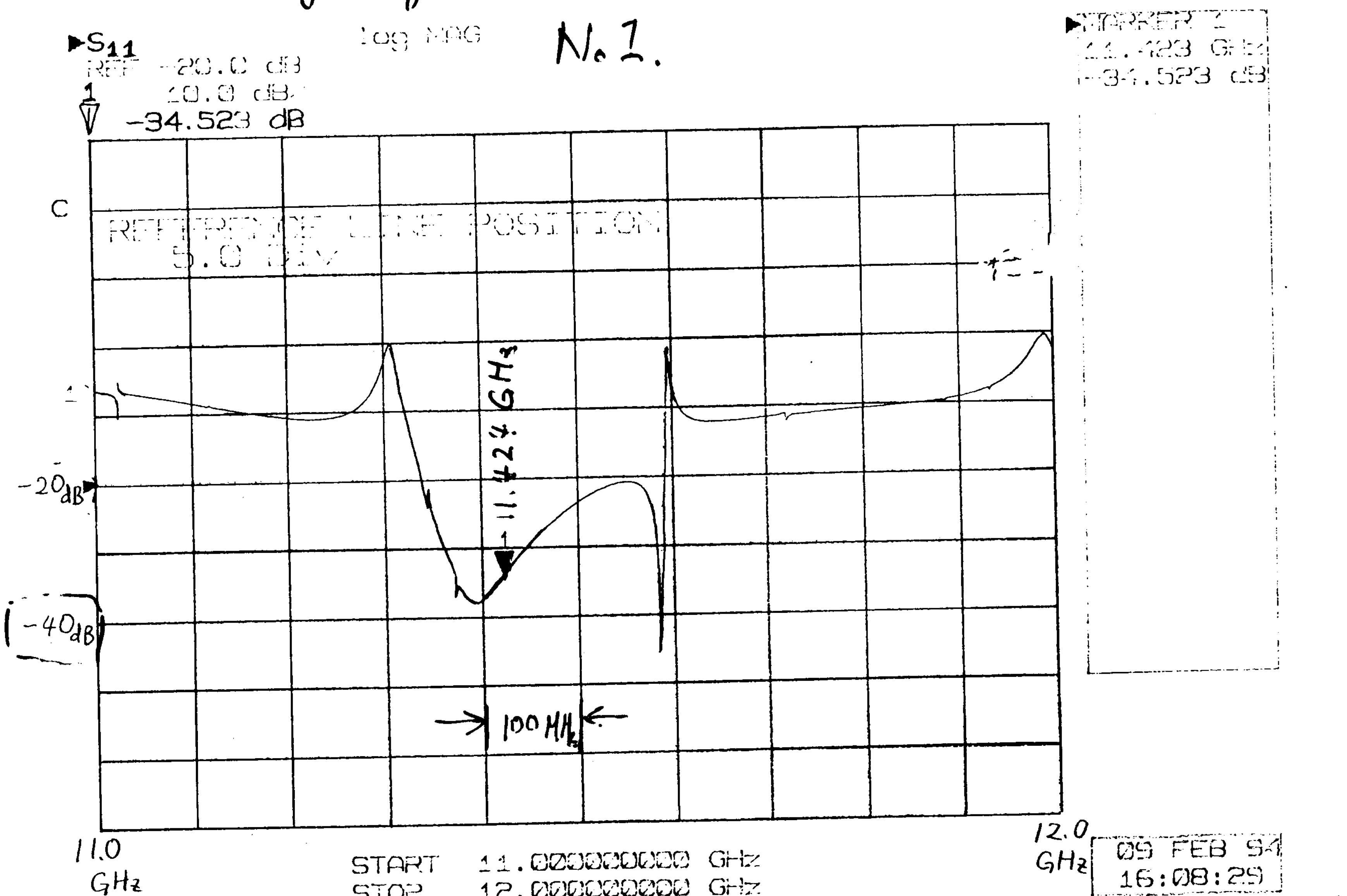

(by Yuji. Ohtake)

162

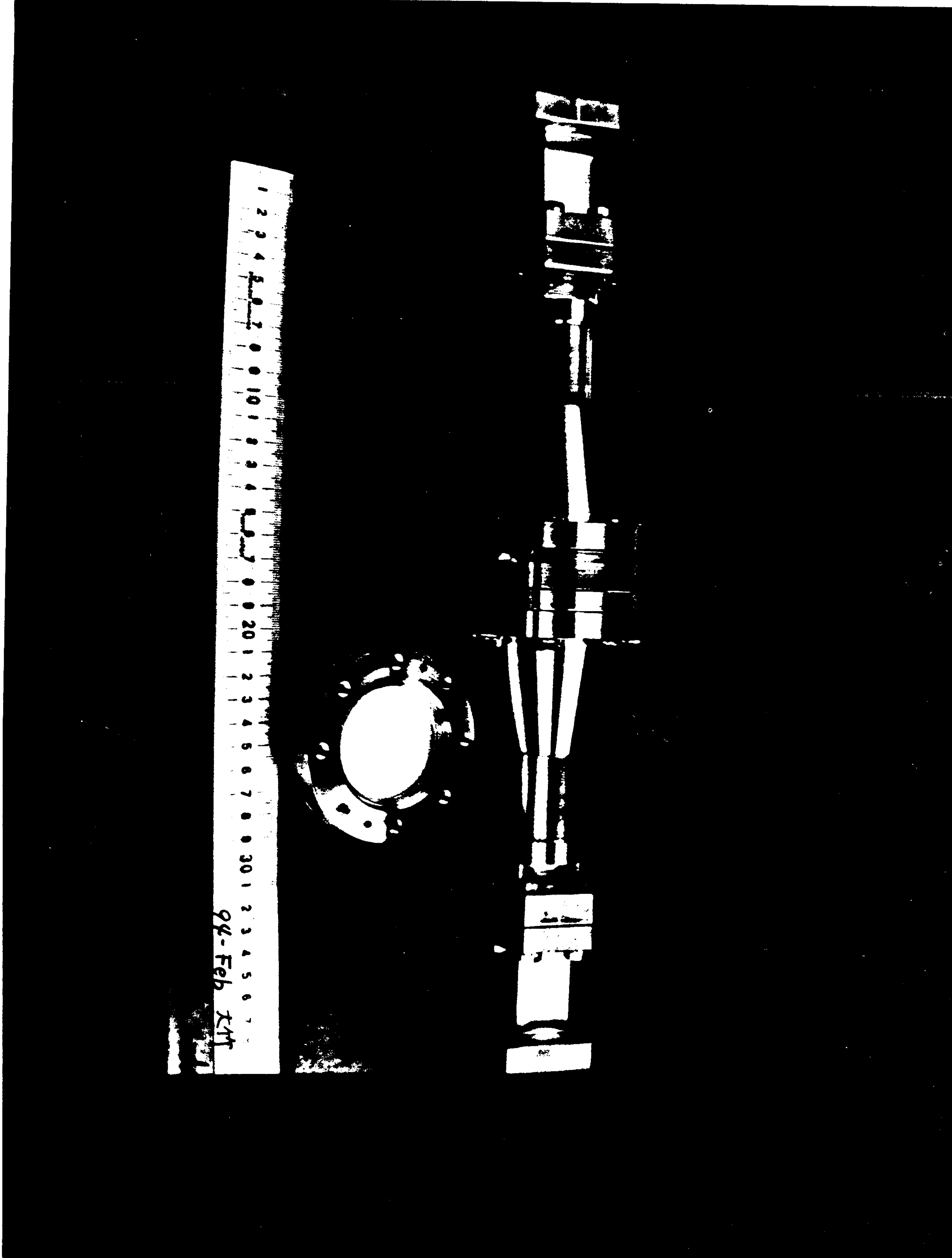

S. Tokumoto J. Odagiri Y. Otake Res. Ring

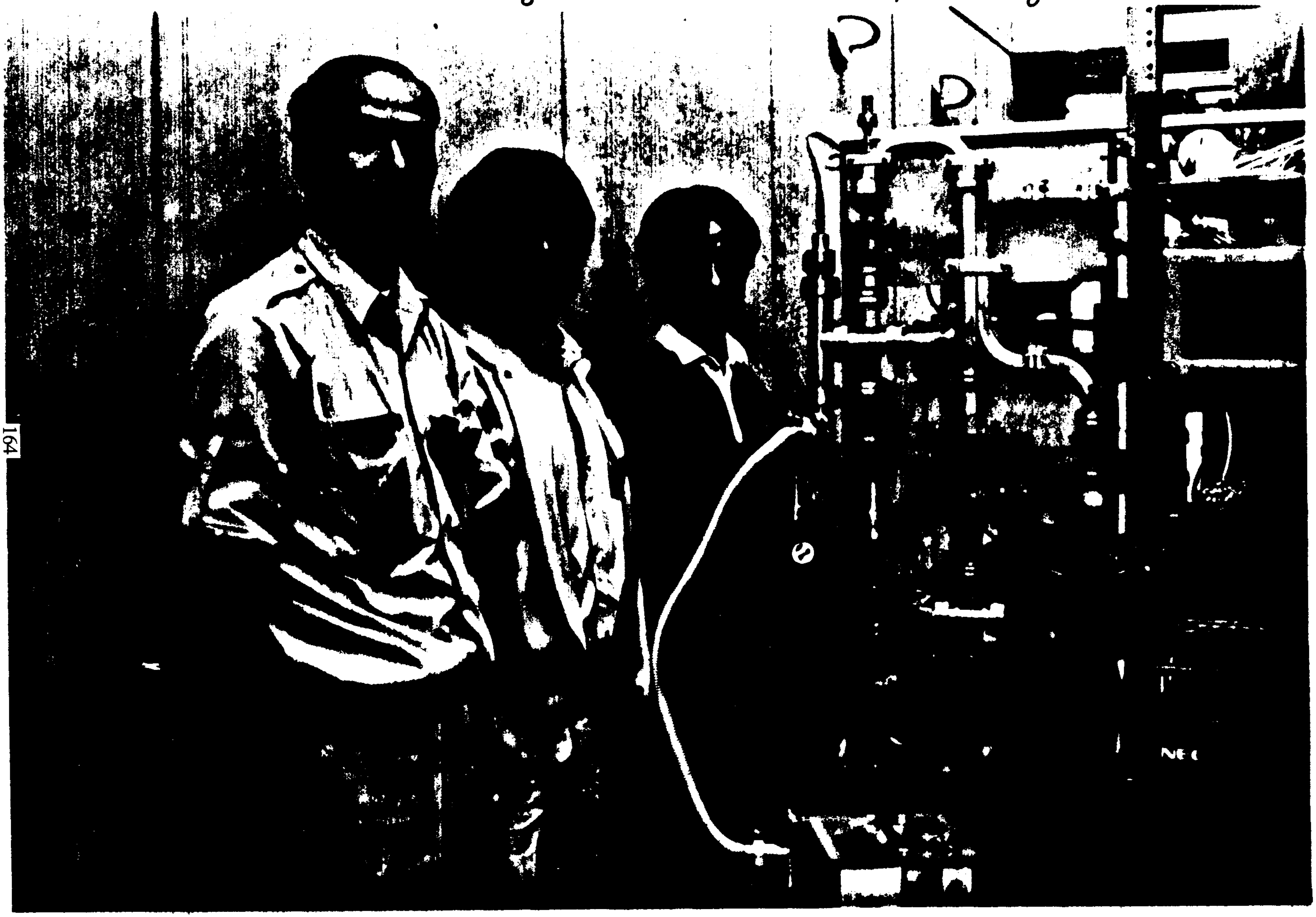

Results of TE1 1-mode RF Window High-Power Test

5/16/94

300 ns input to the resonant ring.

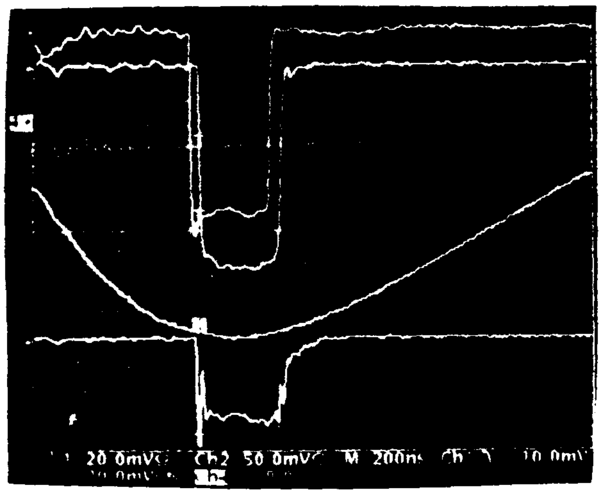

Resonant ring input power
200 ns/Div. 14.5 MW

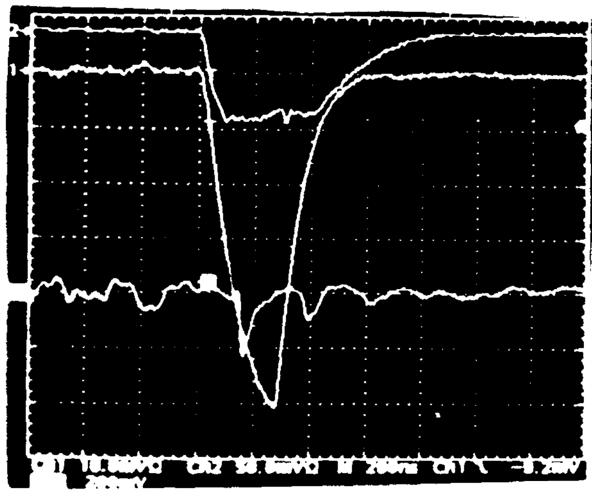

Resonant ring circular power
200 ns/Div. 102 MW

700 ns input to the resonant ring.

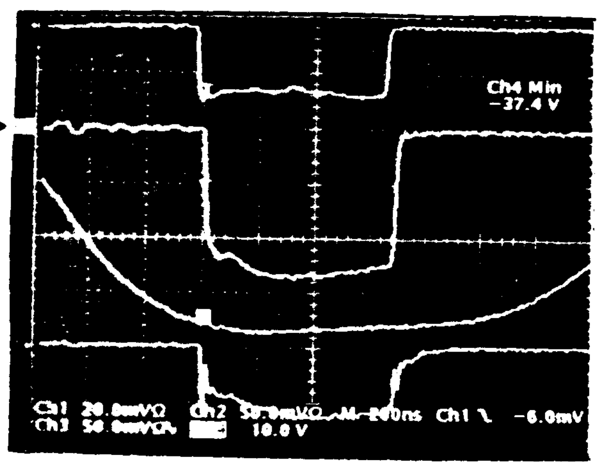

Resonant ring input power
200 ns/Div. 8.6 MW

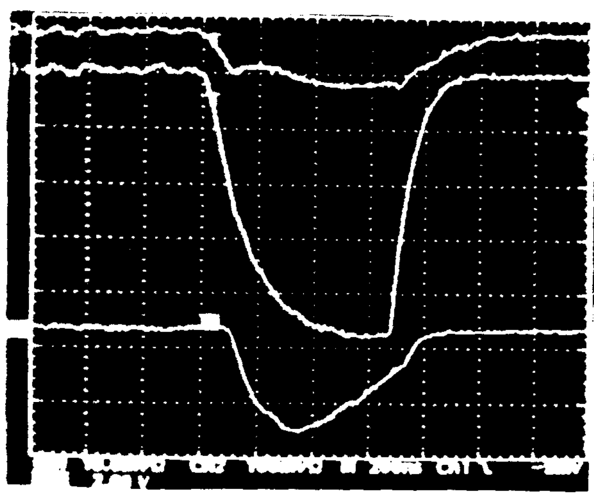

Resonant ring circular power
200 ns/Div. 72 MW

Super Conducting Solenoid (M. Elec.)

Sept. 94' Tested.

- for XB72k.
- Independant Refregerator + Thermal Conduction Cooling.
  - water supply
  - 200V power line
- To reduce Heat Loss
  "High Tc Super Conducting Material"
  for the current lead.
- Total Power Max, 5 kW
  ~3 kW
- Permanent Current Mode in Future,
  need some additional "Switch"
  possible.
- Field Measurement in "SCAC" Jan. 95'?
  effect of "Thermal Cycle"

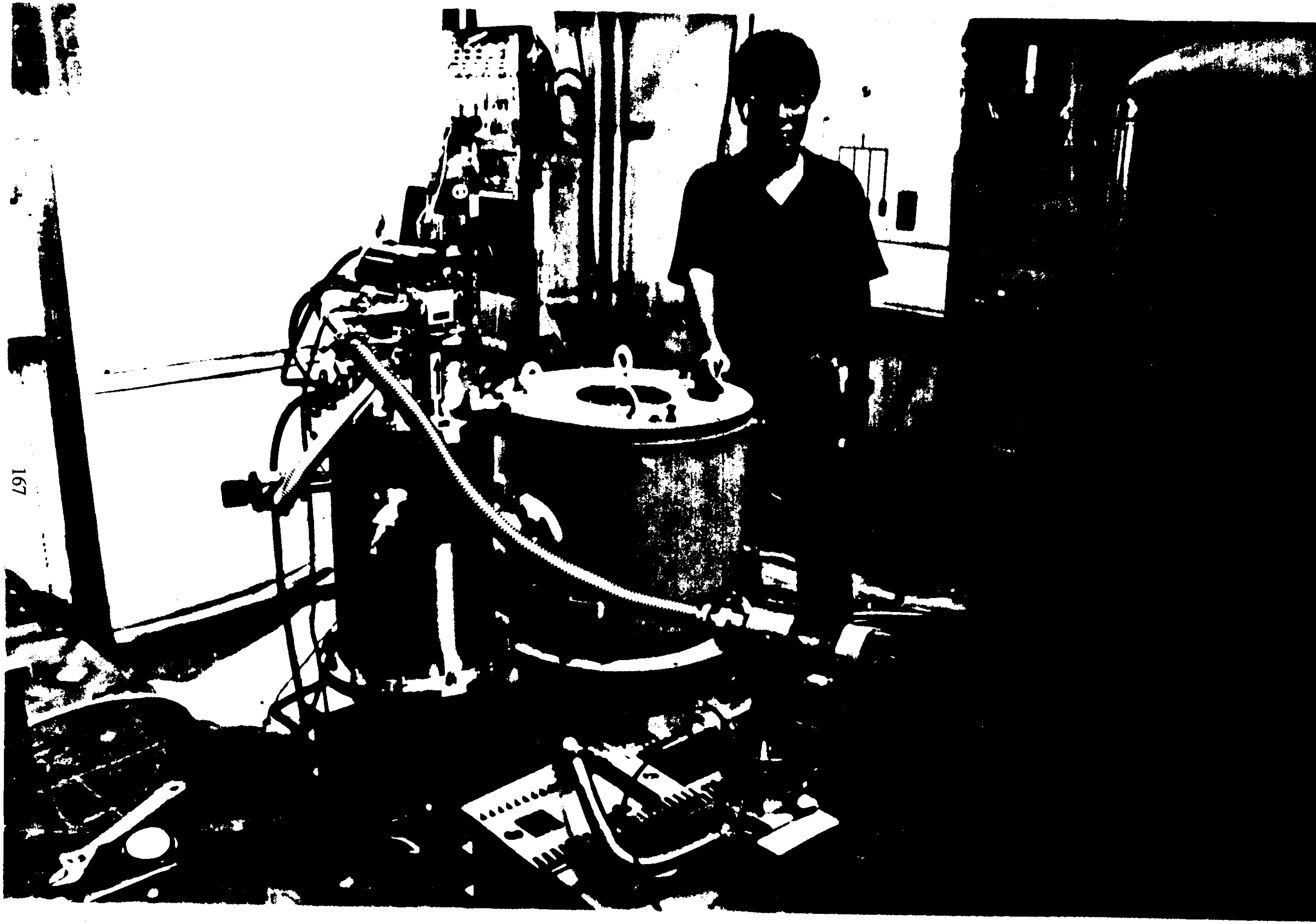

94-09-05
三電 ソレノイド
High Tc
Current Lead
NbTi:
Max 6.5 KG

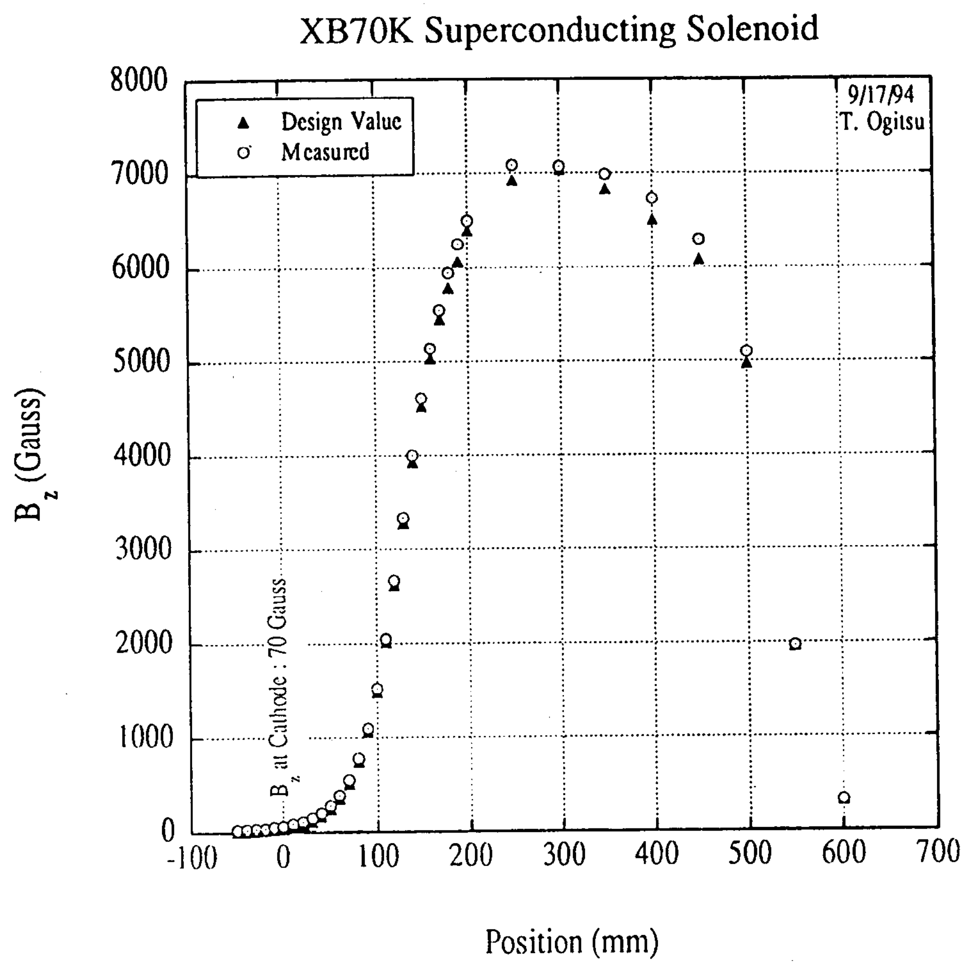

中心軸上 Bz
▲ 72k 設計値
○ 測定値
ホール素子使用
カソード面上の値は
Backing コイルの補正なし
補正可能な値になっている
目標値 35 ガウス

XB70K SC Solenoid
Thermal Cycle

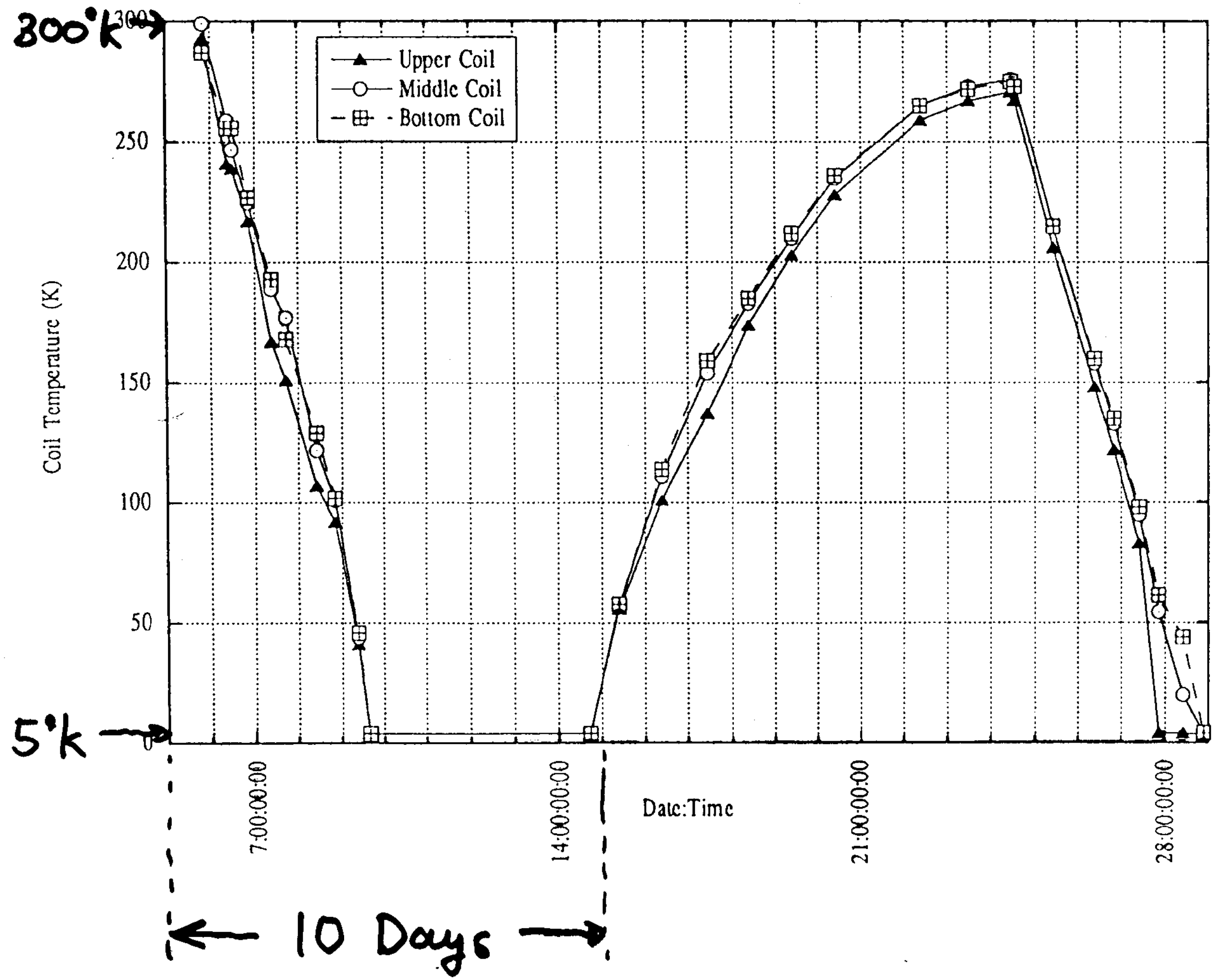

MODULATORS FOR X-BAND KLYSTRON(XB-72K)

1) Conventional modulator(1991)

2) Blumlein type PFN

Under design and construction by IHI(Ishikawajima-Harima Heavy Industry) ~~Will be Completed~~ 1993-Feb.
was tested 1993 - Oct.

Design Parameters

(a)PFN(Blumlein Type)

Also Tested 9-stage Version

Rise Time(with Trans.)	~150 ns
Fall Time(with Trans.)	~230 ns
Flat Top	~500 ns
Number of PFN	12 ~~8~~-stages + 12 ~~8~~-stages { C = 2.6 nF, L = 340 nH }
Output Voltage(=Charging V)	80 kV (1:7 Step-up)
Impedence	23 Ohm(XB-72K 550 kV)

(b)Pulse Trans.(Primary at 80 kV while charging)

Step-up ratio	1:7
Leakage L	830 nH
Stray Capacitance	4 nF (Primary)
Primary L	200 micro-H
Loss at 200 pps	100 W (Hysteresis)
	1000 W (Eddy Current)
※ Rise Time (Trans. only)	~100 ns
※ Fall Time (Trans. only)	~200 ns
Sag.	2.8 % (after 500 ns)
Core Material	Si-Fe (t=25 micron)

※ • Inductance of Lead Wiring etc

" Maxwell " — OK. ? ⇒ (very Promissive)
(Made in USA)

• 1992 Fy ..... Conventional

• 1994 Fy .... In Oil Tank.

1st Test 1995 - Jan.

HM

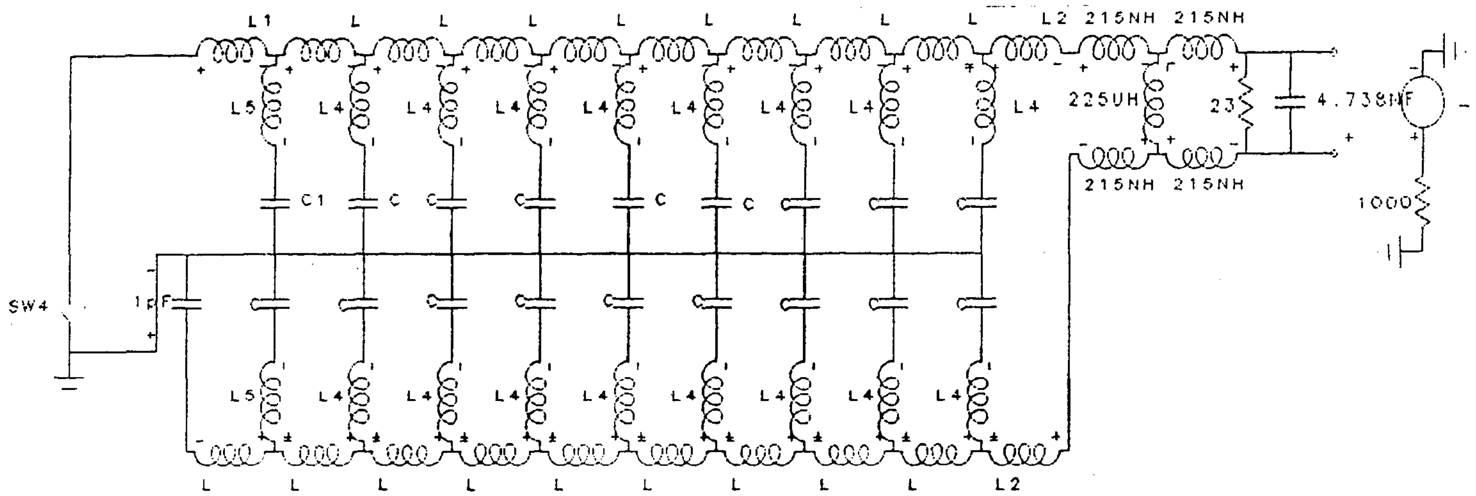


```
.DEFINE SW4 T,0.0000MS,0.05MS

.DEFINE C 3.5NF
.DEFINE C1 3.5NF
.DEFINE L 0.6UH
.DEFINE L2 0.6UH
.DEFINE L4 40NH
.DEFINE L5 40NH
.DEFINE L1 0.6UH
```

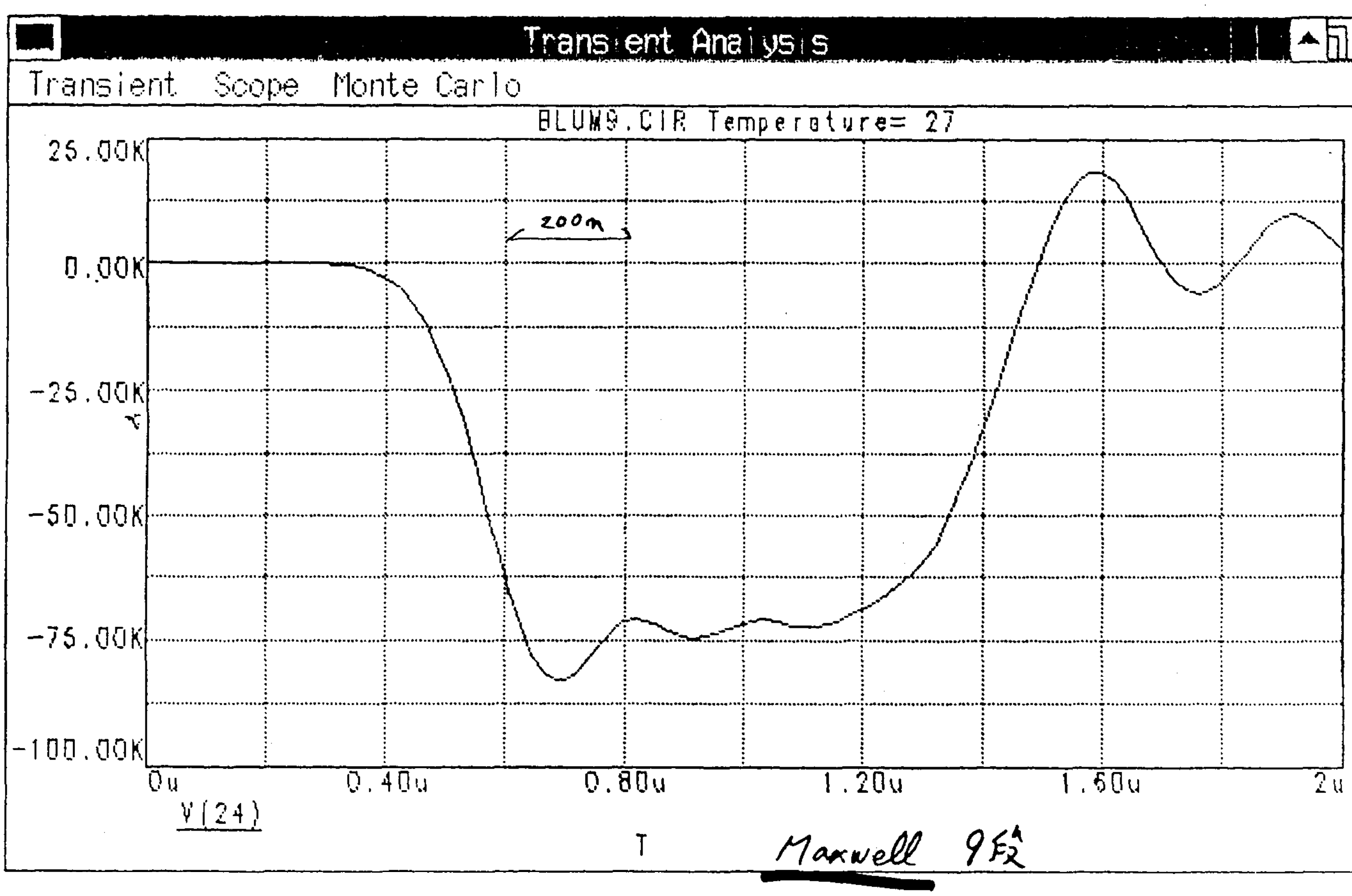

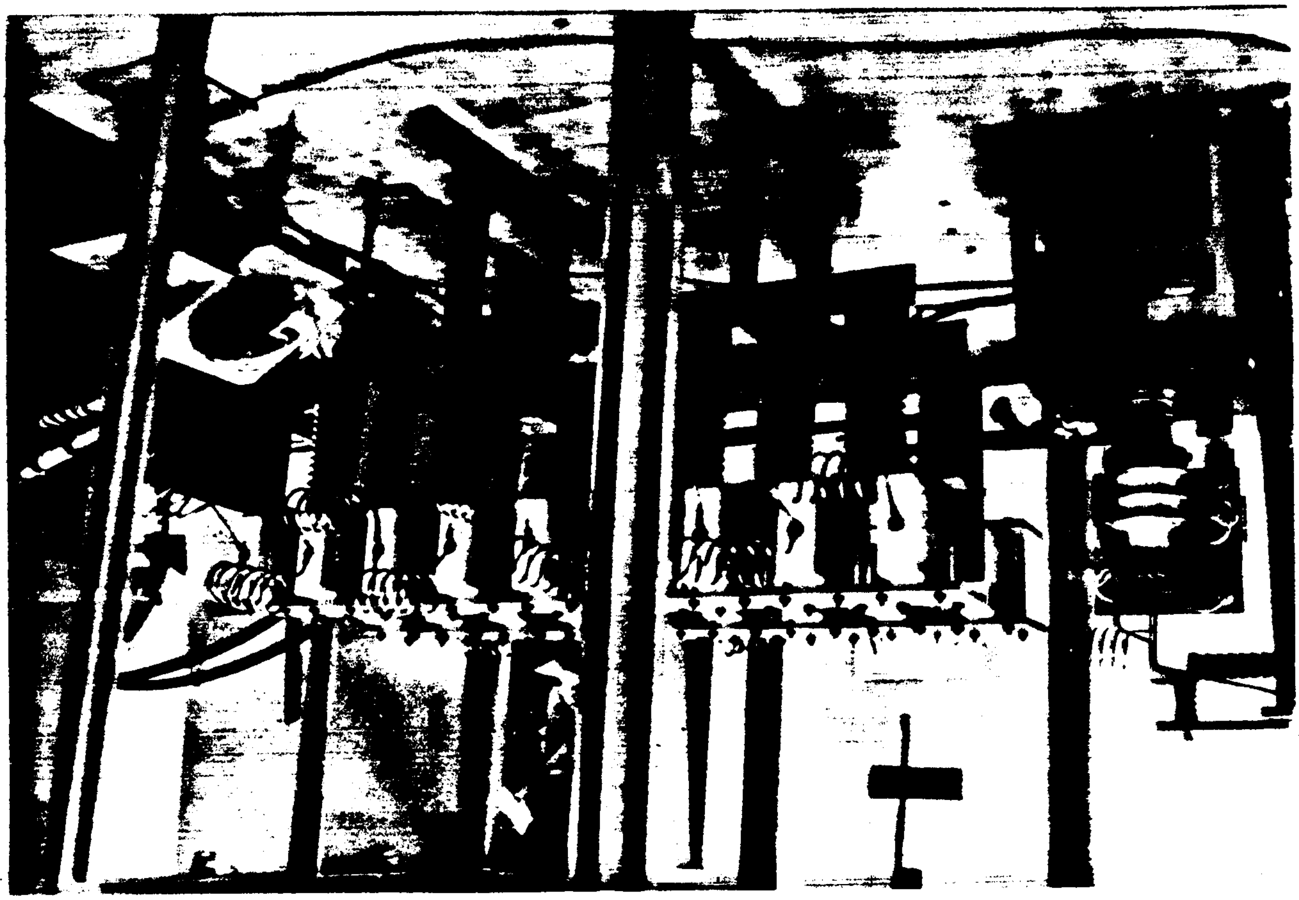

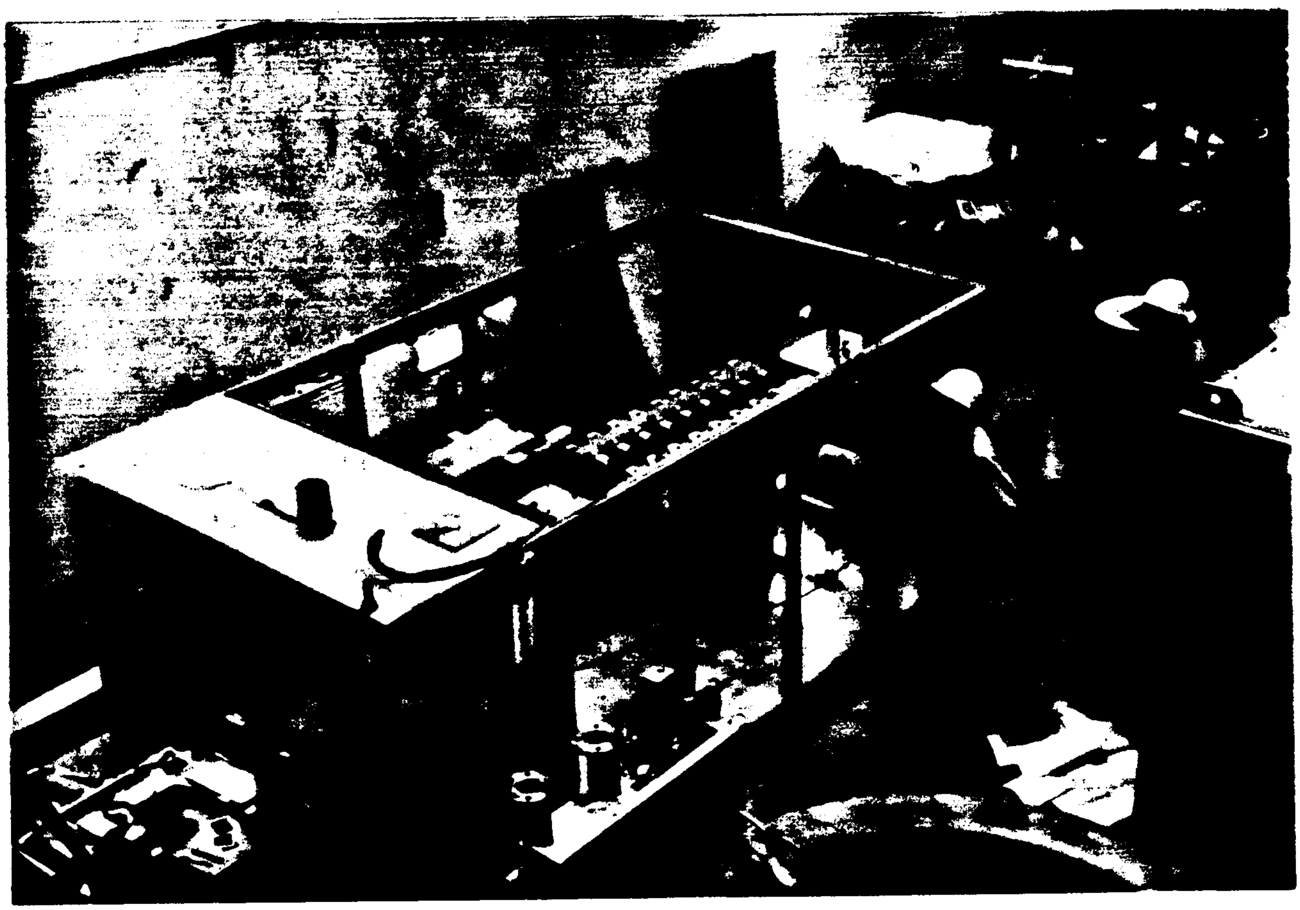

(4) $I_{P\text{-}BIAS} = 15A$

Bias Current

= 15A

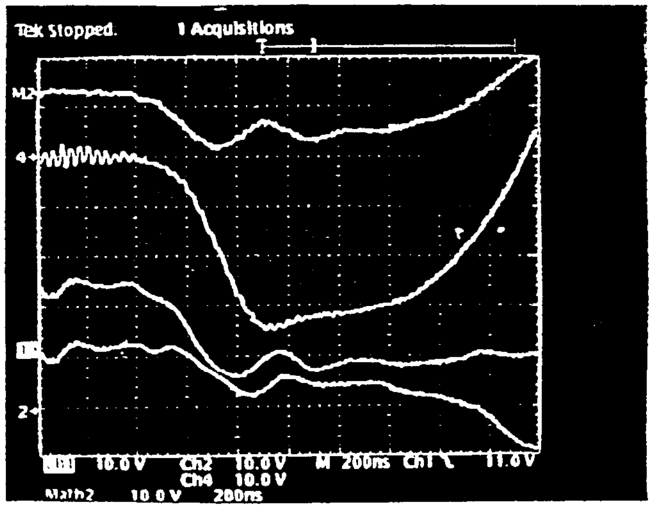

(5) $I_{P\text{-}BIAS} = 20A$

= 20A

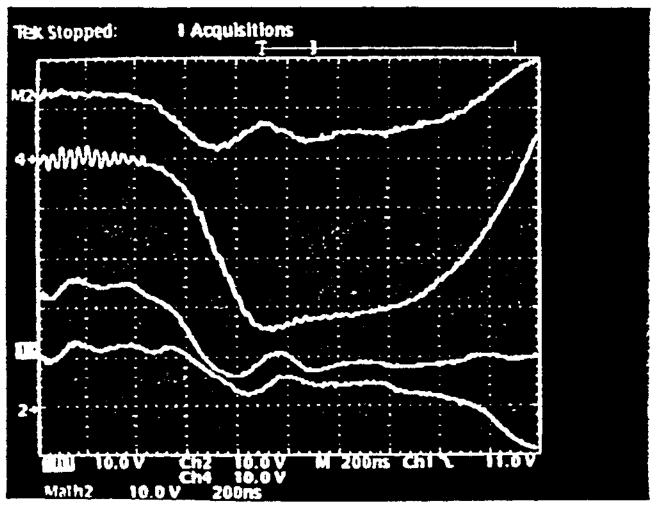

1993-Nov.

(6) $I_{P\text{-}BIAS} = 25A$

400ns

$V_c \sim 450kV$ →

= 25A

$T_{rise} \fallingdotseq 250ns$

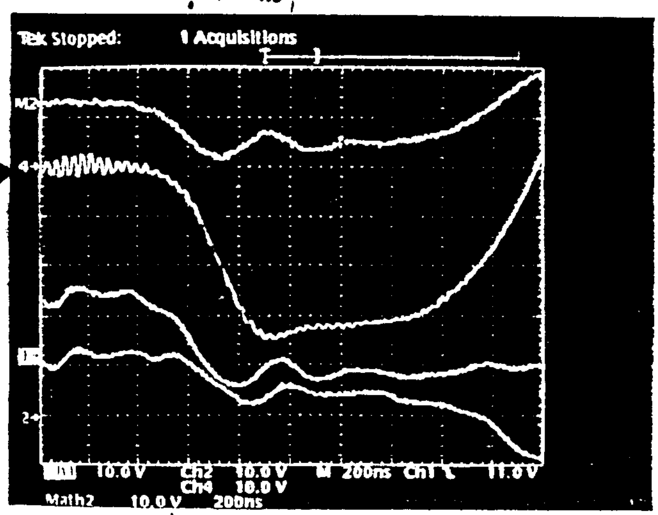

今回のほぼBest
但し Impedance 若干ずれあり
出力電圧に若干問題あり.
Impedance (?)

A NEW RF POWER DISTRIBUTION SYSTEM FOR X-BAND LINAC EQUIVALENT TO AN RF PULSE COMPRESSION SCHEME OF FACTOR 2^n

H.Mizuno, Y Otake,
National Laboratory for High Energy Physics(KEK)
1-1 Oho,Tsukuba-shi, Ibaraki-ken 305 JAPAN

ABSTRACT

As an RF power source system for a future X-band linear colliders, some RF pulse compression system is necessary. A new simple scheme which can provide the better efficiency than the present scheme such as SLED or SLED-2, is proposed. This scheme consist of 2-Klystrons, a 3-dB coupler and a TE01 mode delay line one half of the necessary delay time. The output RF pulse of 2-klystrons are combined through 3-dB coupler and the first half of the pulse is transported to the upstream of a linac through the TE01 mode wave guide. Then, by reversing the phase of the one of 2-klystrons, the last half of the RF pulse is directly fed to the linac structure located close to the klystrons. The RF power loss in this system is determined by the loss in the transporting waveguide. In the case of 400nsec pulse. ie 200nsec pulses at the input of 2-different accelerating structures, the estimated efficiency is more than 95%.

③ H.M

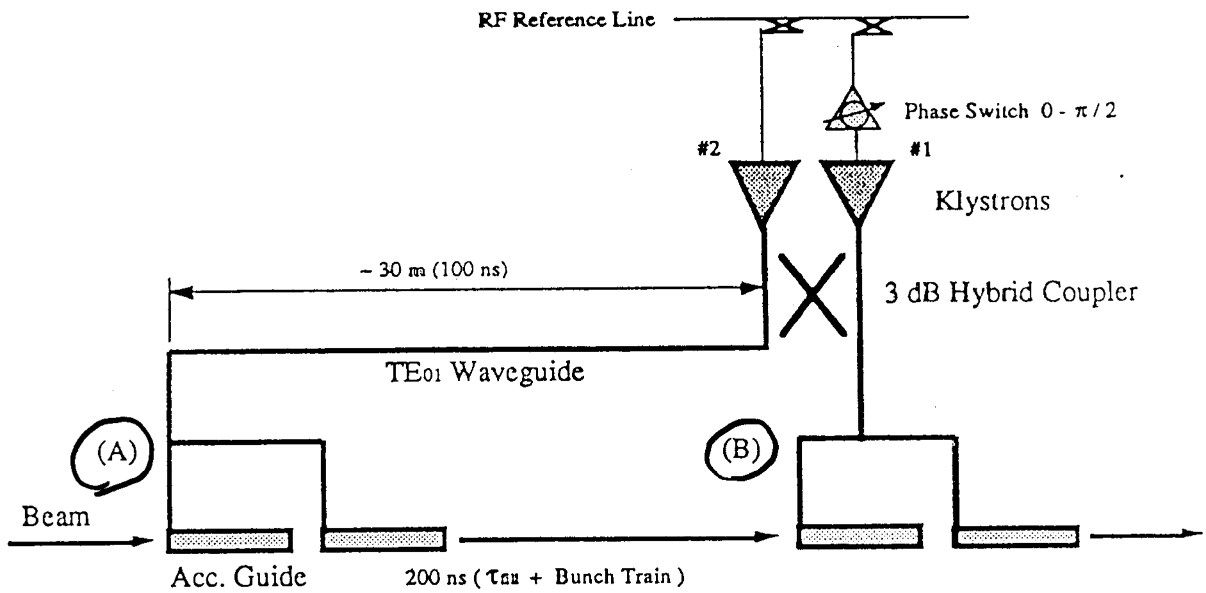

図 1　A Schematic Diagram of an RF Power Distribution System

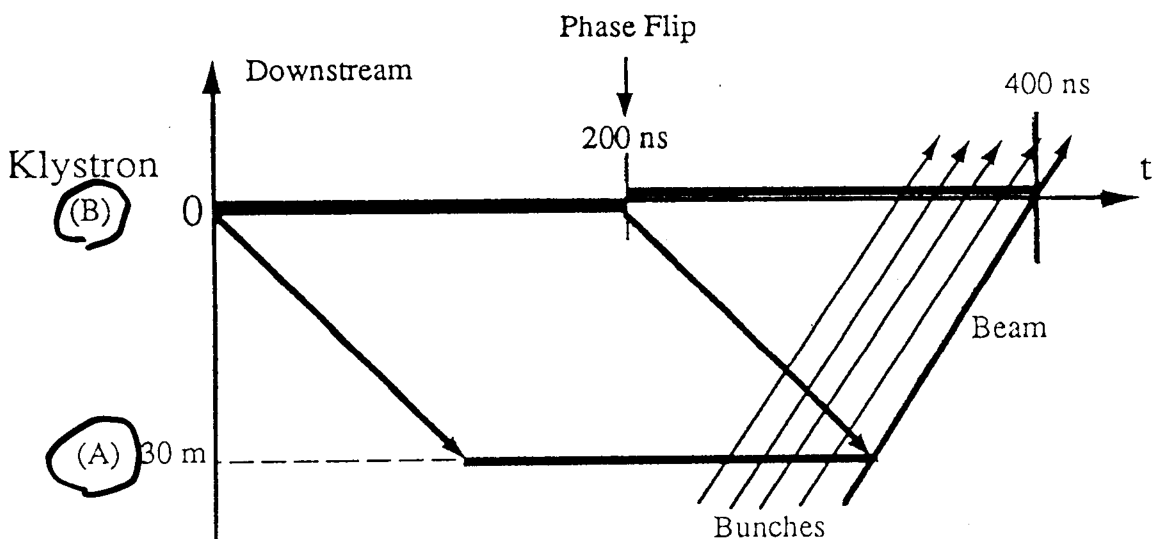

図 2　A Railroad Diagram of RF Distribution

X3 or X4 Delay Line Scheme

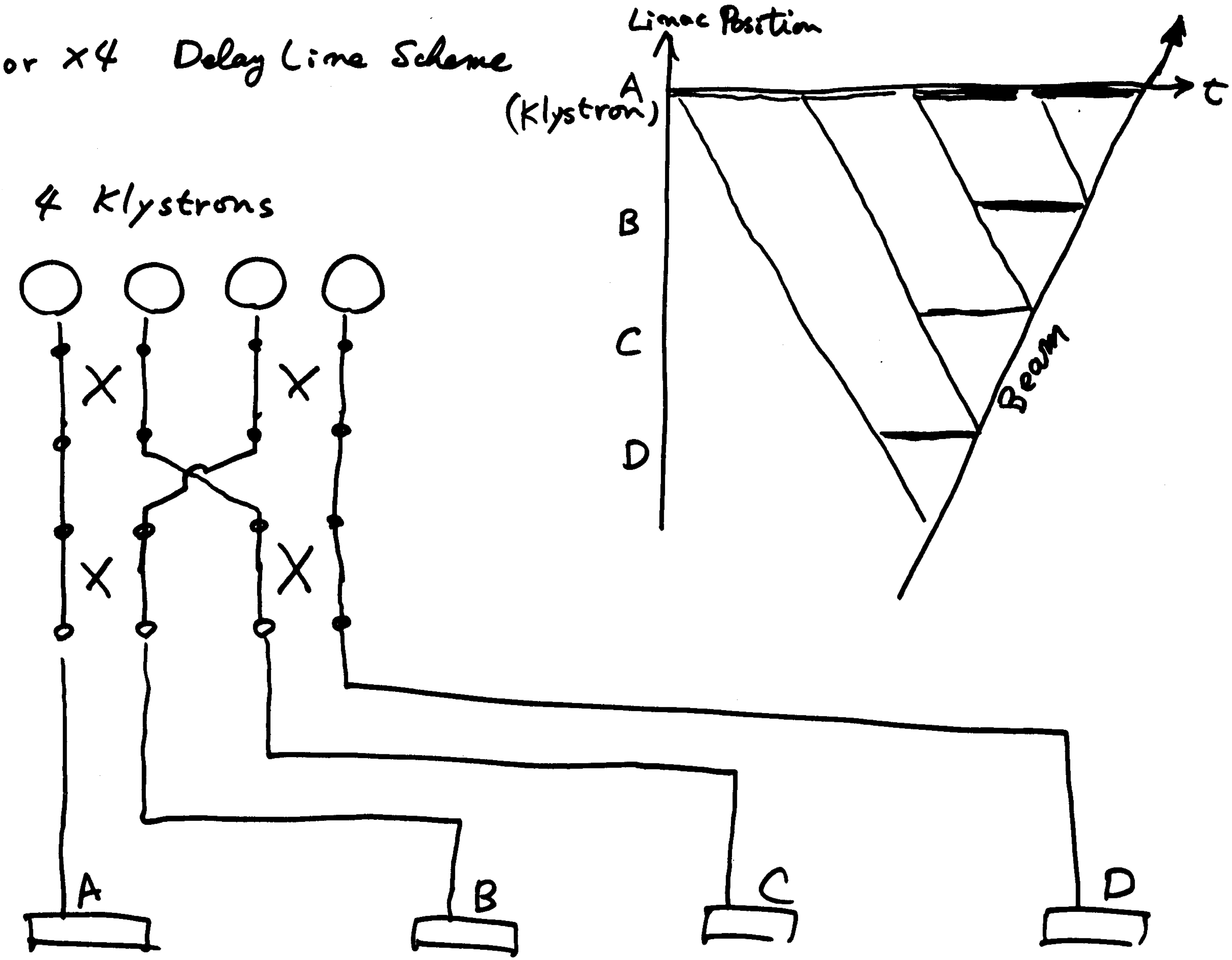

Table-1)

Transfer losses in the waveguides*

1)TE01 mode

Waveguide (Diameter)	Loss (dB/m)	Vg/c	Line loss (200ns)
51mm	1.3e-2	0.7733	8.02%
69mm	4.5e-3	0.886	2.82%
118.1mm	8.3e-4	0.9625	0.56%

2)TE11 mode

Waveguide (Diameter)	Loss (dB/m)	Vg/c	Line loss (200ns)
51mm	1.22e-2	0.9626	7.93%
69mm	8.44e-3	0.9748	5.60%
118.1mm	4.7e-3	0.9951	3.18%

*The loss in the system is 1/2 of these values.

Conclusion

1)A factor 2^n RF pulse compression equivqlent system can be constructed without any RF power storage devices such as a cavity or cavities.

2)In case of the X-band linear colliders, this system can have very high efficiency. The energy loss in the delay line is less ththan 2%, while an ordinary RF pulse compression system may suffer energy loss of about 25% or even more.

3)No narrow band component such as an energy storage cavity is necessary. therefore this system can be as flexible as aconventional electron linac RF power system.

4)Practically, factor x2 or x3 equivalent system are preferable, therefore, the number of klystrons must be 2 or 1.5 times more.

5)A 500nsec class modulator and the pulse transformer system could ahieve more than 75% efficiency.

NLC RF Parameters

	500 GeV		1.0 TeV		1.5 TeV
Active Str. Length(1) (km)	13.5	10.7	16.2		24.5
Accelerating Gradient(2) Unloaded/Loaded (MV/m)	50/37.3	60/44.8	85/63.4		85/63.4
Input Power to Str.(2) (MW/m)	50	72	145		145
No. 7.2m RF Stations(3)	1877	1487	2254		3404
Particles per Bunch (10^{10})	0.65	0.78	1.10		1.10
Repetition Rate (Hz)	180		120		120
Bunches per RF Pulse	90		75		75
RF Pulse Length(4)	240		220		220
Pulse Compression System	SLED-II (x5)		SLED-II (x5)	BPC (x8)	BPC (x8)
Power Gain/Comp. Efficiency(5)	3.6 / 72%		3.6 / 72%	7.2 / 90%	7.2 / 90%
Klystron Pulse Length (μs)	1.20		1.10	1.76	1.76
Klystron Efficiency	60%		65%		65%
Peak Pwr. per RF Station (MW)	100	145	289	145	145
No. Kly. per Station @ Peak Pwr. (MW)	2 @ 50	2 @ 72	4 @ 72	2 @ 72	2 @ 72
Total No. Klystrons(6)	3754	2974	9016	4508	6808
Modulator Efficiency(7)	PFN @ 75%		PFN @ 80%		PFN @ 80%
Energy per Pulse per Station(8) (J)	267 ~~278~~	385 ~~401~~	611	489	489
Net RF System Efficiency	32%		37%	47%	47%
Wall Plug Power(9) (MW)	90	103	165	132	200

Status of Klystron R&D

XL series: $K_\mu = 1.2$, $V_0 = 440\ kV$

	Achieved XL1	Achieved XL2	Jan '95 XL3
Output structure	3 cell SW		4 cell TW
Output Power (MW)	50 (58)	50	85 (simulation)
Pulse Length† (μs)	1.5 (0.4)*	1.5	1.5
Efficiency (%)	37 (42)	36	54 (sim.)

* Limited by TE_{11}-mode oscillation (3 penultimate cavities tuned to same frequency)

Windows

TE_{01} TW window using isostatic pressed ceramic
Reached 100 MW in resonant ring at 60 Hz
In progress: 50 MW (and still going up) at 120 Hz

† 1.5 μs needed for x 6 pulse compression in NLCTA
1.2 μs design value for 500 GeV NLC

XL1 Klystron

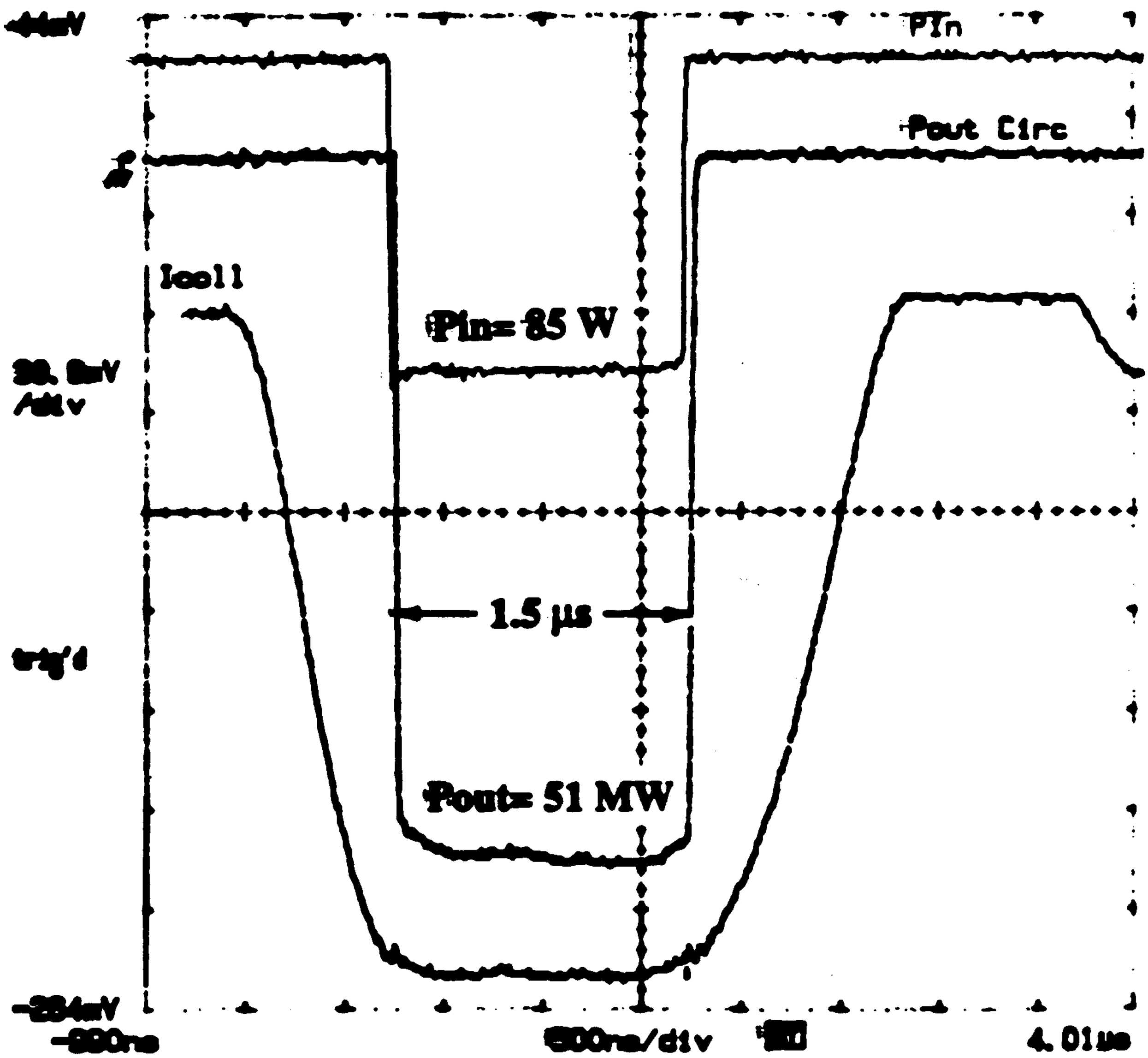

Vo= 440 kV
Io= 332 A
fo= 11.455 GHz
Efficiency= 34.9 %

FREQUENCY	SATURATED OUTPUT POWER
11.420 GHz	47 MW
11.4266 GHz	50 MW
11.440 GHz	52.5 MW
11.460 GHz	52.7 MW
11.480 GHz	47 MW

60 PPS
WINDOW ΔT ≈ 25 °C

PPM - Focused Klystron for NLC

5 cell TW output circuit
short magnet period
$K_\mu = 0.6$

Simulated results at $V_0 = 470$ kV

- $P_{out} = 55$ MW
- $\eta = 66\%$

Beam stick ready ≈ May '95
will test both immersed + Brillouin flow

Video available (K. Eppley)

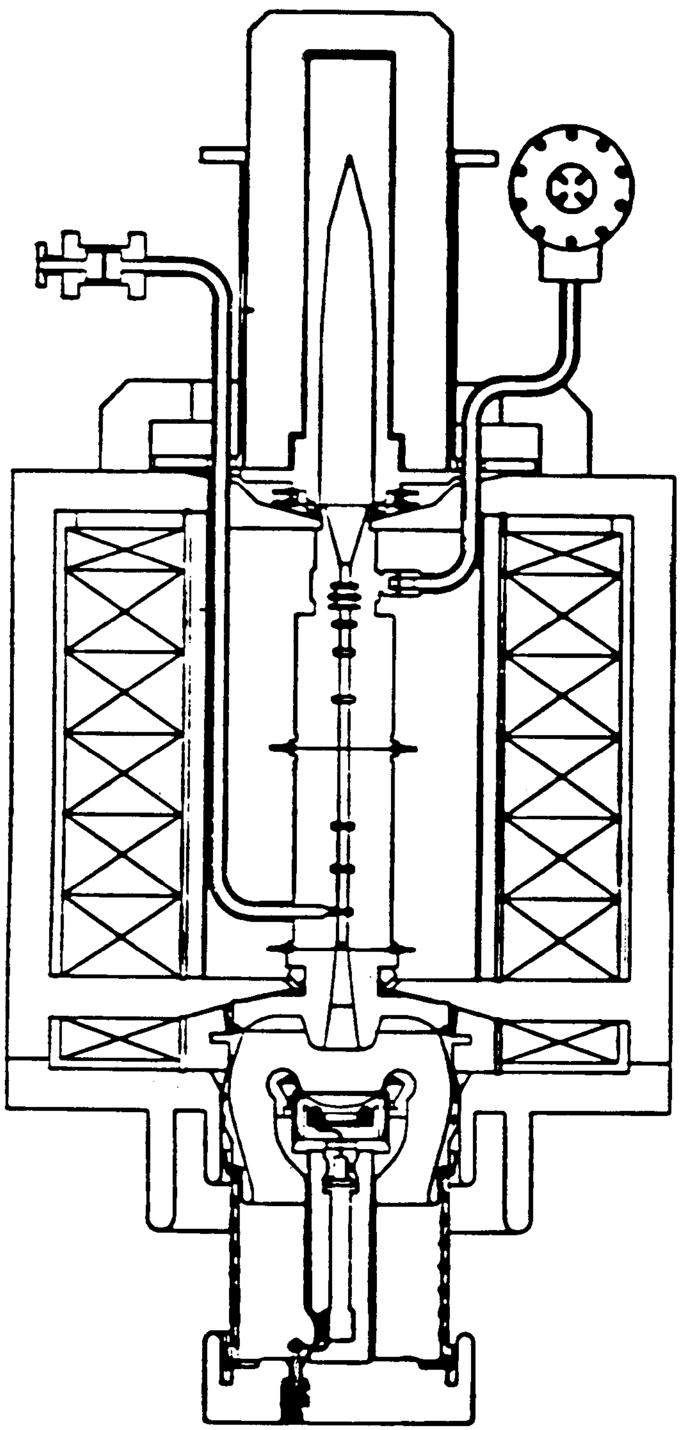

XL1

SOLENOID POWER: 24 KW

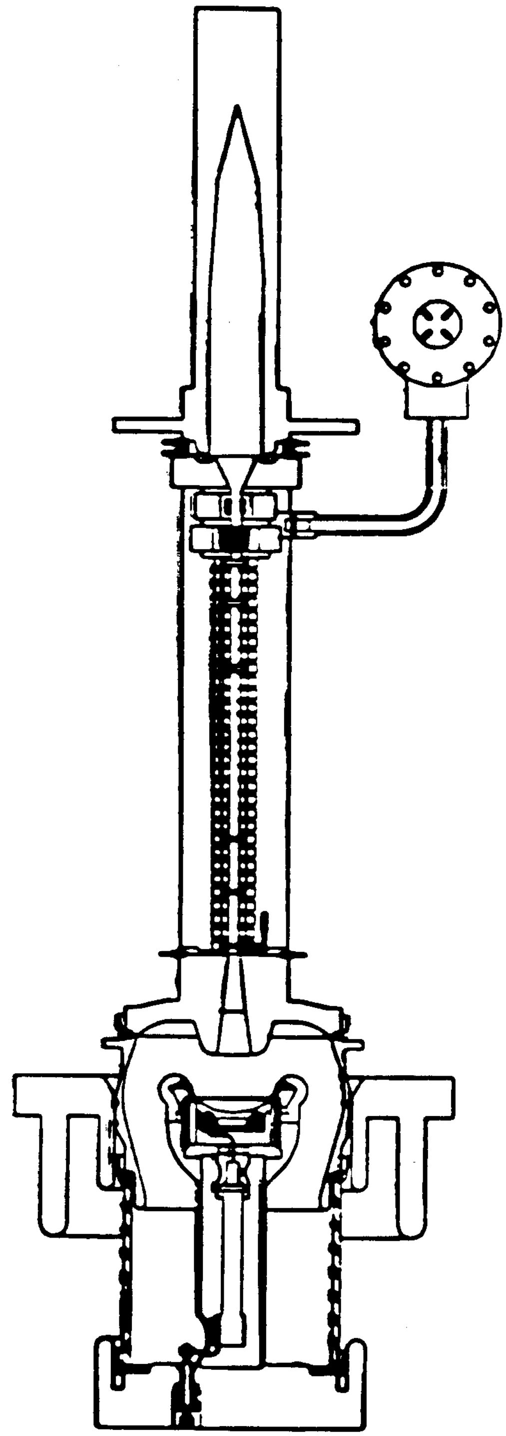

PPM FOCUSED DESCENDANT

NO FOCUSING POWER

Modulators

	n	$T_K(\mu s)$	$V_{ch}(kV)$	$V_o(kV)$	η_E	η_{tot}
Existing						
5045	15:1	3.6	46	345	0.74	—
DESY Kly.	23:1	2.1	46	525	0.60	—
XC Kly	20:1	0.9	46	460	0.50	—
In Progress						
NLC TA (1)	24:1	1.6	48	580	0.70 (sim)	—
Cassel (2) 3-stage	6.5:1	1.0	65	600	0.80 (sim)	—
? Future						
NLC (3) 2-stage	8:1	1.2	67	535	0.80	0.75
1.0 TeV (4) 2-stage	6:1	3.5	70	420	0.85	0.80

(1) Designed for 2×100 MW klystrons

(2) Ready for high power tests ≈ Feb. '95

(3) For PPM-focused tube: $K_\mu = 0.6$, $\eta = 0.6$, $\hat{P} = 75$ M

(4) For klystron matched to a X16 BPC system: $K_\mu = 0.5$, $\eta = 0.70$, $\hat{P} = 40$ MW

Overmoded TE_{01}-mode Components

Based on flower petal mode converter

$\frac{1}{2}$-1% loss 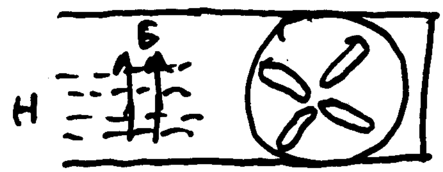 } narrow wall of rectangular guide

Rt. ∠ bend = 2 FP's + rectangular bend 1%

3db coupler = 4 FP's + rect. hybrid 2%

4.75" delay line 1.3% / μs

WC 293 transmission line .06% / meter

WR 90 1% / meter

Flower petal tested to 150 MW in ASTA

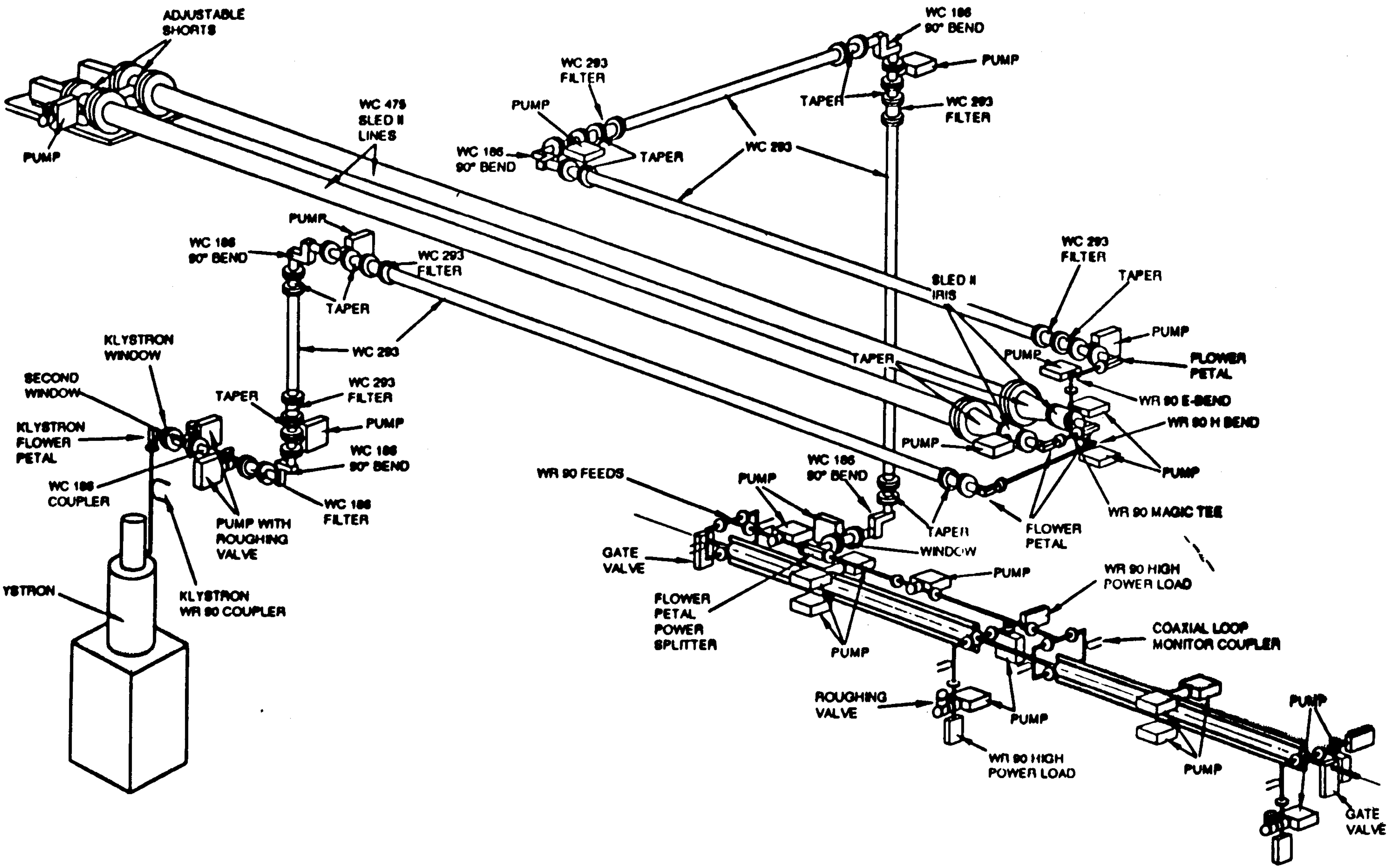

UNLESS OTHERWISE SPECIFIED ALL DIMENSIONS IN INCHES TOLERANCES: .X ± .02, .XX ± .01, .XXX ± .005 ANGLES ± .1° INTERNAL CORNERS .015 R MAX SURFACE FINISHES 32/ MAX	STANFORD LINEAR ACCELERATOR CENTER ENGINEERING SKETCH
	ISOMETRIC VIEW OF NLCTA HIGH-POWER RF DISTRIBUTION SYSTEM FOR ONE STATION
PREPARED BY K HOAG	SK - HH - 850 - R2
	5 - 17 - 94

RF Pulse Compression Parameters for ASTA and NLCTA

	ASTA		NLCTA
	Achieved	Planned	Design
Klystron peak power	32 MW	50 MW	50 MW
Klystron pulse length	0.9–1.05 μs		1.5 μs
Accelerator pulse length	0.15 μs		0.25 μs
Compression ratio	6–7		6
Intrinsic SLED-II efficiency	75–70%		75%
Inefficiencies due to component losses			
Delay line	−3%*		−4%*
Mode transducer (R.T. loss)	−2%		−2%
Magic Tee (R.T. loss)	−7%	−1%	−1%
Non-optimal reflection coef.	−(8–5)%	—	—
Net efficiency due to component losses	80–83%	94%	93%
Net SLED-II efficiency	60–58%	70–66%	70% *
Power gain	3.6–4.1	4.2–4.6	4.2

*Mode conversion losses equal to wall losses (−5%/μs).

x 85% transmission efficiency
net P.C. efficiency = 0.6
Power Gain = 3.6

TLL 7/13/94

UPGrades to 1.0/1.5 TeV

Higher Klystron Power

$2 \times 72 = 144$ MW sheet beam klystron

Low K_μ per □ ⇒ $\eta > 65\%$

Grid Switched Klystron

$\eta \approx 90\%$?

More Pulse Compression

SLED-II with active switch
(Sami Tantawi)

X16 compression
1% RT Loss

$\left\{ \begin{array}{ll} \eta = .35 & \text{passive} \\ \eta = 0.8 & \text{active switch} \end{array} \right.$

X16 BPC with discrete cavities for delay line

$$Q_0 = \frac{25,800}{y^3 + \frac{1.2}{n}}$$

TE_{01} cavity copper

$y = 0.61\,\lambda/a$

n = no. wavelengths long

Can of course go superconducting -- Easy for TE_{01} mode cavities!

For the Future ??

Pulse compression

×16 BPC system with $\eta = 80\%$, $PG = 12.8$
uses 6 TE_{01} mode cavities / stage.

compact: ≈ 6m long × 2m high

Klystron

$T_K = 16 \times 220\,ns = 3.5\,\mu s$ $\quad K_\mu = 0.5$, $\eta = 0.70$

$$P_K = \frac{1}{2} \times \frac{144\ MW/m \times 7.2\,m}{12.8} = 40\ MW$$

Modulator

Long pulse (3.5 μs), low output voltage (420 kV)
low turns ratio (6:1), high eff. $\eta \approx 80\%$

Net rf system efficiency

$$\eta_{Kly}(70\%) \times \eta_{mod}(80\%) \times \eta_{p.c}(80\%) \approx 45\ \%$$

XL '94 Dec
T. Higo

JLC X-band Structure

Present design & R&D principle

① Single bunch emittance growth

alignment ~10 μm → $\langle \frac{a}{\lambda} \rangle \sim 0.16$

② Multi bunch emittance growth

detuned : $w_0 \times \frac{1}{100}$ → 150 cell

⇒ Start fabrication study $\frac{\delta f}{f} < 10^{-4}$ alignment cell ~ a few μm

precise machining & bonding

③ XB-72k

130 MW 500 ns × 2 klystrons & power distribution

→ 130 MW / structure 250 ns

∴ $T_f \sim 120$ ns $n T_b \sim 120$ ns

$\langle E_{NL} \rangle \sim 73$ MV/m

$\langle E_{LD} \rangle \gtrsim 50$ MV/m (?), $L_{acc} \sim 20$ km for 1 TeV.

---

detuned ; medium damping ?

choke mode : initial / operational cost ? later

Dec. 94

941203
940216 T. Higo

JLC-X parameters

RF pulse Nb × tb + Tf = ~~90~~ × 1.4ns +Tf= ~~253~~ nsec
Field E_{NL} = ~~40~~MV/m, E_{LD} = ~~28~~MV/m

Detuned structure of a/λ=~~0.16~~ 0.166 with medium damping

Frequency	11.424	GHz	
<a/λ>	~~0.16~~ 0.166		a = 3.3 ~ 5.1
Number of cells	150		
Effective length	1.31	m	
Filling time	~~126.5~~ 106.4	nsec	
τ	~~0.69~~ 0.578		

E_{NL}	~~40~~ 73	MV/m	
(E_{LD}	~~28**~~	MV/m)	~~(JLC-I)~~
P_{IN}	~~23.8~~ 130	MW/structure	

Q0	6550 ~ 6750		
Qex	< 2000		
Iris width	4	mm	⇒ Qex=1600
Iris height	2	mm	
$\sigma f_{d_1} / f_{d_1}$	~~2.4~~ 2.24	%	gaussian sigma *
$\Delta f_{d_1} / f_{d_1}$	~~12.5~~ 11.2	%	total distribution *
$\pm 3\ \sigma f_d / f_d$	$<10^{-4}$		incase Qex=∞

Cell alignment	~1	µm
Cavity alignment	~10	µm

To realize the damping of the wake field down to a few % during 126ns
QL should be < 1500 ----> since Q0 = 6600 ---> Qex = 2000.
Iris width w = 3.5 ~ 3.8 mm to obtain Qex=2000.
If iris width w=4mm ----> Qex=1600 in ideal matched case.
----> No degradation of accelerating mode
Qex=1600 --> 2000 when $|\Gamma|$ = 0.45 (VSWR = 2.6)
Disk thickness 2mm (K. Bane ! to 2mm for higher modes > 1st & 2nd)
** artificially cited from JLC-I and should be calculated.

		f	σf	Δf
*	1st mode	15.6 GHz	0.35 GHz	1.75 GHz
	6th mode	36.3 GHz	0.26 GHz	1.30 GHz

X-band structure studies at KEK

[1] Fabrication of 30cm CZ structure

"Establish reliable fabrication technique"

• IHI	Au	890°C	10g/mm^2	'93
• NKC	Au	800°C	5g/mm^2	Apr.'94
• MHI	Ag-plating	800°C	3g/mm^2	vac leak !!
• MHI	Cu-Cu	800°C	3g/mm^2	Dec. '94

[2] Fabrication of 1.3m detuned structure

Fabrication of full size structure $< a/\lambda > = 0.166$

---> gaussian detuned in 1st and 6th dipole modes
---> machining of 150 different cells
---> study the frequency controllability
---> high field characteristics
E_{av} = 73 MV/m at Pin = 130 MW)

•1.3m [#1] with damping port without load
---> fabrication with
damping / vacuum port milling ~1µm
good alignment of cells < a few µm

•1.3m [#2] without damping port
---> check vacuum 10^{-8}Torr inside --> need baking, material?
---> wake feild measurement (ASSET) if calculation precise
→ fab. machining & joining by company

[3] Precision machining of cells for SLAC 1.8m structure

→ fine machining & brazing

[4] High field experiment

- 20cm-long structure (CERN)

    ---> further conditioning the CERN structure
    at >100MV/m and >100ns
    peak acclerating field = 100 MV/m at 30 MW

- 30cm-long structures

    ---> high power performance of diffusion bonded structure
    peak acclerating field = 100 MV/m at 131 MW

- 1.3m-long structures

    ---> high field characteristics of full-size structures
    ---> average acclerating field = 73 MV/m at 130 MW
    ---> dark current, amount, emittance, multiplication
    ---> VAC level inside structure
    ---> break downs, fault rate

[5] Wake field related studies

---> in order to confirm the idea of "detuned structure"

- developement of wake field calculation
  for practical design

  treatment of rounded beam holes
  coupler cells
  how to damp through medium damping ports

- trial of electrical measurement

  for checking the calculation

- measurement using ASSET at SLAC

  1.3m structure
  with medium damping
  or without damping port (pure detuned)

- estimation of tolerances

  considering beam dynamics with corrections

Cells for MHI 30cm structure

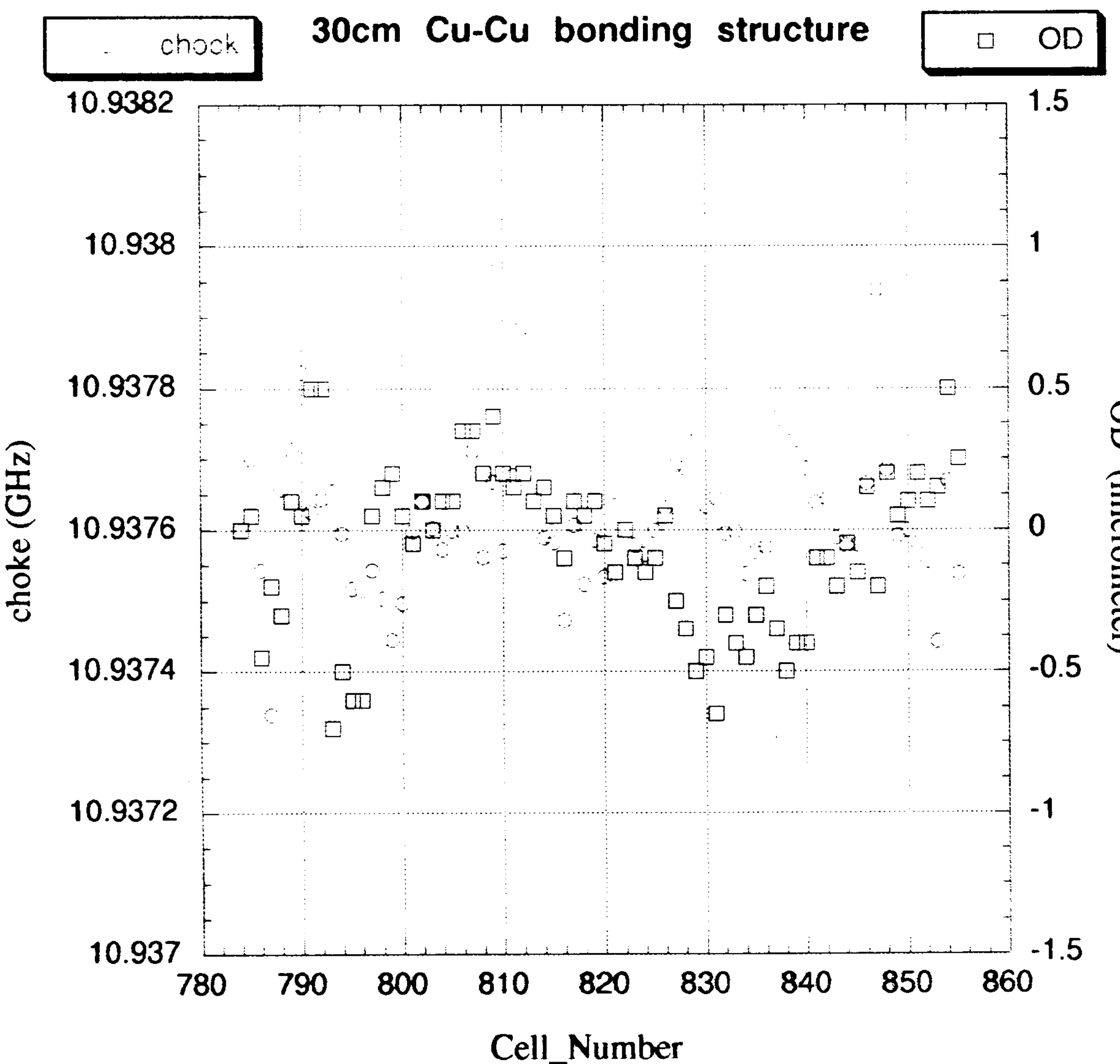

$\frac{\partial f}{\partial 2b} = -0.47$ MHz/μm

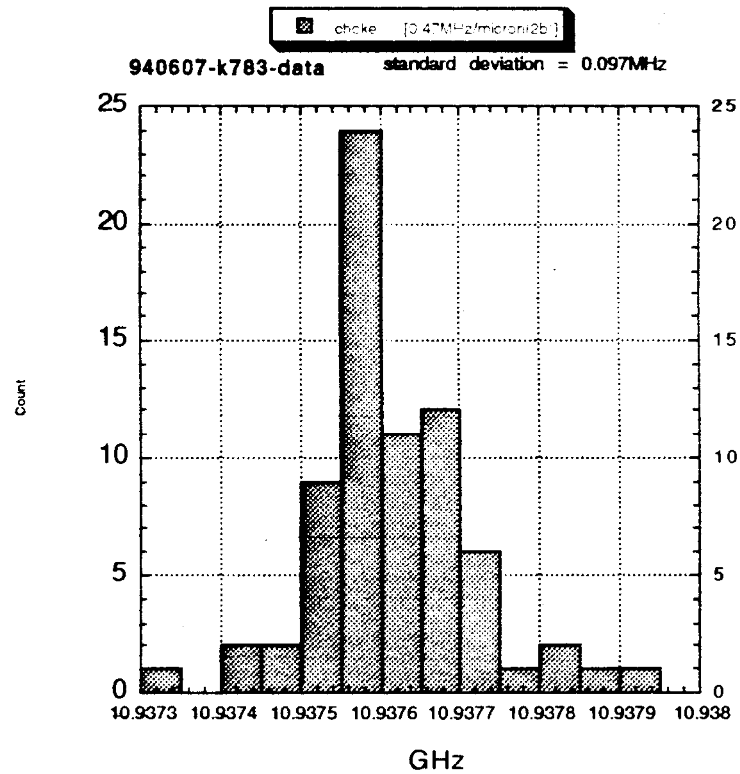
choke
940607-k783-data
standard deviation = 0.097MHz
25
20
15
10
5
0
Count
10.9373
10.9374
10.9375
10.9376
10.9377
10.9378
10.9379
10.938
GHz

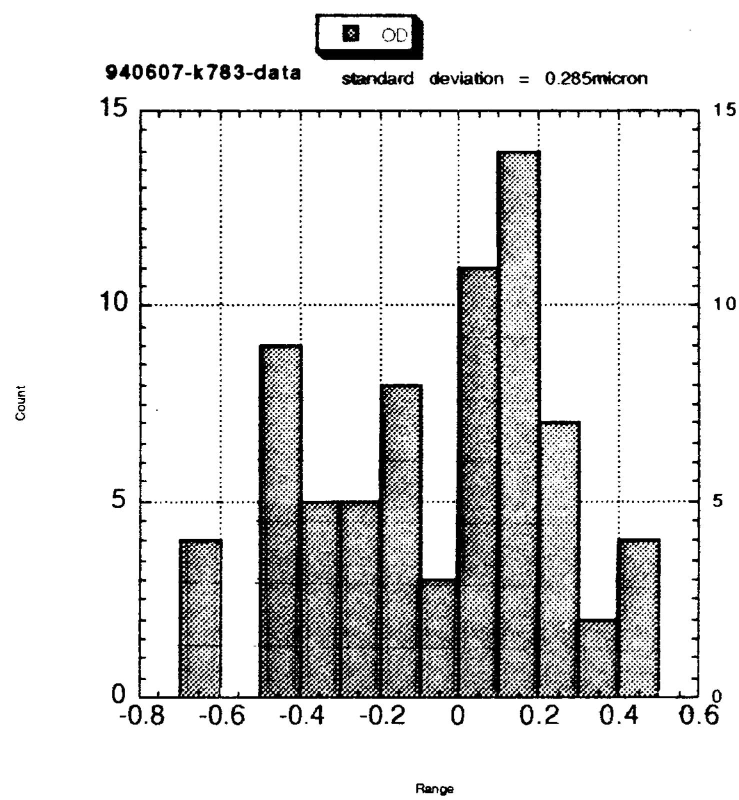
OD
940607-k783-data
standard deviation = 0.285micron
15
10
5
0
Count
-0.8
-0.6
-0.4
-0.2
0
0.2
0.4
0.6
Range

931005 T.Higo

Summary of MHI 17cell Ag-LTD bonding [redacted]

930916 T. Higo 700°C 1h

MHI 17cell measurement (each cell)
with dummy half cells
or with two plungers

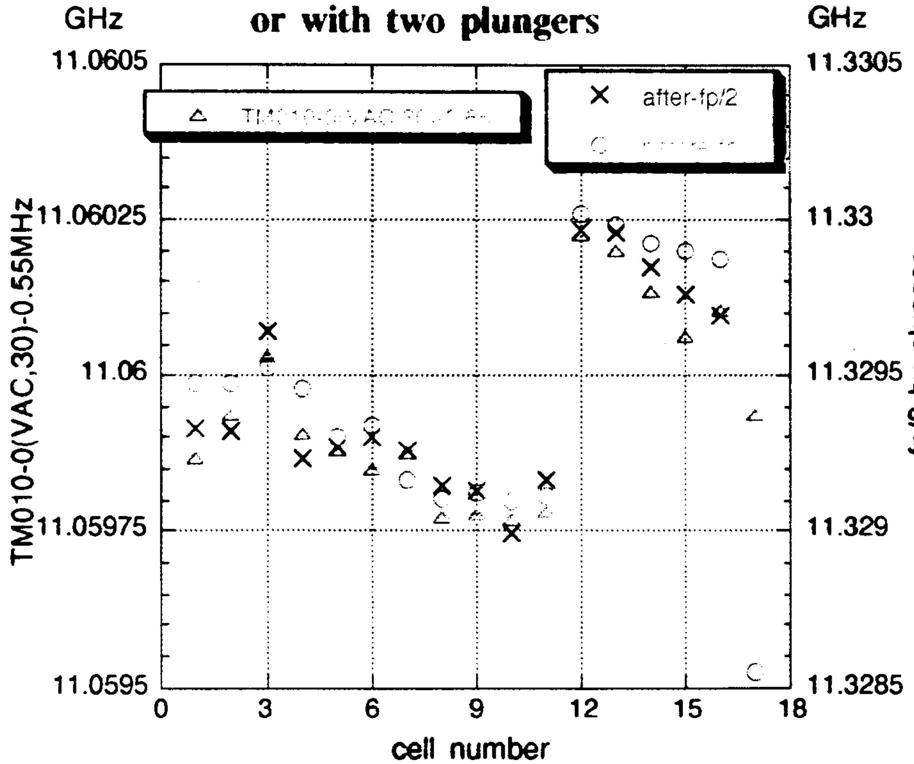

930812

17cell alignment after diffusion bonding

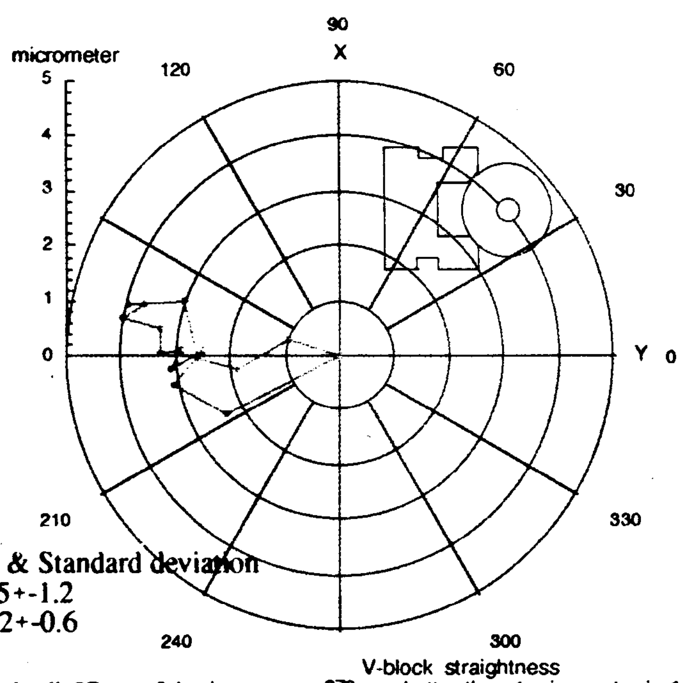

Mean & Standard deviation
x=-2.5+-1.2
y= 0.2+-0.6

machined cell OD = +-0.4 micrometer

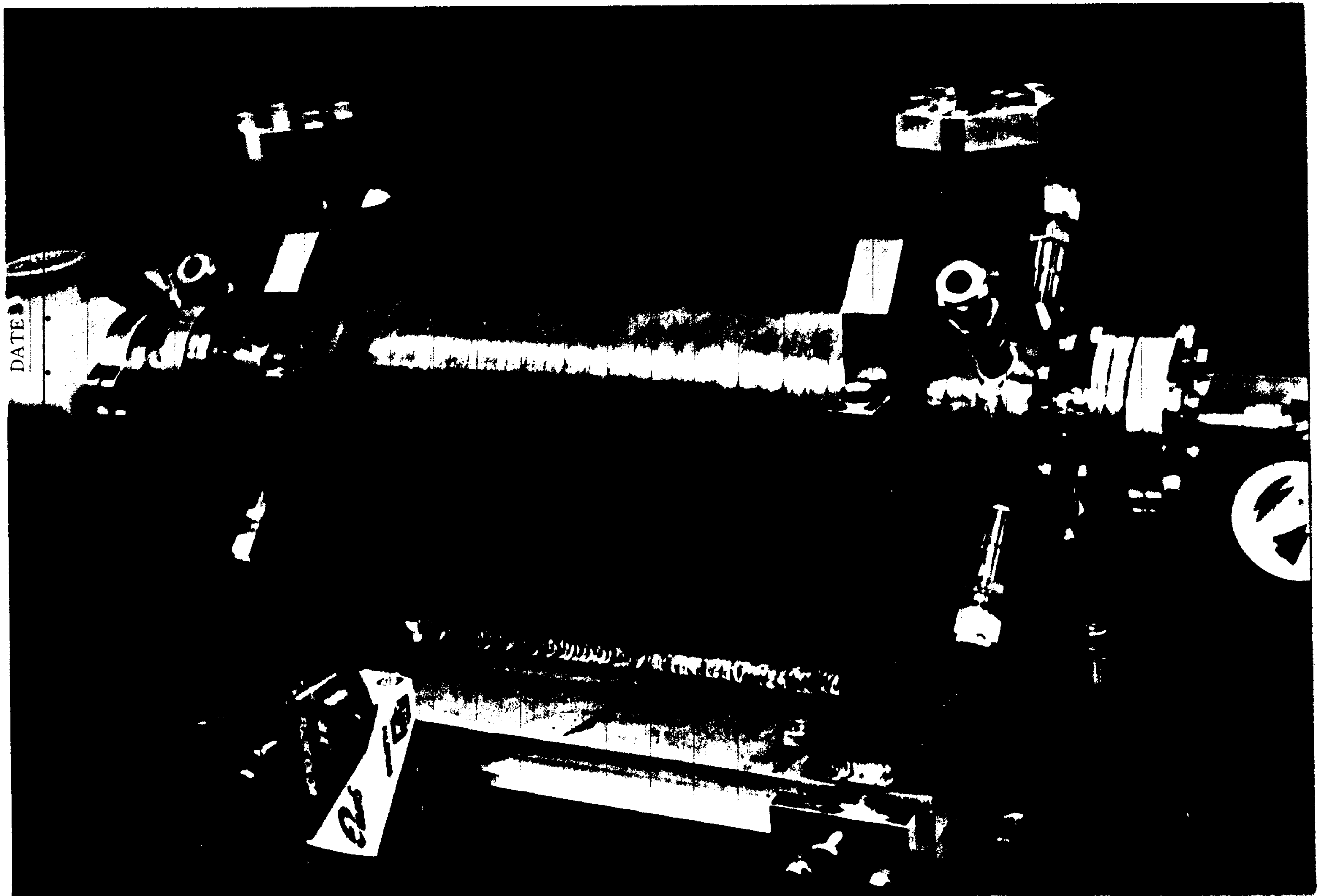

IHI Au 1μ Diffusion Brazing 30cm

930914 T. Higo

Summary of IHI 30cm structure

890° 1°min

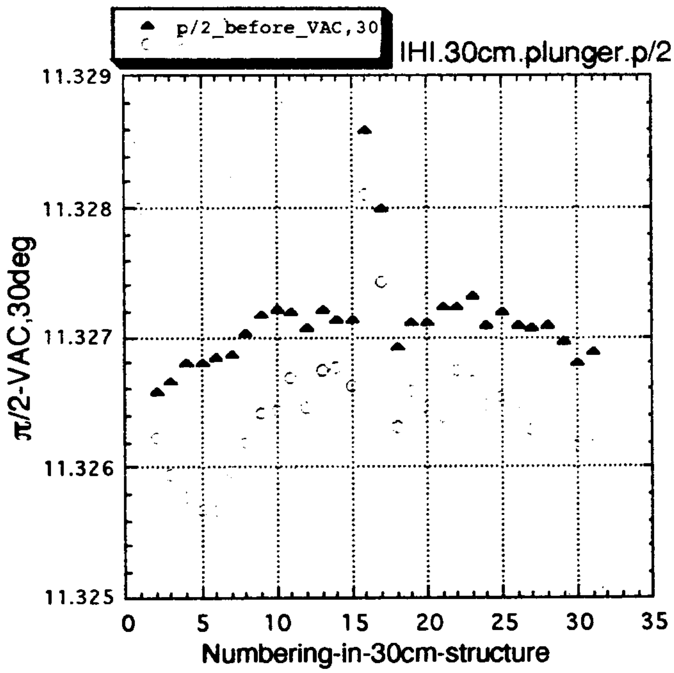

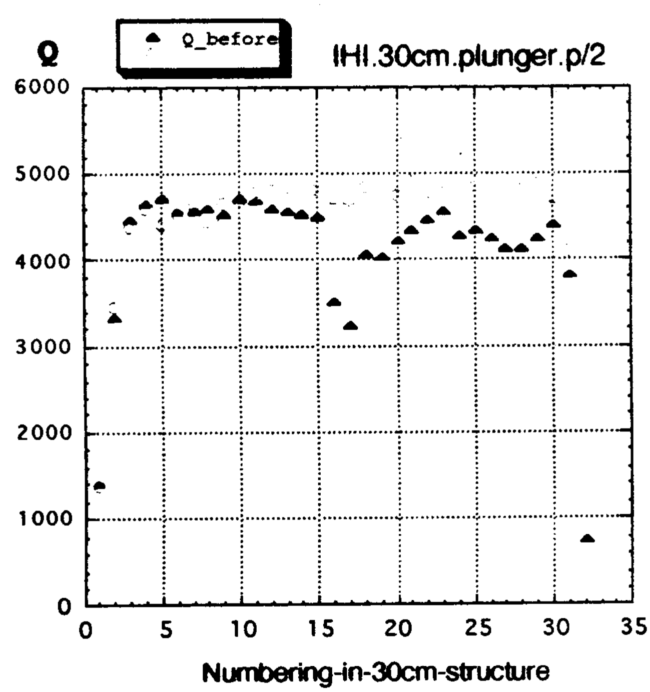

LC

931005 T.Higo

Results of alignment IHI 30-cm structure bonded by diffusion brazing 890° 10 min

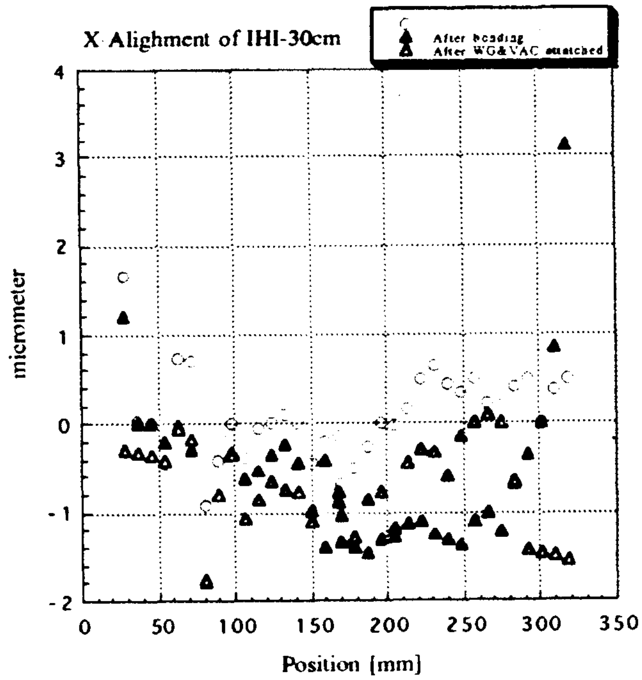

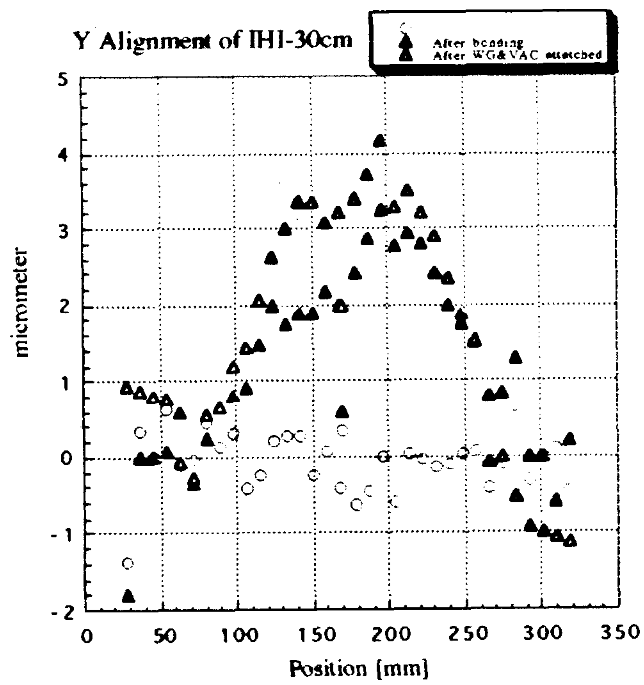

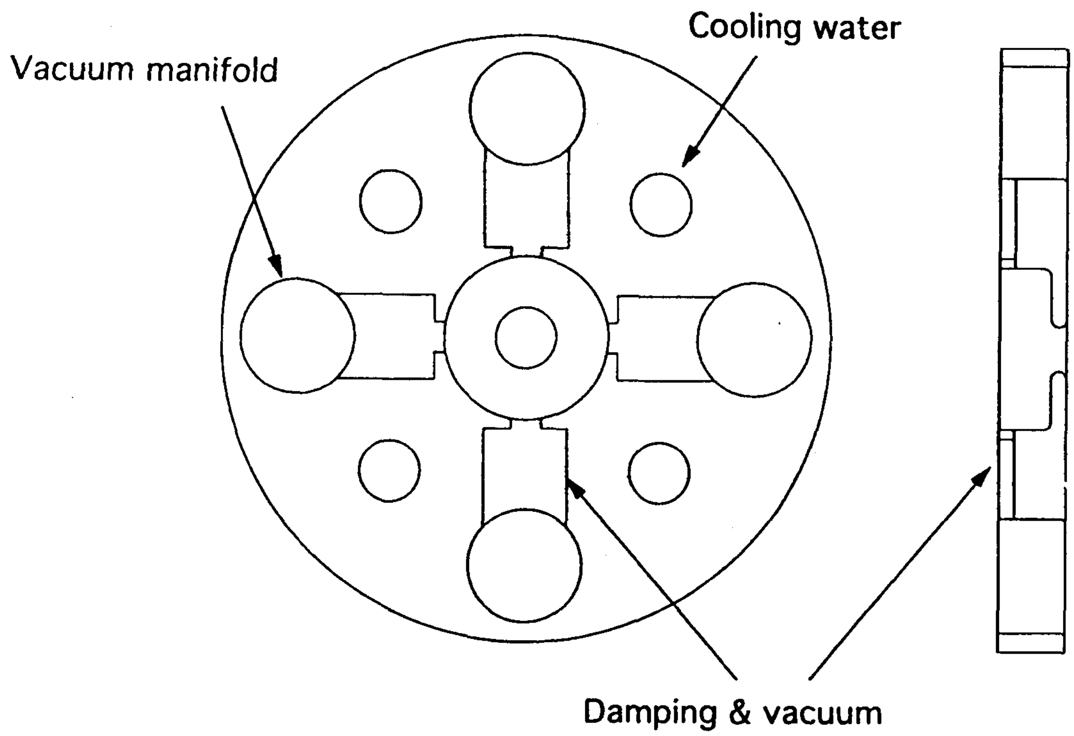

Schematic drawing of a regular cell

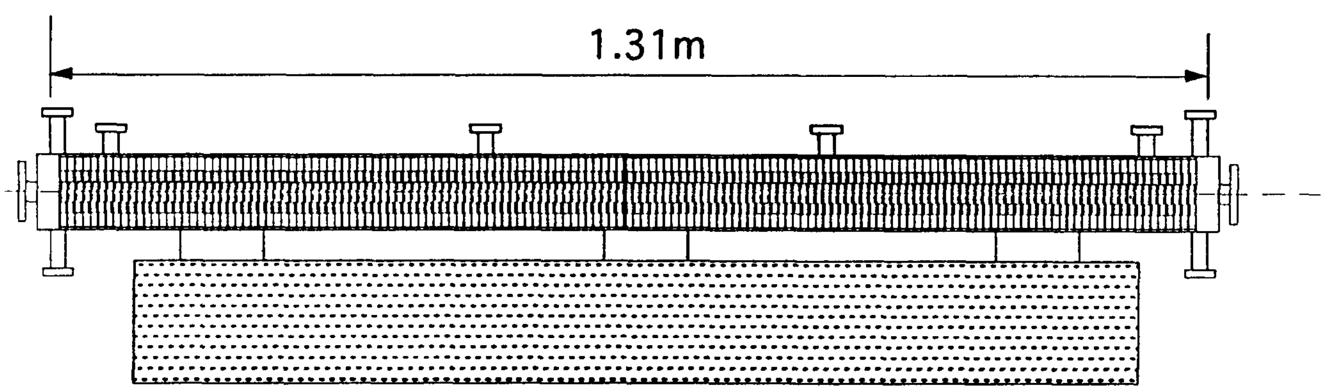

Schematic drawing of 150-cell detuned structure

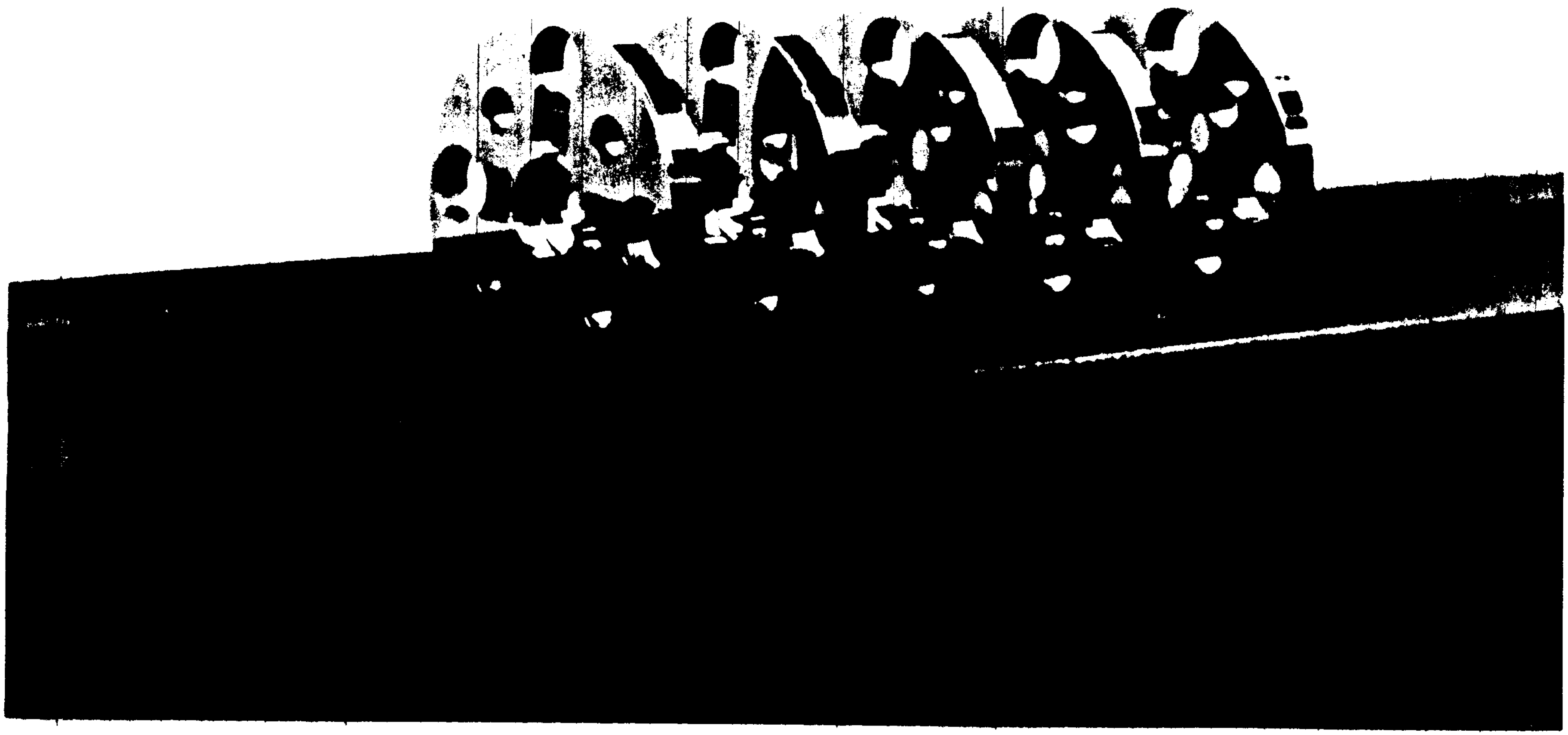

Regular cells for 1.3m Detuned Structure with Medium Damping

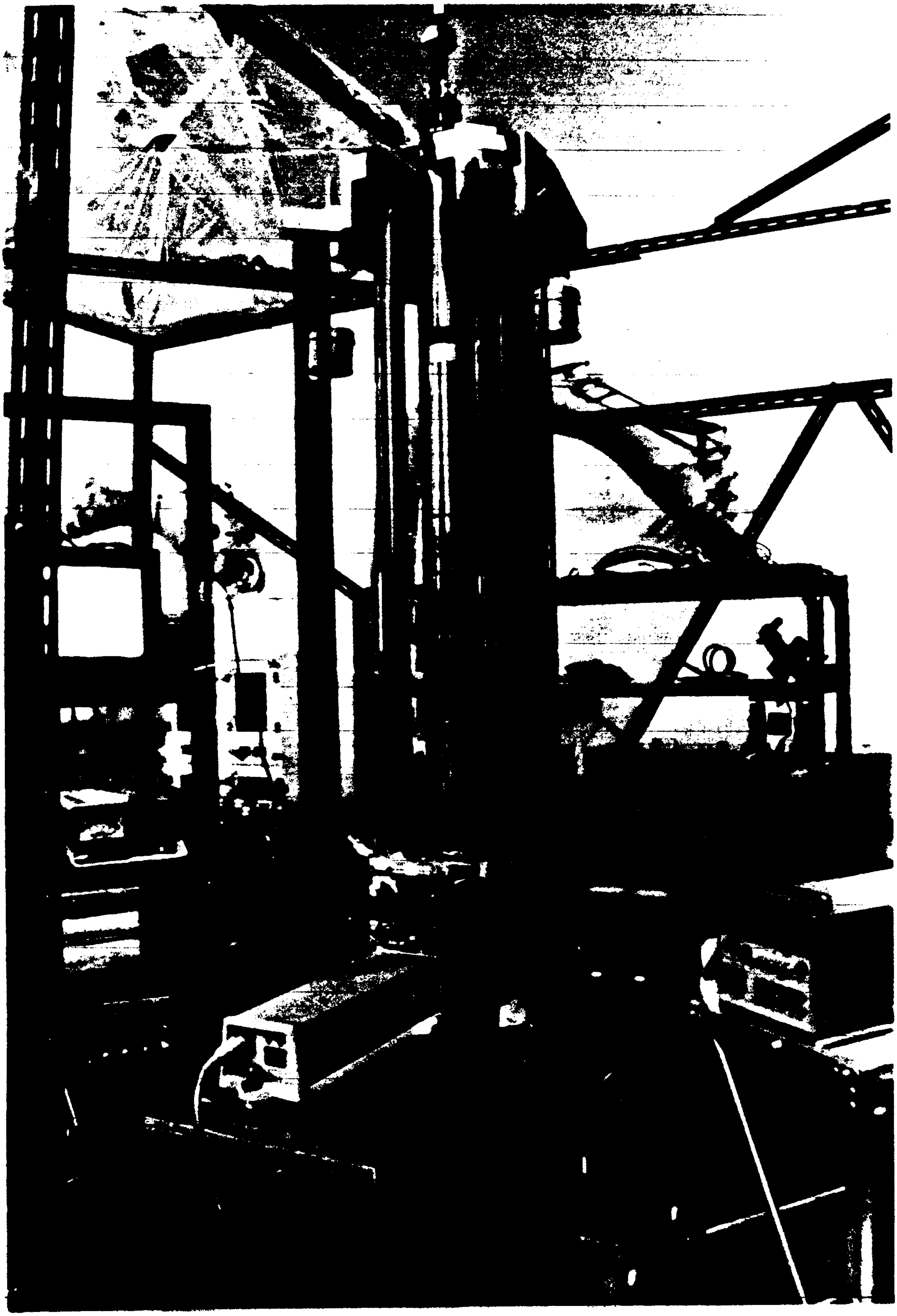

132 cell stack Aug. '94

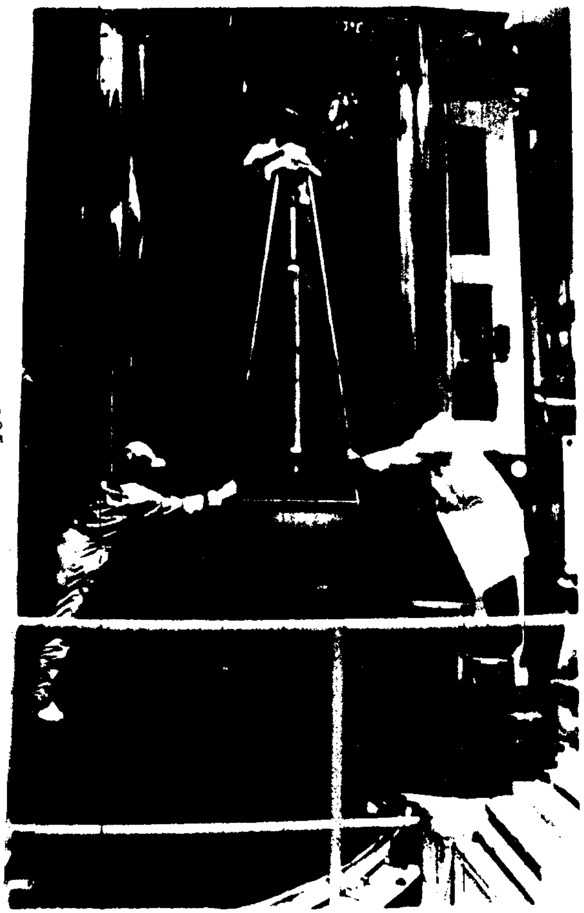

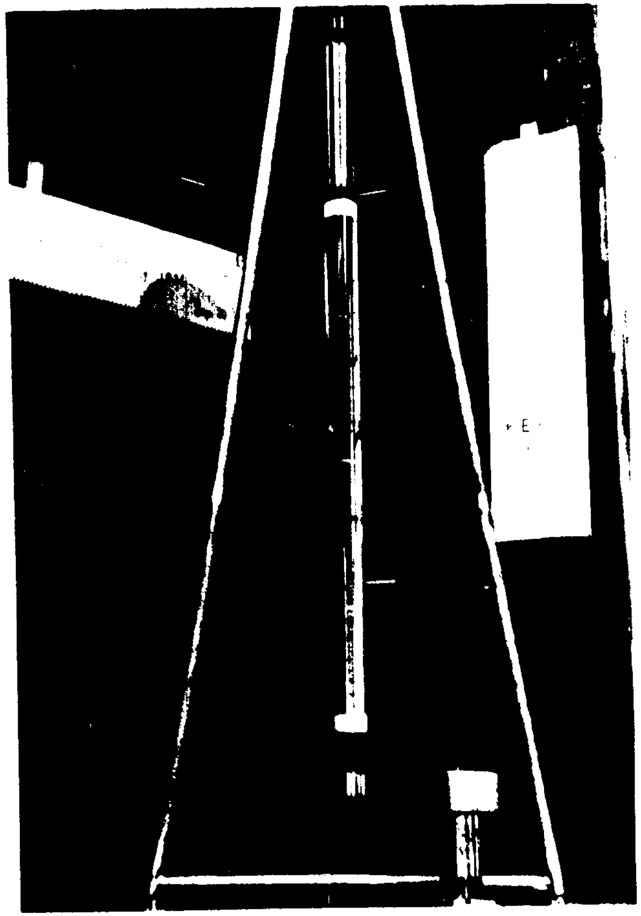

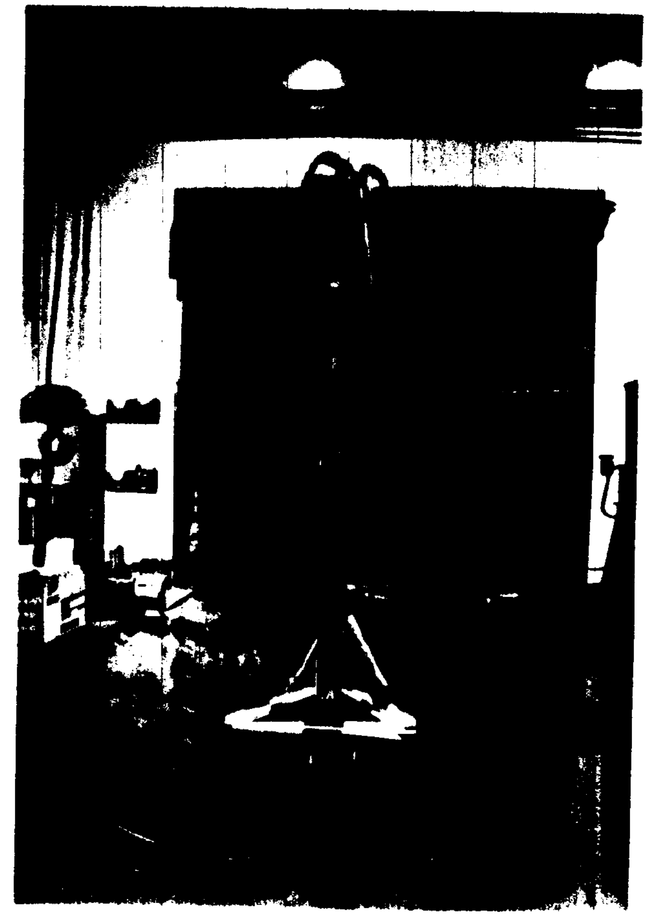

132. cell into furnace

Aug. '94

132 cell Cu-Cu diffusion bonding at 800°C 1hr.

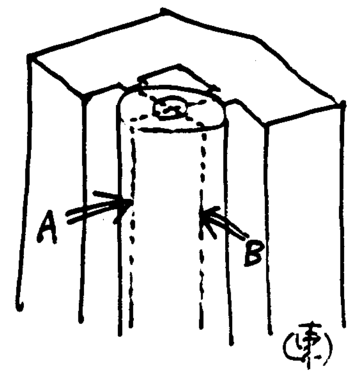

Xband Acc Tube (図1－1)

常温時と拡散接合１回のAの曲がり比較
点

Alignment (A)
曲がり量 (μm)

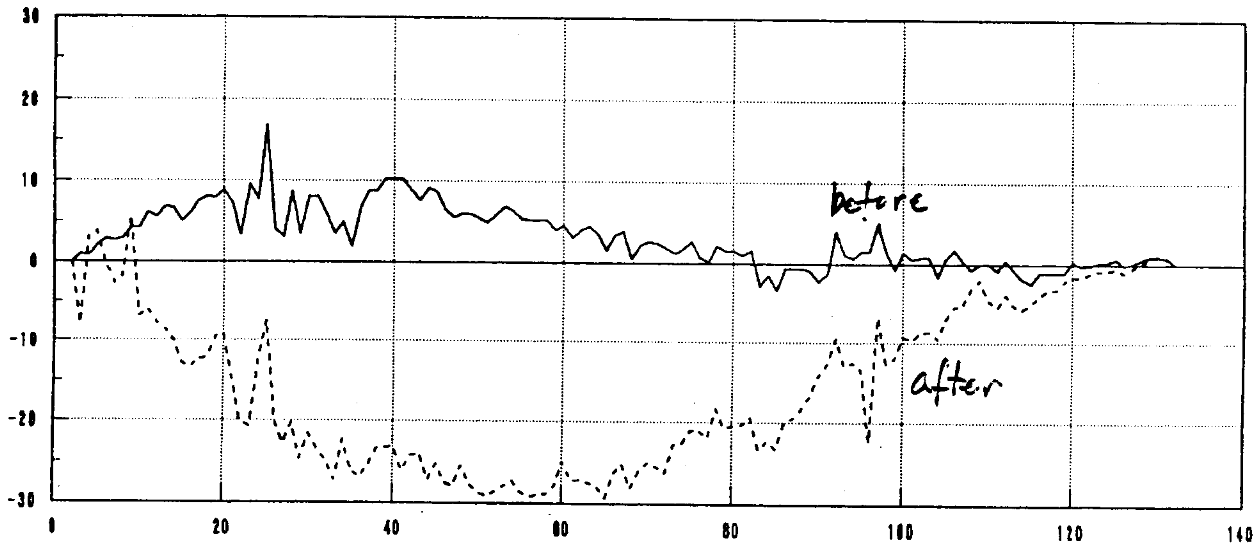

セル番号

常温時 拡散接合一回実施後

常温時と拡散接合１回のBの曲がり比較
点

Alignment (B)
曲がり量 (μm)

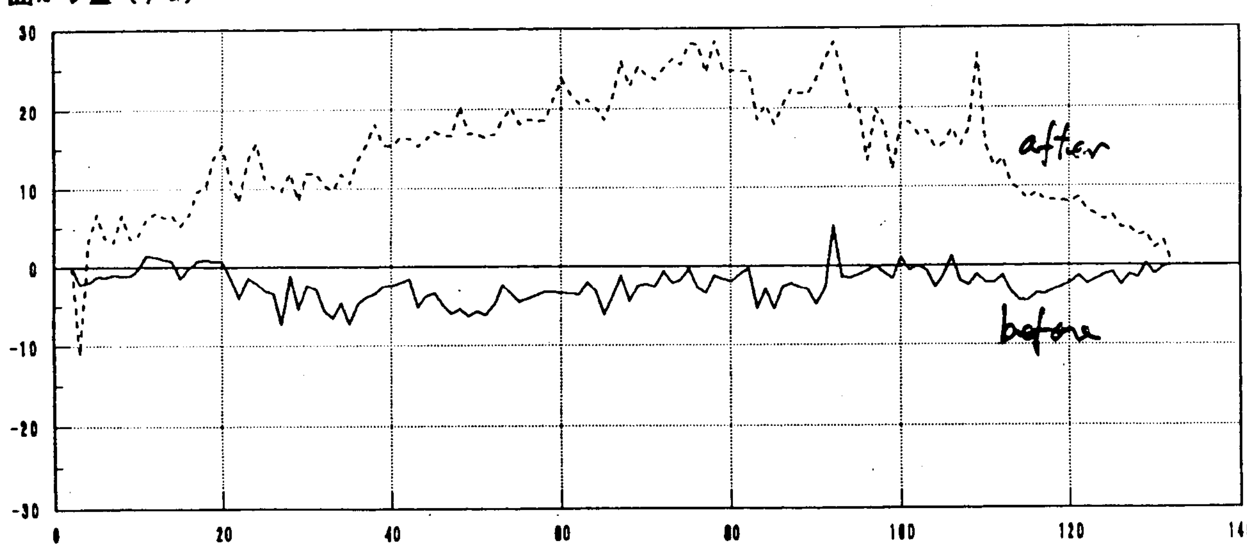

セル番号

常温時 拡散接合１回実施後

表1-2のデータ 表2-2のデータ

132 cell Cu-Cu diffusion bonding at 800°C 1hr.

~10kg weight, 3 g/mm² pressure

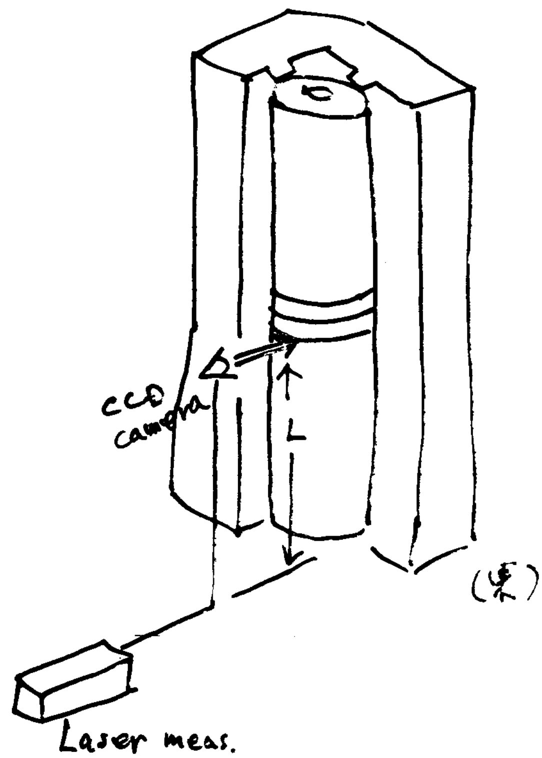

Xband Acc Tube (図2)

常温と拡散接合１回との差

長さの

$(L_{after} - L_{before})$

寸法差(mm) [mm]

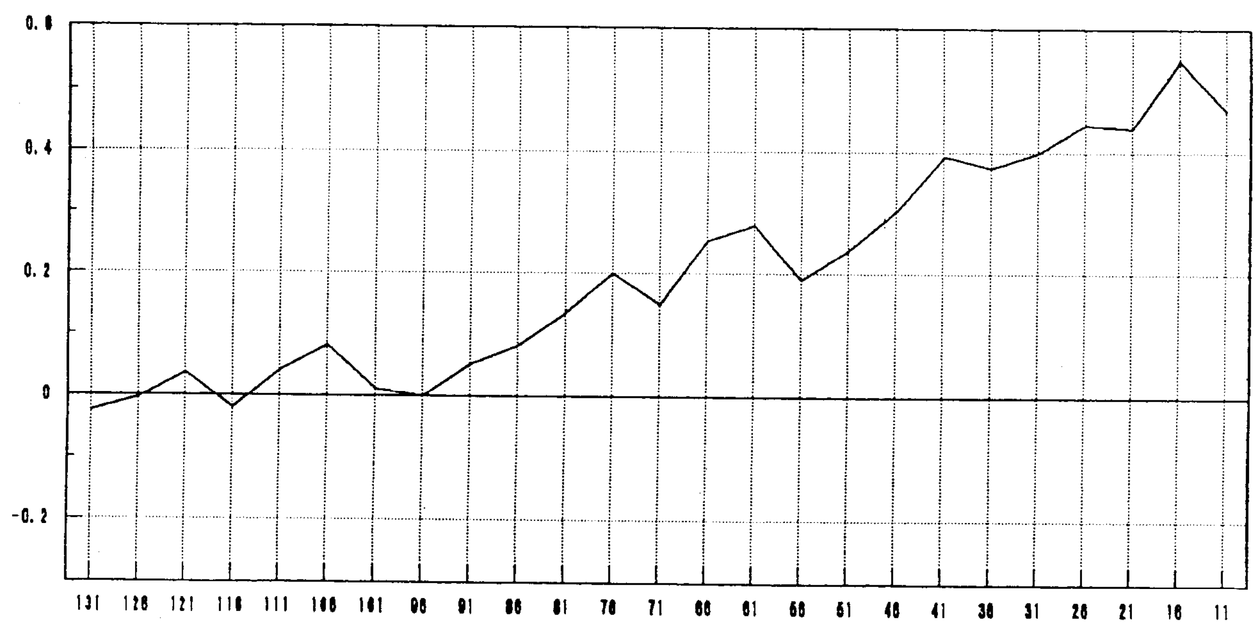

セル番号

注：セルNo132は１セル故使用せず

：表-3のデータ参照

'94 Dec

Summary on Precise Fabrication

① Machining cells

{ f_{acc} — $\sigma \sim 0.1$ MHz — full ± 0.5 MHz
{ OD — full $\pm 0.5\ \mu m$

OK.

② Alignment of cells — need fabrication of diff. cells.

• assembling
  10 ~ 30 cells ------- 130 cells
  a few μm — ~10 μm → will be better
• bonding ↓ ↓
  kept — <u>30 ~ 40 μm</u> (800°C, 1h)
  should be better. → 10μ or less

③ Shrinkage along z

(3 μm / junction or 3 μm / cell at 890° 10 min
(~500 μm / 132 cell at 800°C, 1h

need understanding of mechanism + perturbation to freq. on dipole modes.

④ Frequency Control.

δf_{acc}. (~0.1 MHz at 700°C
(~1 MHz at 890°C 10 min
(? 800°C 1h

temp. dep.
need summary of data.

δf_{d_1} ~ same as δf_{acc}.
δf_{d_2} or others : larger?
need control of hom in add. to f_{acc}.

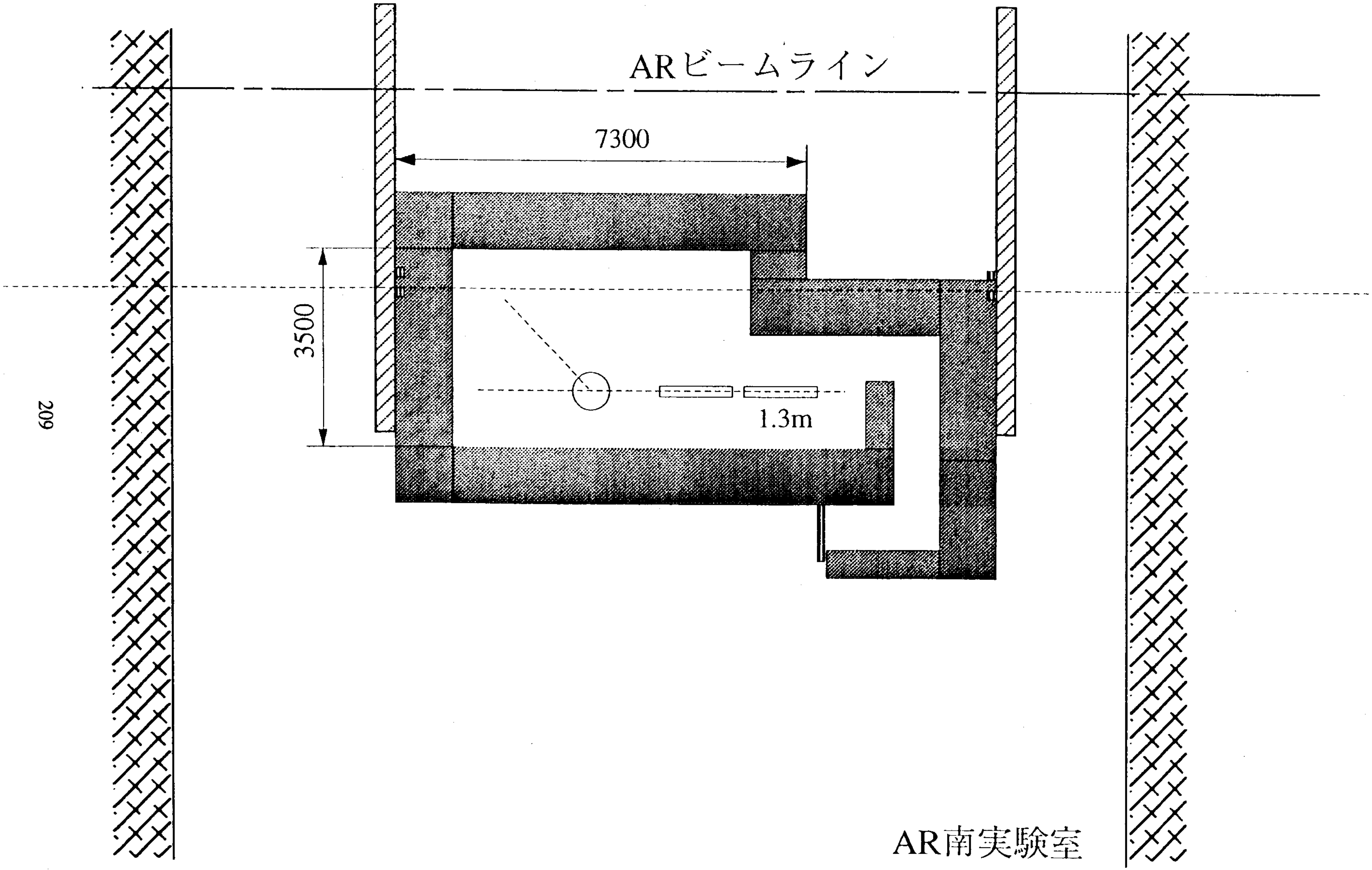
ARビームライン
7300
3500
1.3m
AR南実験室

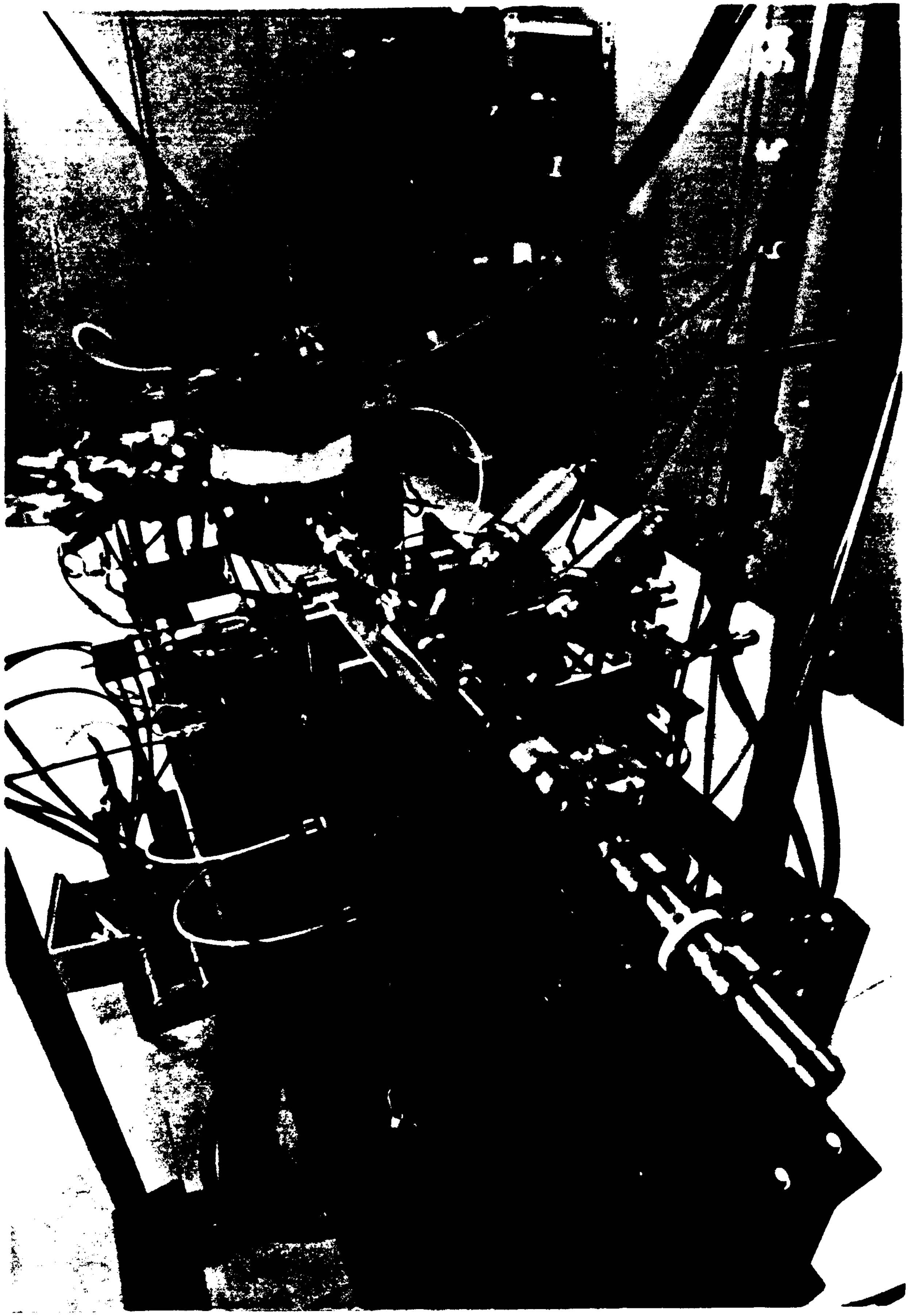

Accelerating Structure Test Setup   May '94

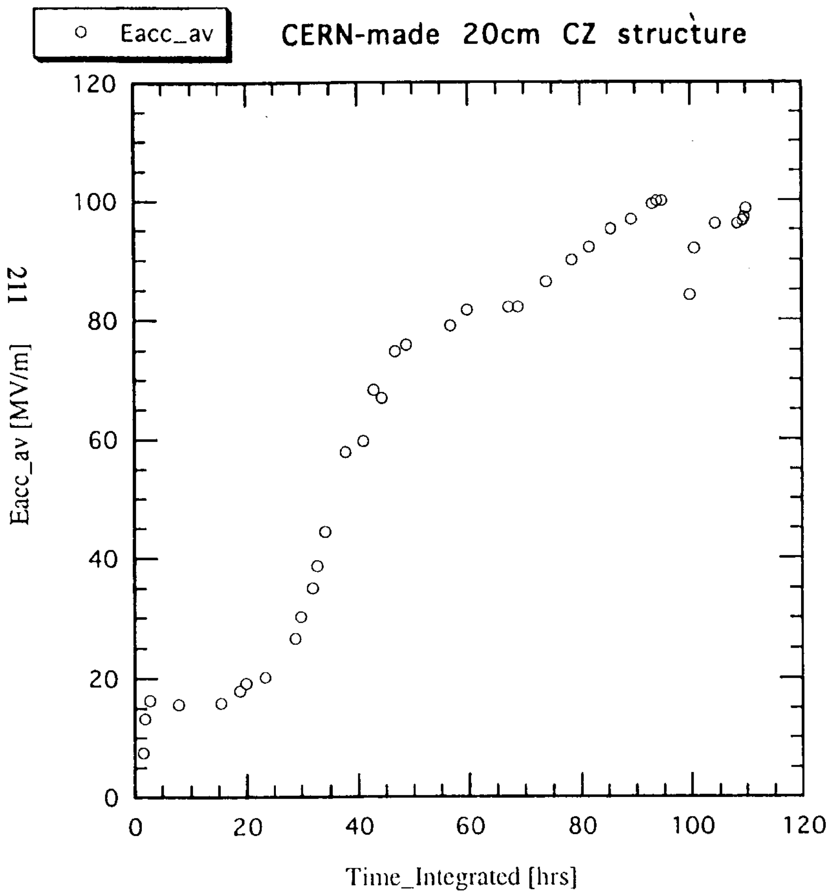
Eacc_av
CERN-made 20cm CZ structure
Eacc_av [MV/m]
Time_Integrated [hrs]
0
20
40
60
80
100
120

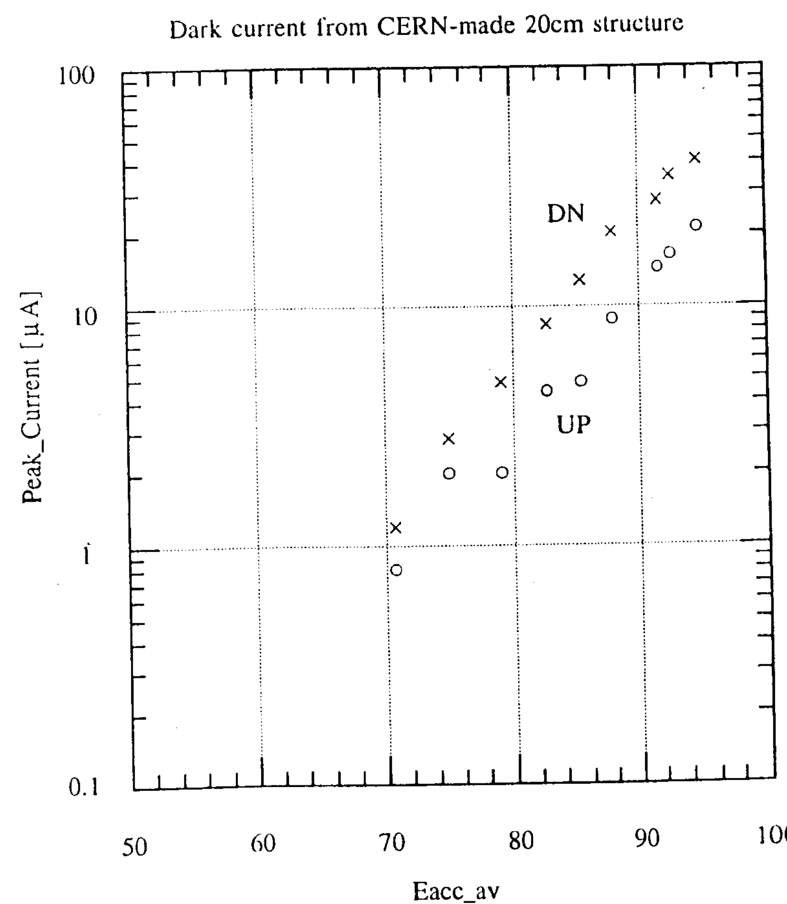
Dark current from CERN-made 20cm structure
Peak_Current [μA]
Eacc_av
DN
UP
100
10
1
0.1
50
60
70
80
90
100

Electron Trajectry Simulator (Yamaguchi)

on $\begin{cases} a = 3\ \text{mm} \\ t = 2\ \text{mm} \end{cases}$ X-band $\frac{2}{3}\pi$ structure

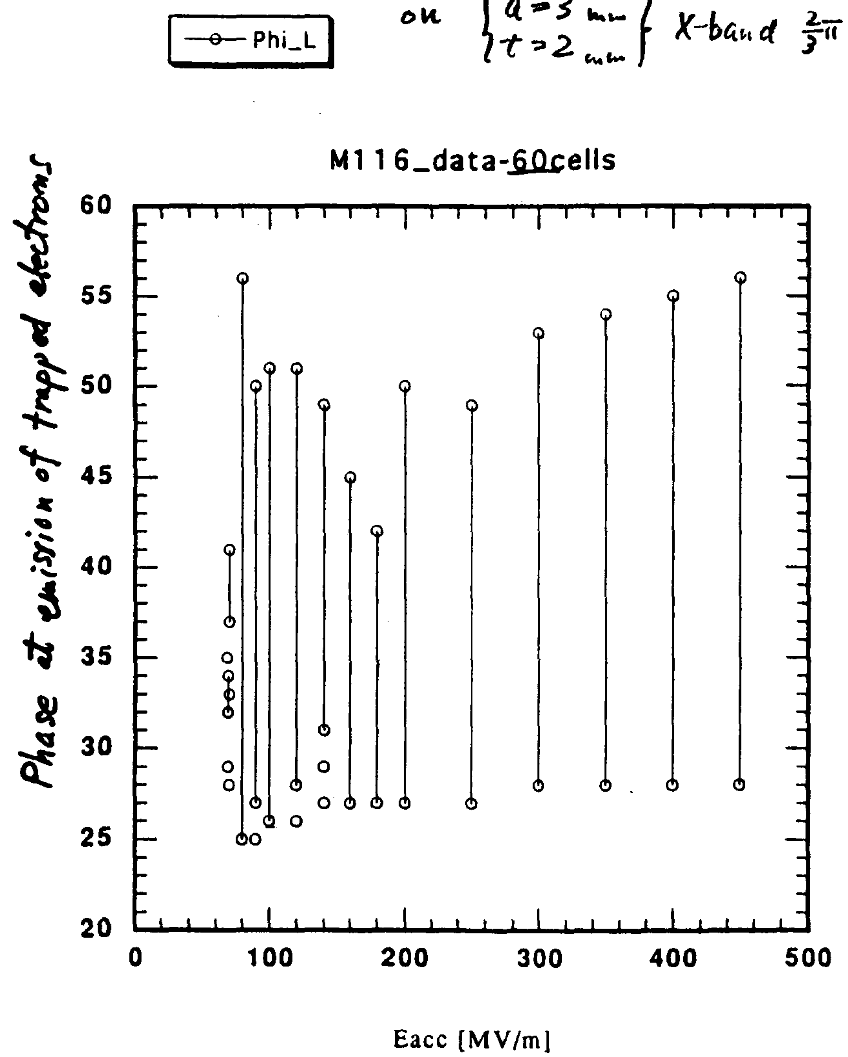

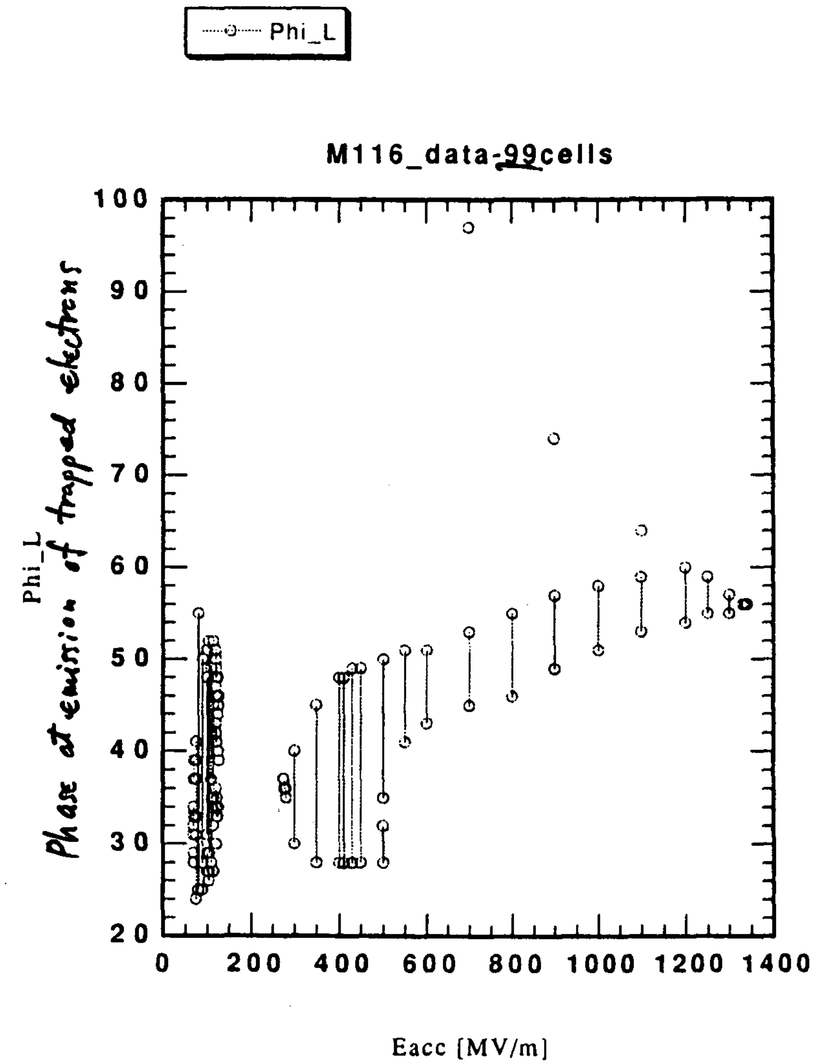

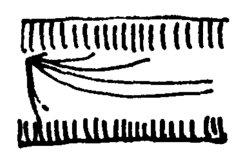

(dep. on Eacc.)

212

Dec.
col. 孫
IHE

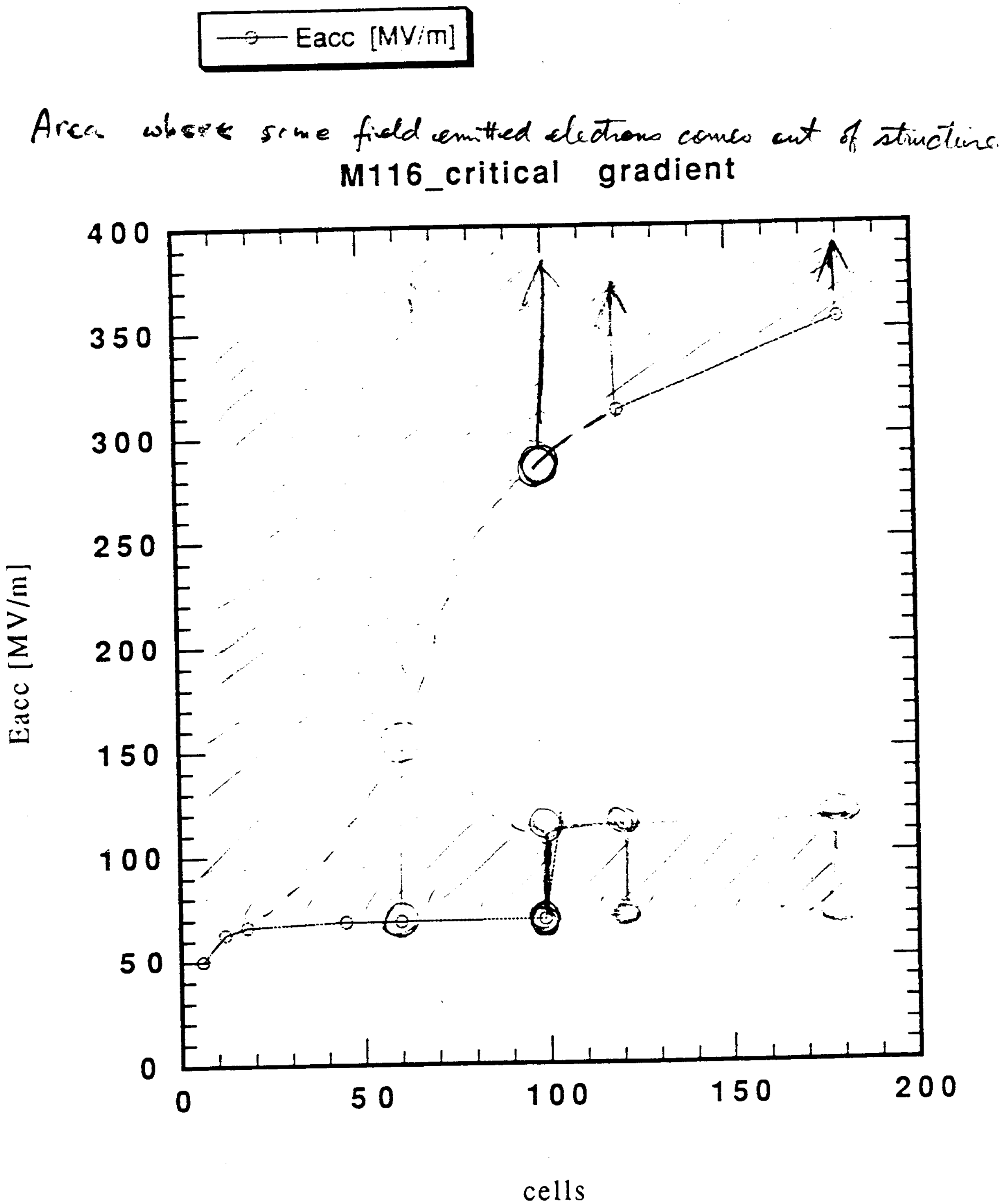

Eacc [MV/m]
Area where some field emitted electrons comes out of structure.
M116_critical gradient
400
350
300
250
200
150
100
50
0
Eacc [MV/m]
0
50
100
150
200
cells

Geometry of "Open Mode Expansion"　Yamamoto (KEK)

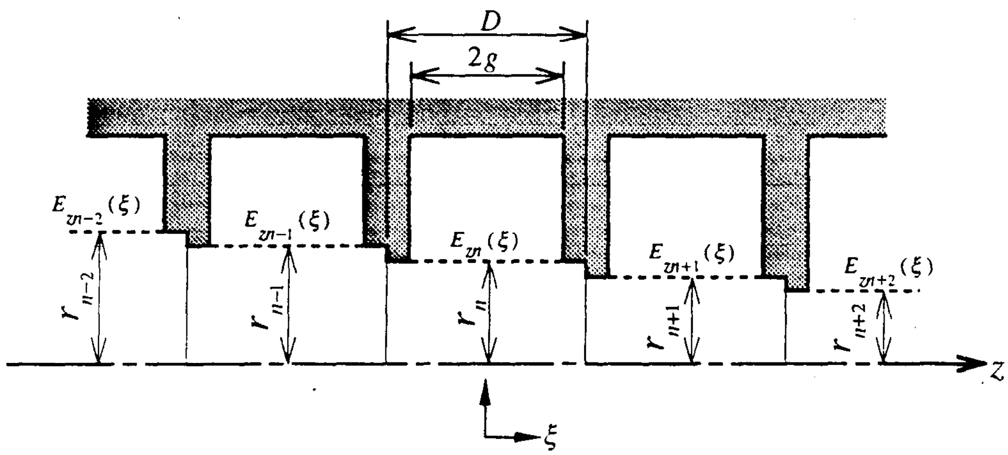

図 G.1: 非周期構造の電場の積分経路。点線に沿って E_z の線積分を行う。

Open Mode Expansion

Basic Modes

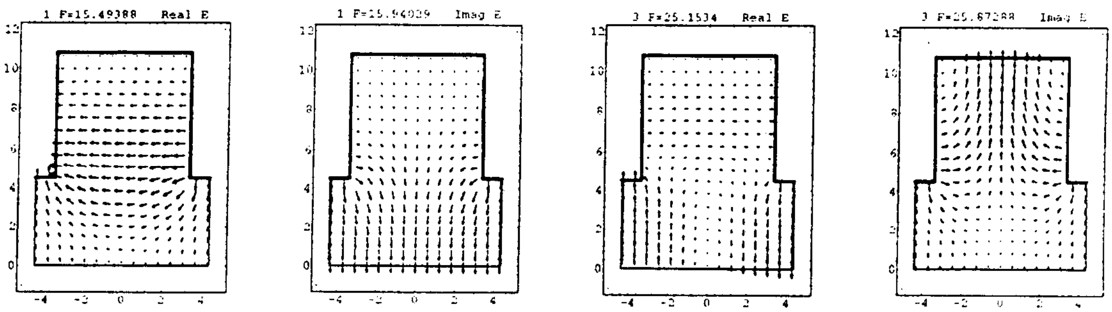

(a); open 1 ($\acute{e}_1$) (b); open 2 ($\acute{e}_2$) (c); open 3 ($\acute{e}_3$) (d); open 4 ($\acute{e}_4$)

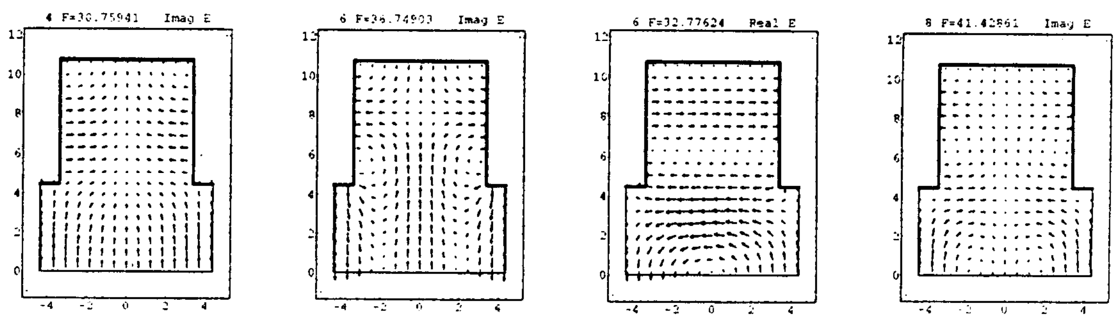

(e); open 5 ($\acute{e}_5$) (f); open 6 ($\acute{e}_6$) (g); open 7 ($\acute{e}_7$) (h); open 8 ($\acute{e}_8$)

Electric Fields of the open mode. Resonant modes of the detuned structure was calculated by open mode expansion using base function as shown above.

'94 D.
SLAC

from Maxwell's eq.

$$\left\{\left(\frac{\omega}{c}\right)^2-\left(\frac{\bar{\omega}_i}{c}\right)^2\right\}\int_V \bar{\boldsymbol{e}}_i^*\cdot \boldsymbol{E}dv=\int_S\left(\frac{\bar{\omega}_i}{c}\boldsymbol{E}\times\bar{\boldsymbol{h}}_i^*\right)\cdot \boldsymbol{n}dS$$

$$\boldsymbol{E}=\sum_{j=1}^{\infty}a_j\acute{\boldsymbol{e}}_j$$ ← open mode expansion

$$\acute{\boldsymbol{e}}_i(L)=\acute{\sigma}_i\acute{\boldsymbol{e}}_i(R)$$
$$\bar{\boldsymbol{h}}_i^*(L)=-\bar{\sigma}_i\bar{\boldsymbol{h}}_i^*(R)$$

$$\left\{\left(\frac{\omega}{c}\right)^2-\left(\frac{\bar{\omega}_i}{c}\right)^2\right\}\int_V \bar{\boldsymbol{e}}_i^*\cdot \boldsymbol{E}dv=\frac{\bar{\omega}_i}{2c}\sum_{j=1}^{\infty}a_j(\bar{\sigma}_i e^{i\phi}+\acute{\sigma}_j e^{-i\phi}+\bar{\sigma}_i\acute{\sigma}_j+1)\int_R\{\acute{\boldsymbol{e}}_j(R)\times\bar{\boldsymbol{h}}_i^*(R)\}\cdot\boldsymbol{n}_R dS$$

$$v_{ij}=\int_V\bar{\boldsymbol{e}}_i^*\cdot\acute{\boldsymbol{e}}_j dv$$
$$m_{ij}=\int_R\acute{\boldsymbol{e}}_j(R)\times\bar{\boldsymbol{h}}_i^*(R)\cdot\boldsymbol{n}_R dS$$

$$\boldsymbol{a}=\begin{pmatrix}a_1\\a_2\\a_2\\\vdots\end{pmatrix}$$

$$\bar{\boldsymbol{\Omega}}_{ij}=\bar{\omega}_i\delta_{ij}$$

$$\boldsymbol{U}_{ij}=\frac{\bar{\omega}_i^2}{\acute{\omega}_j^2-\bar{\omega}_i^2}\left[\acute{\sigma}_j\bar{\sigma}_i+1\right]m_{ij}=\frac{\bar{\omega}_i}{c}v_{ij}$$

$$\boldsymbol{T}_{ij}=\frac{1}{2}\left[\bar{\sigma}_i e^{i\phi}+\acute{\sigma}_j e^{-i\phi}+\bar{\sigma}_i\acute{\sigma}_j+1\right]m_{ij}$$

$$\boxed{\boldsymbol{X}\boldsymbol{a}=\omega^2\boldsymbol{a}}$$

$$\boldsymbol{X}=\boldsymbol{U}^{-1}\bar{\boldsymbol{\Omega}}^2(\boldsymbol{T}+\boldsymbol{U})$$

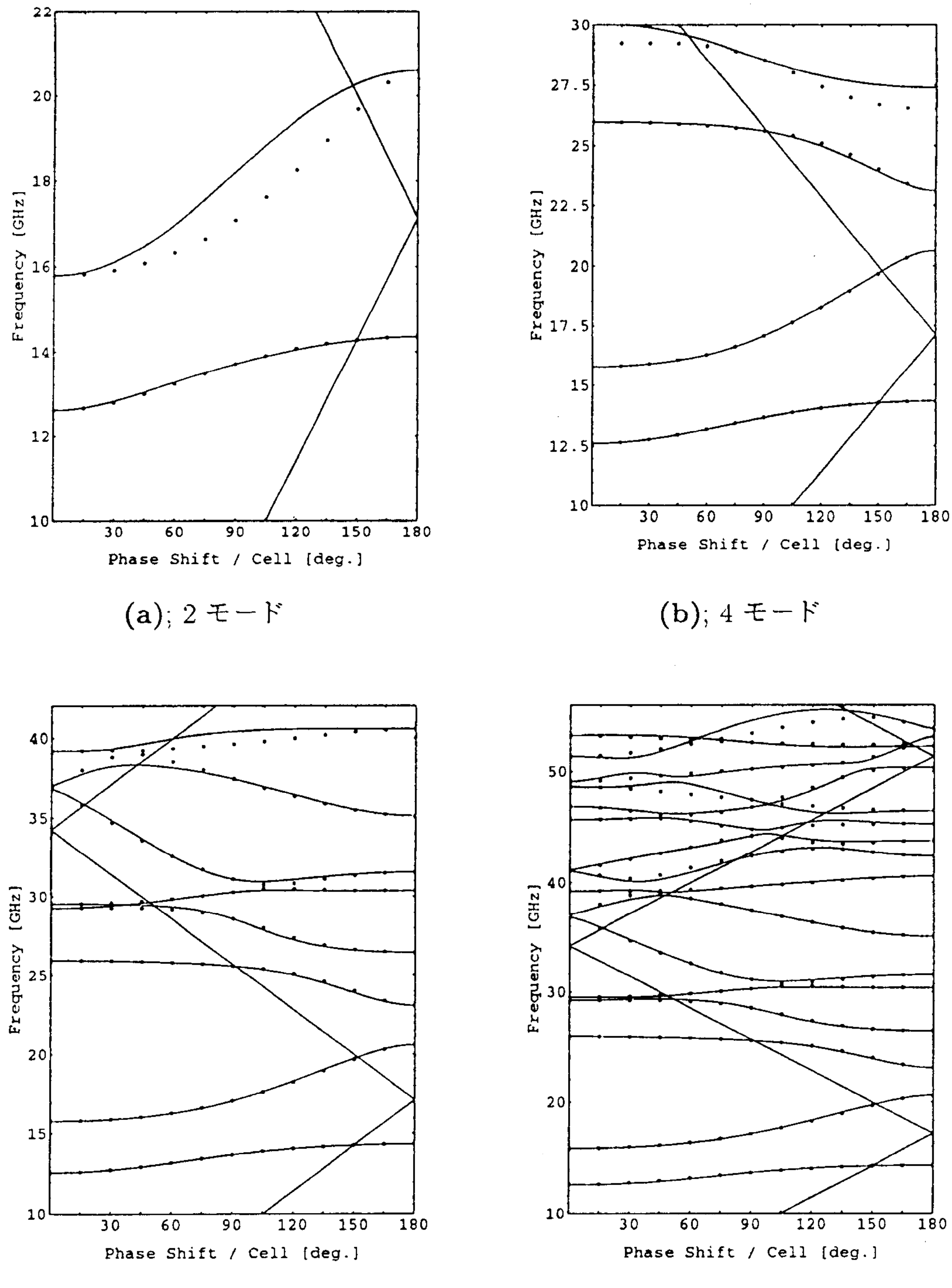

図 J.3: VMXをエルミート行列にしたときの分散関係 (a=6.0mm)。黒丸はフィールドマッチング、実線はオープンモード展開で計算した結果である。それぞれの図は展開するモード数が異なる。

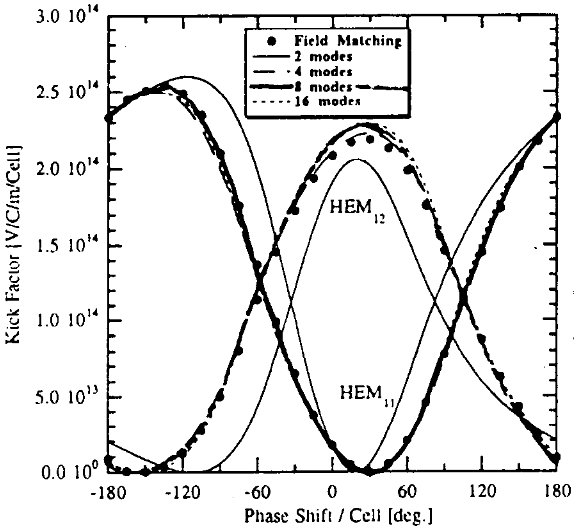

(a); HEM_{11} と HEM_{12}

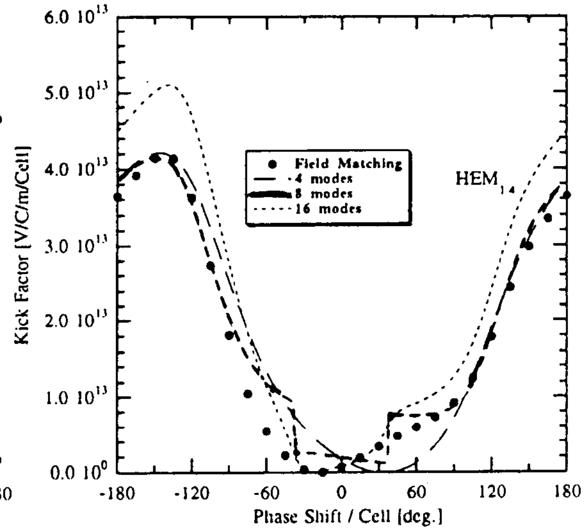

(b); HEM_{14}

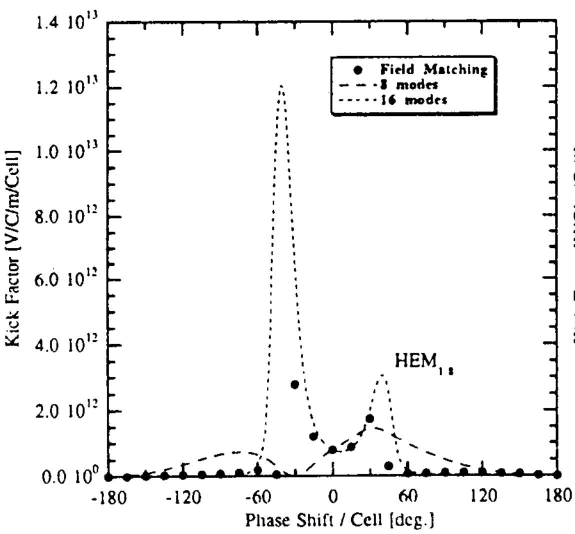

(c); HEM_{18}

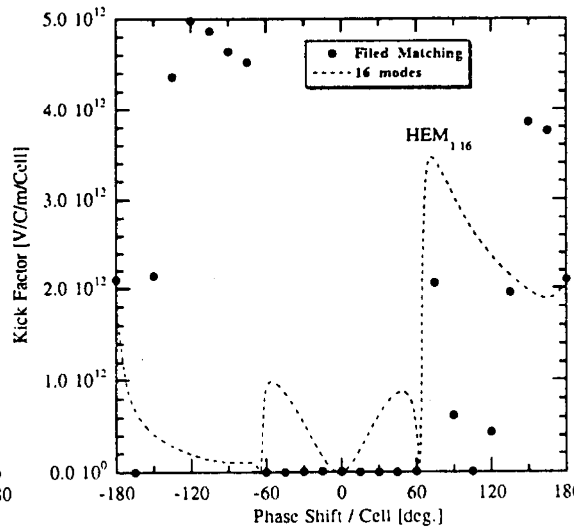

(d); HEM_{116}

図 J.6: VMXをエルミート行列にしたときのキック因子 (a=6.0 [mm])。黒丸はフィールドマッチング、実線や破線はオープンモード展開の結果を示す 。

Basic Parameters of Structure under Fabrication Test

detune181

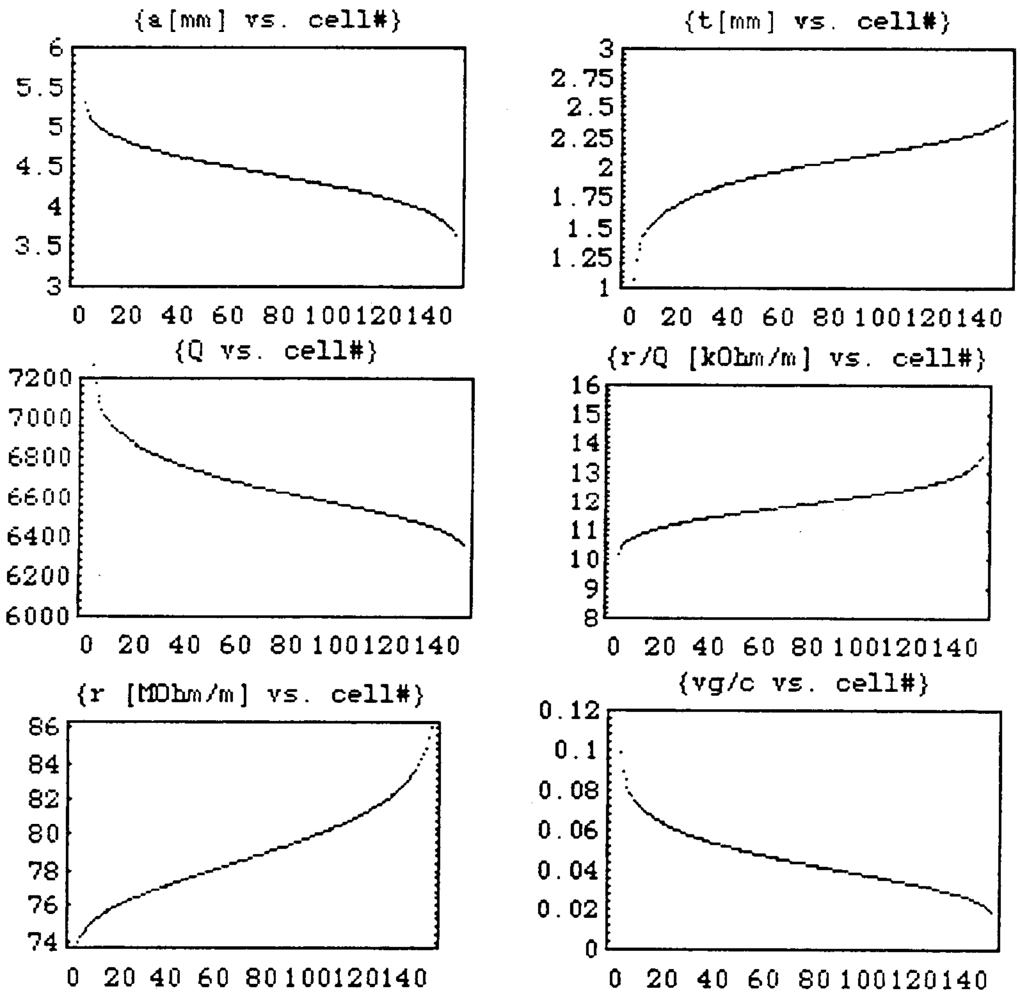

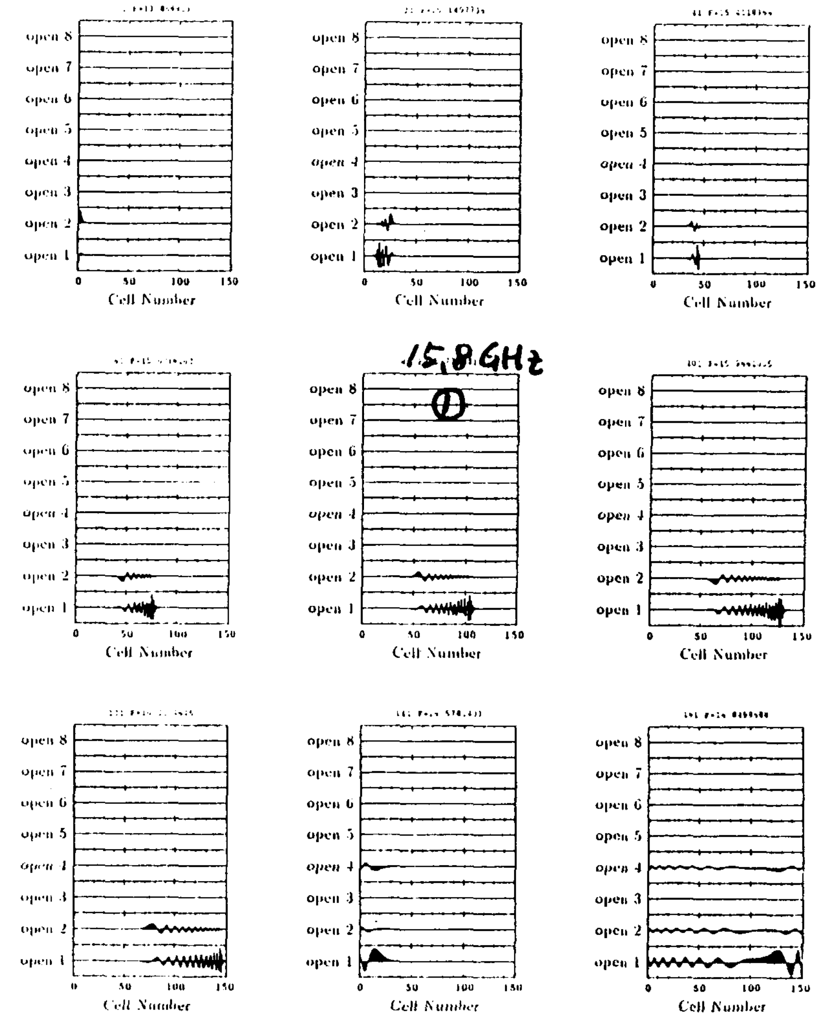

図 4.12: 周波数分散構造の固有ベクトル。横軸はセルの番号、縦軸はオープンモードの固有ベクトルの成分を示す。固有ベクトルの最大値を 1 に規格化している。各グラフ上部の数字は、共振モードの番号と周波数である。

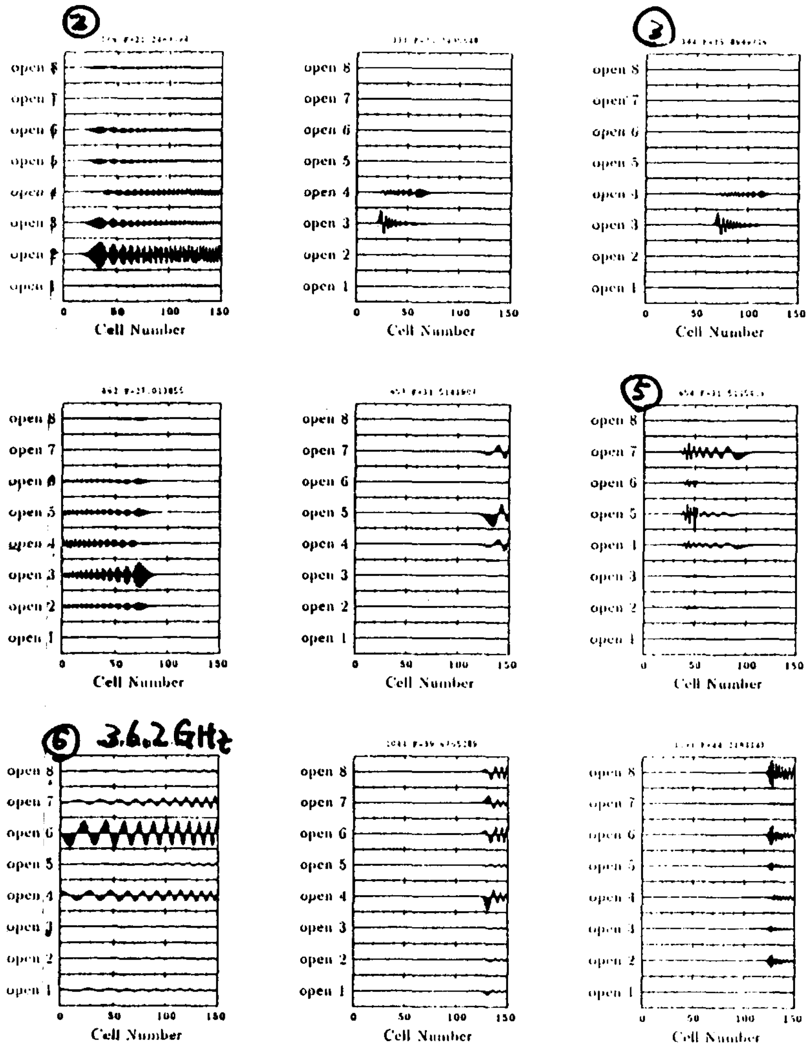

図 4.13: 周波数分散構造の固有ベクトル。横軸はセルの番号、縦軸はオープンモードの固有ベクトルの成分を示す。固有ベクトルの最大値を 1 に規格化している。各グラフ上部の数字は、共振モードの番号と周波数である。

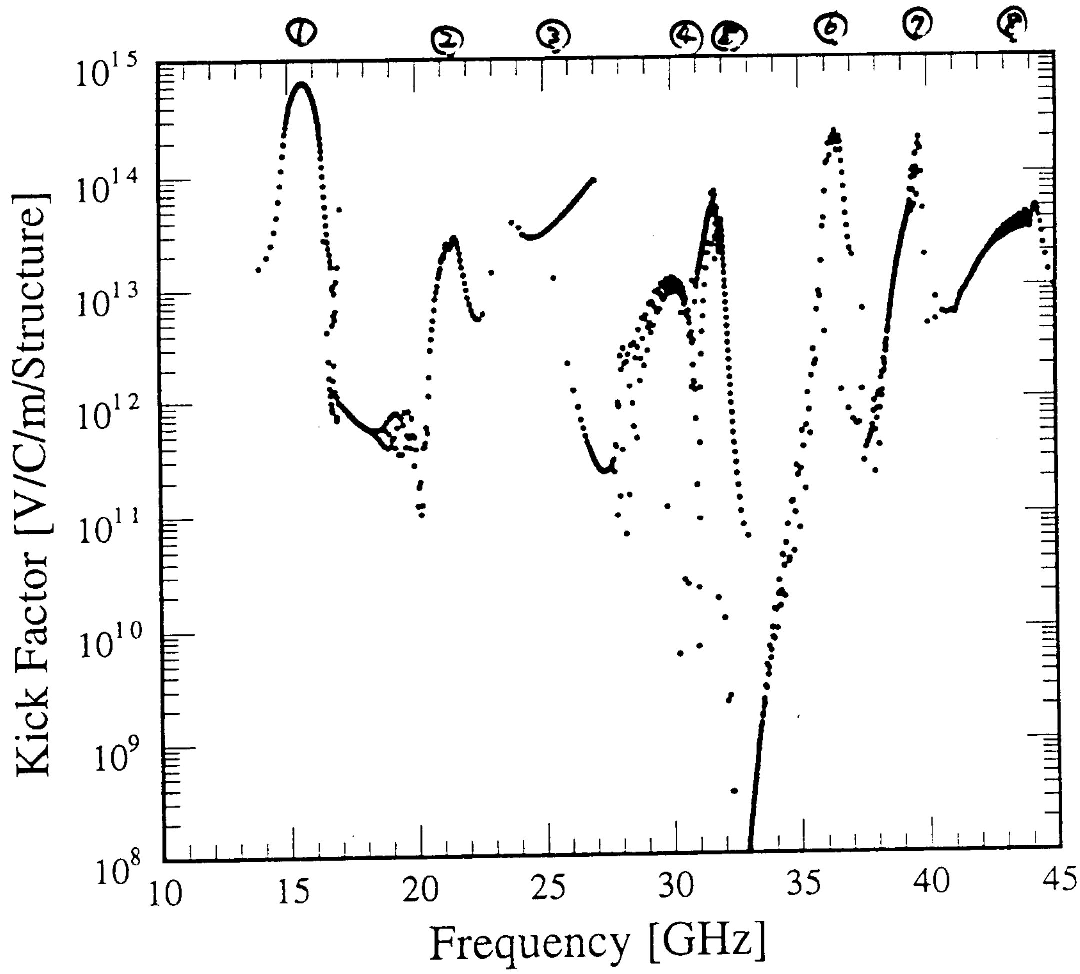

図 4.11: 周波数分散構造のキック因子

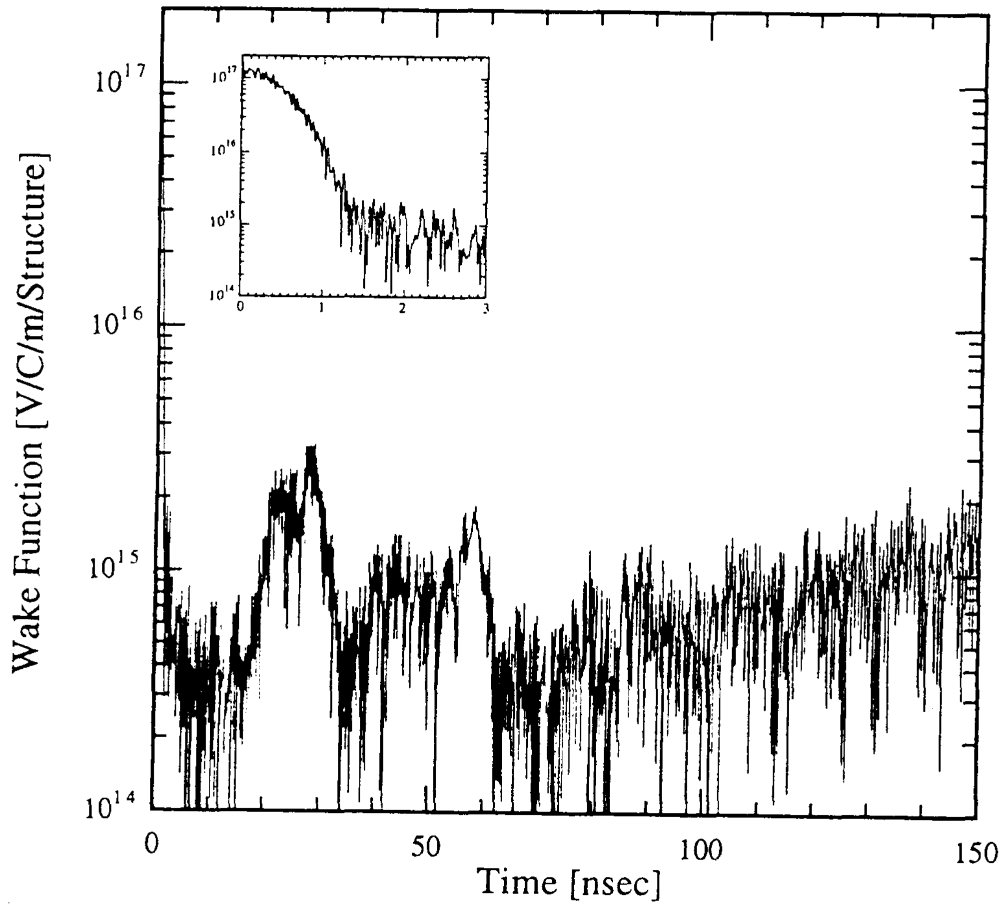

図 4.18: 少しづつ形状の異なる 4 個の周波数分散構造のウェーク関数の絶対値の包絡線

○ $\sum_{\ell=1}^{n-1} W_\perp(\ell t_i)$

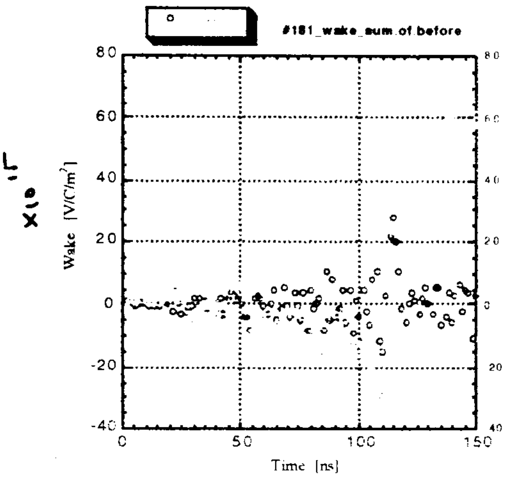

#181

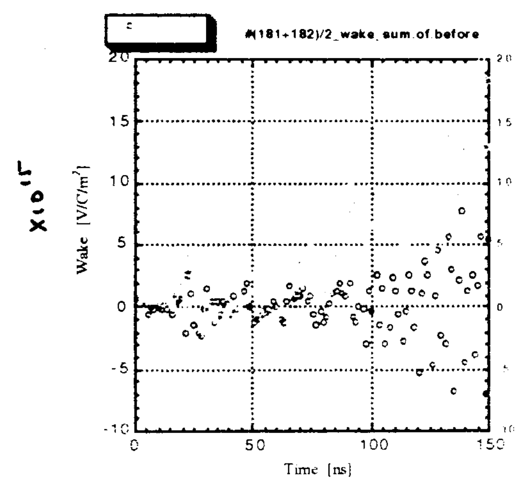

#181&2

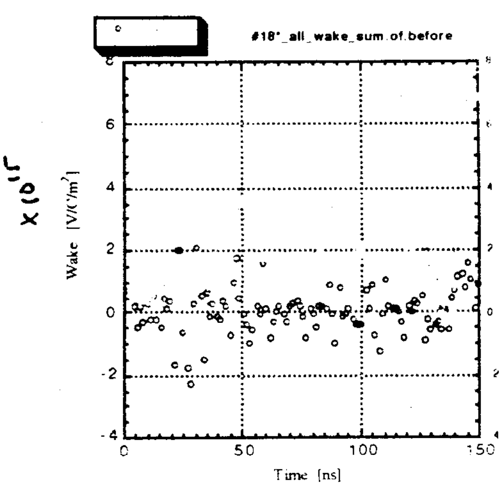

#181all

detune 181

average a / λ	= 0.165824	in 150. cell structure	
τ	= 0.578477		
Filling time	= 106.404	[ns]	
Voltage/structure	= 84.3924	[MV]	in 100MW input
Eav	= 64.3181	[MV/m]	in 100MW input

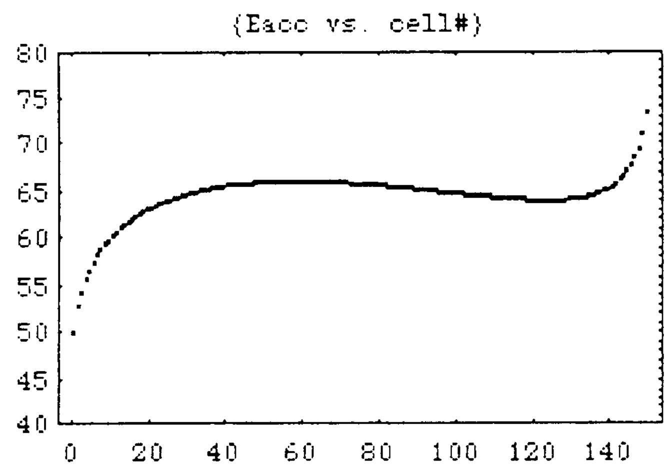

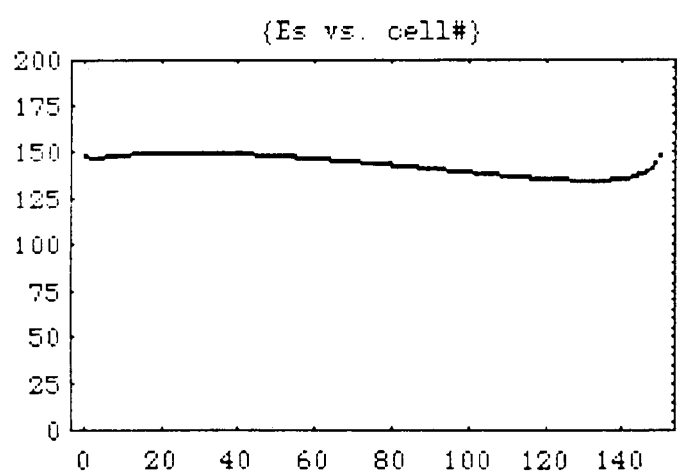

Comparison of "open mode expansion" + "MAFIA 2D" … (Yamamoto) (K.Ko)

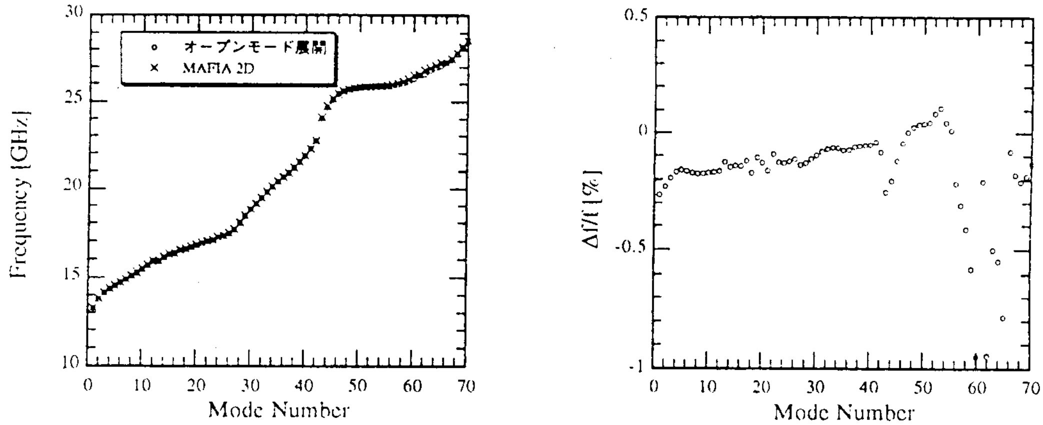

(a): 共振周波数 (b): 共振周波数の差

図 4.6: MAFIA とオープンモード展開の共振周波数。横軸は周波数の低い順に並べたモードの番号である。

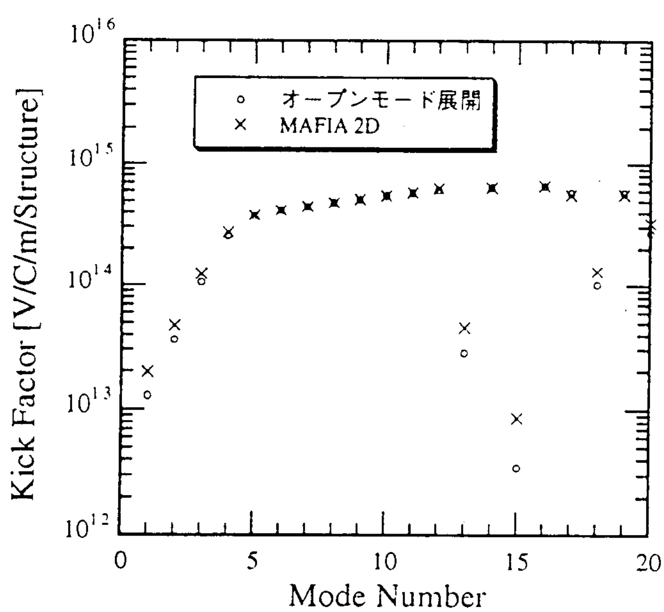

図 4.7: MAFIA とオープンモード展開で計算されたキック因子。横軸は周波数の低い順に並べたモードの番号である。

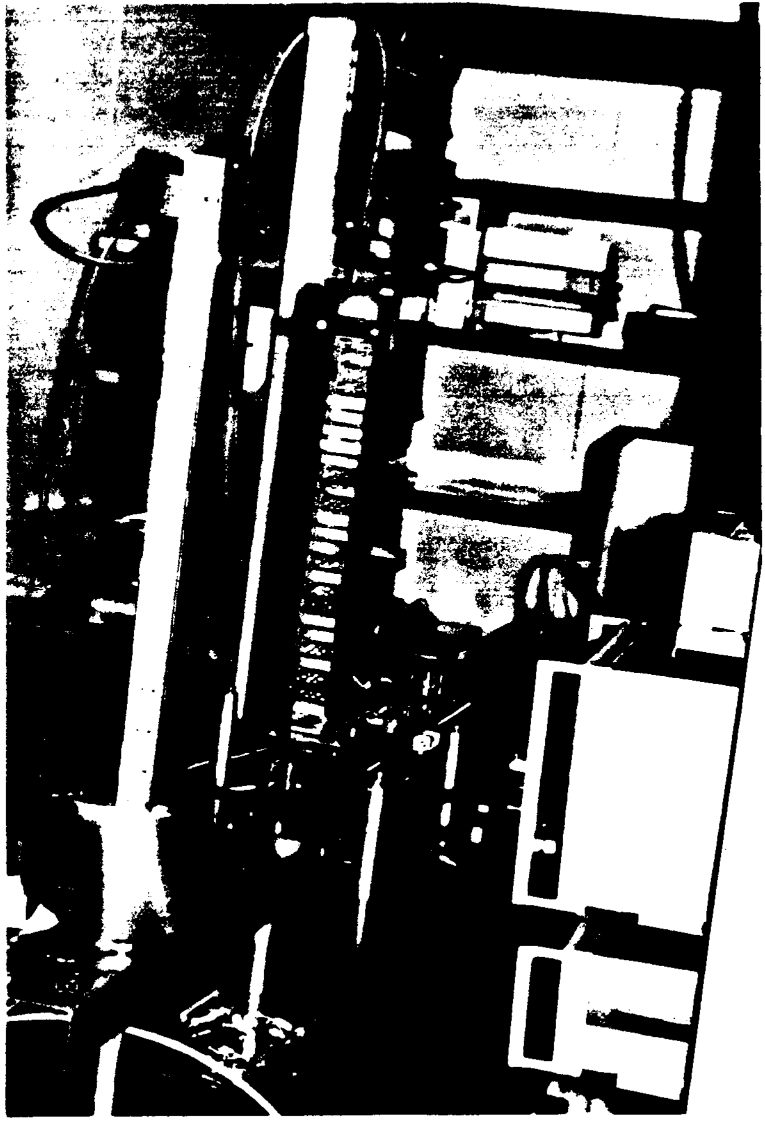

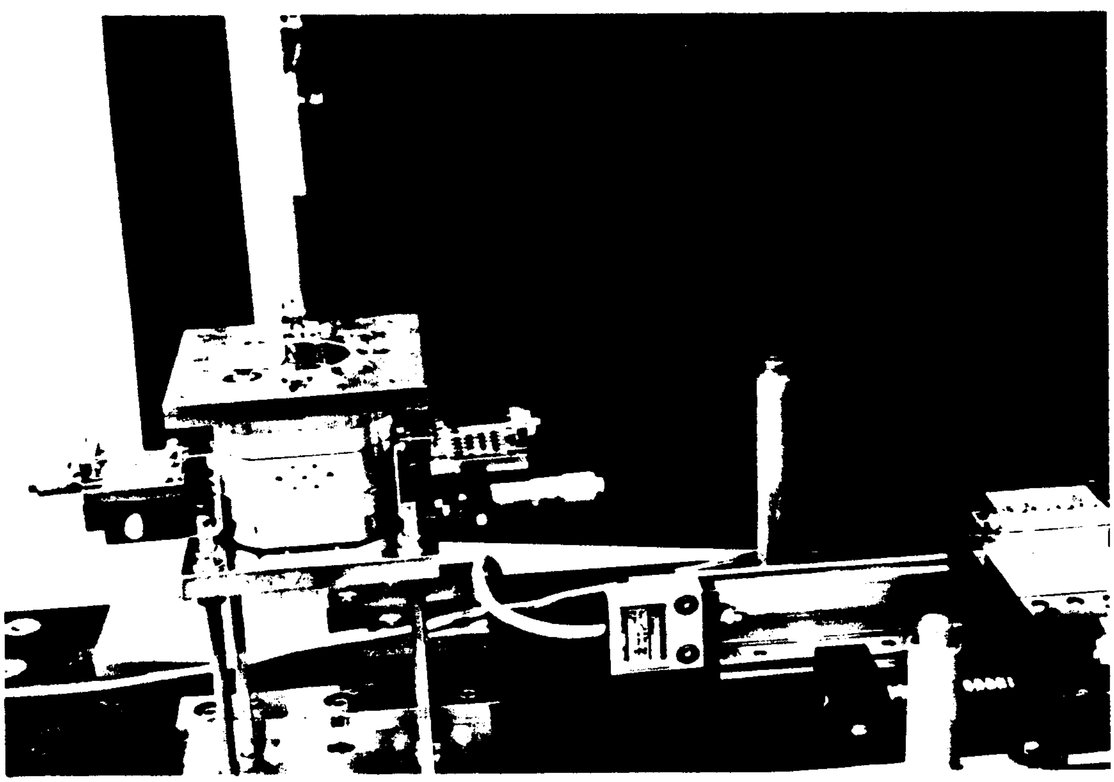

Field Measurement by bead perturbation

Frequency in ascending order.

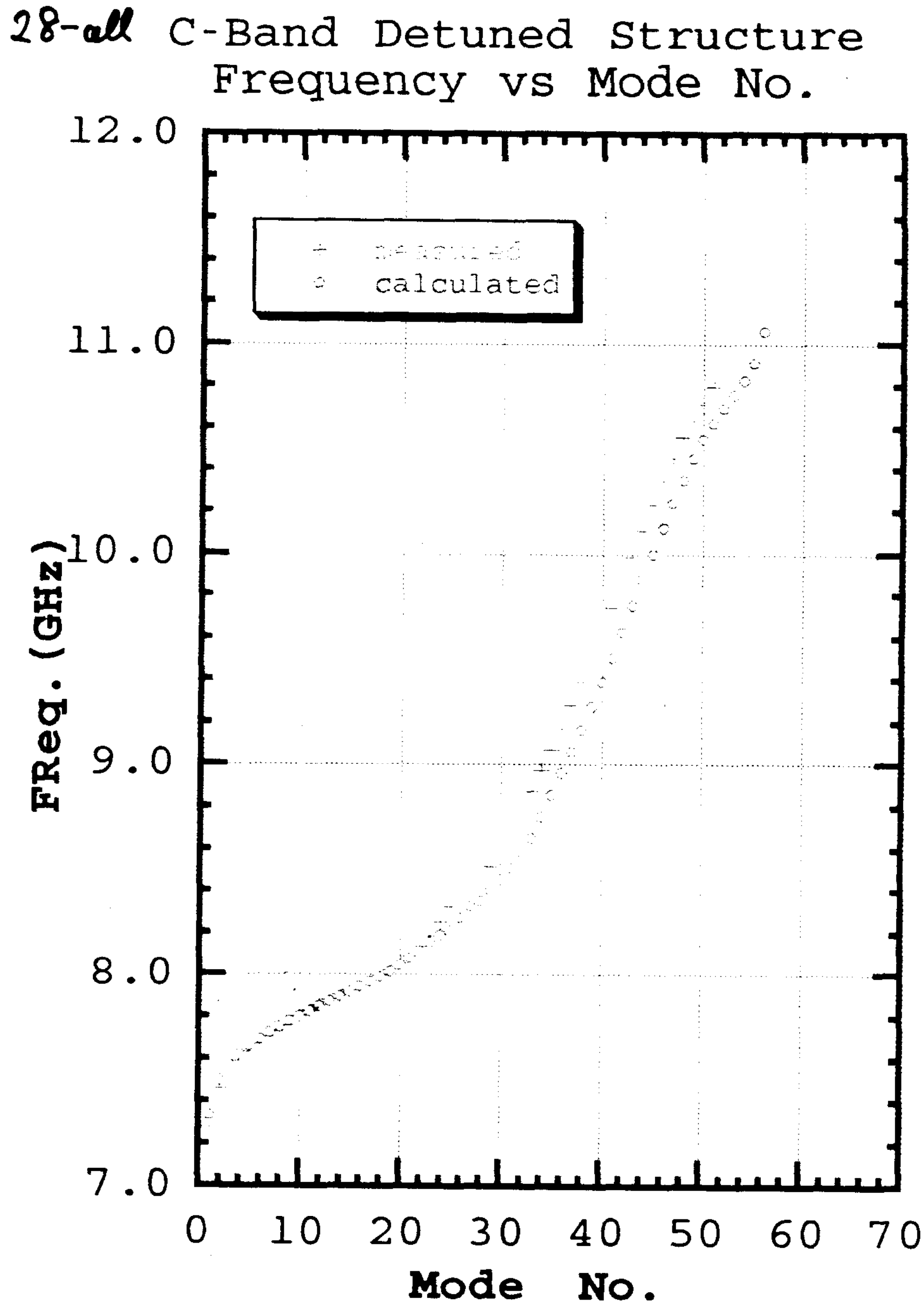

(· higher freq. resonance not yet measured.
· some in middle freq. range seem missing

'94 Dec

Design for reduction of Long Range Dipole Wake "remains"

① Open mode expansion

- extension to more modes than 8
  rounded iris
  non symmetry

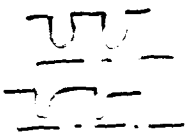

② Equivalent Circuit

- medium damping
- coupling to WG & Beam tube

③ Choke mode cavity

④ Checking Wake field
What to check?
gross structure of wake
or
fine structure of wake at $m t_b$
necessary information on structure parameters?

⑤ design of feedback with beam with BPM's etc.

PROGRESS REPORT ON STUDIES OF ACCELERATOR STRUCTURES

Juwen Wang

Accelerator Theory and Special Projects Department

SLAC

December/1994

WORK
on
ACCELERATOR STRUCTURES

1. Theoretical Calculations

- Design and RF Parameter Calculation
- Equivalent Circuit Models
- Field Matching Technique and Applications
- Beam Loading Calculations
- Resonant Phenomenon
- Multibunch Effects, Misalignment, interleaving, ...
- Numerical Simulations (Couplers, Pumping Holes...)
- Weak Damping for Detuned Structure
- Vacuum System Calculations

2. Low-Power Measurements

- Matching, Tuning and Mode Studies

3. High-Power Tests

- 7-cavity X-Band SW Section
- Four Types of X-Band TW Sections

4. Wakefield Measurements

- Argonne's AATF for Detuned Structure Models
- ASSET for 1.8m Detuned Section in SLC

5. Fabrication Technique Studies

- Design and Machining (75cm and 1.8m Sections)
- Brazing and Alignment
- CMM Machine Measurements

Design of First 1.8 m Detuned Section

$f_1 = f_1(a.t)$

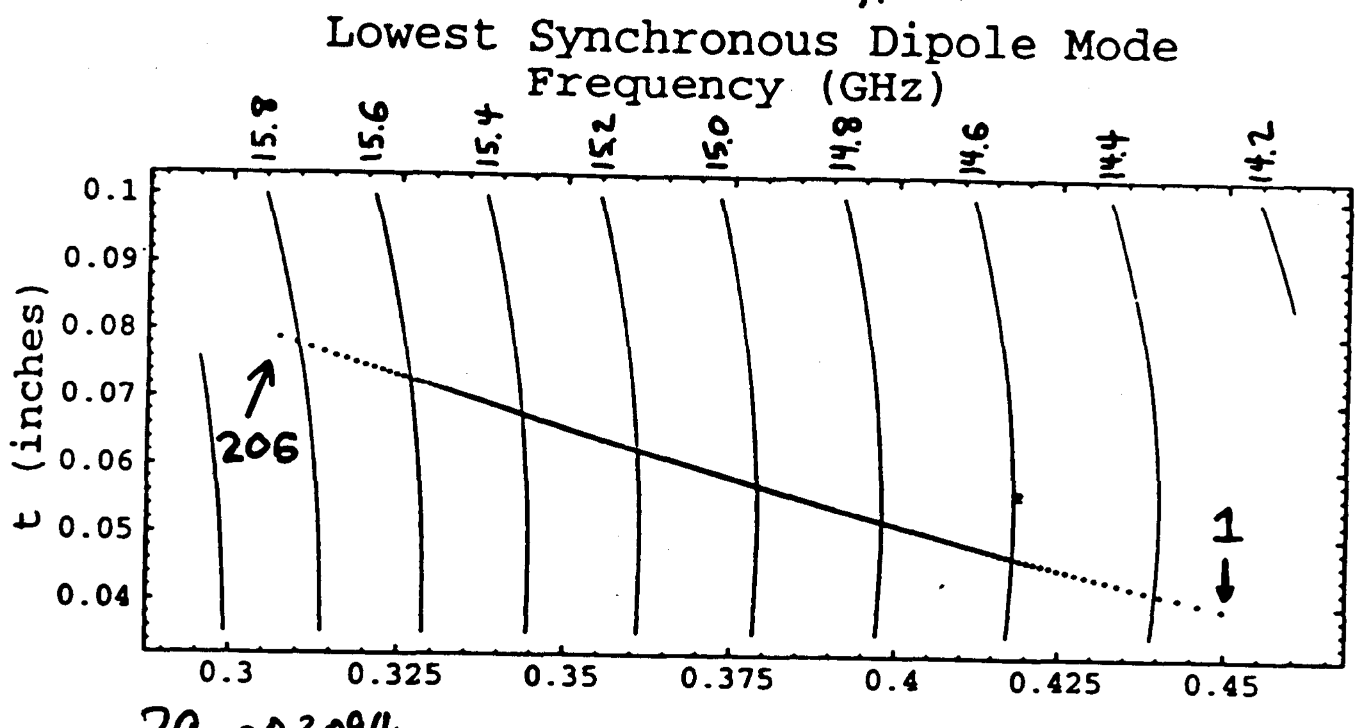

$2a_{206} = 0.3094$ $2a_1 = 0.4464$

$2b_{206} = 0.8413$ inches $2b_1 = 0.9010$ inches

t: 1 mm – 2 mm

$f_0(a.b.t) = 11.424$ GHz

YAP: 2-D Finite Element Code

Bane/Gluckstern

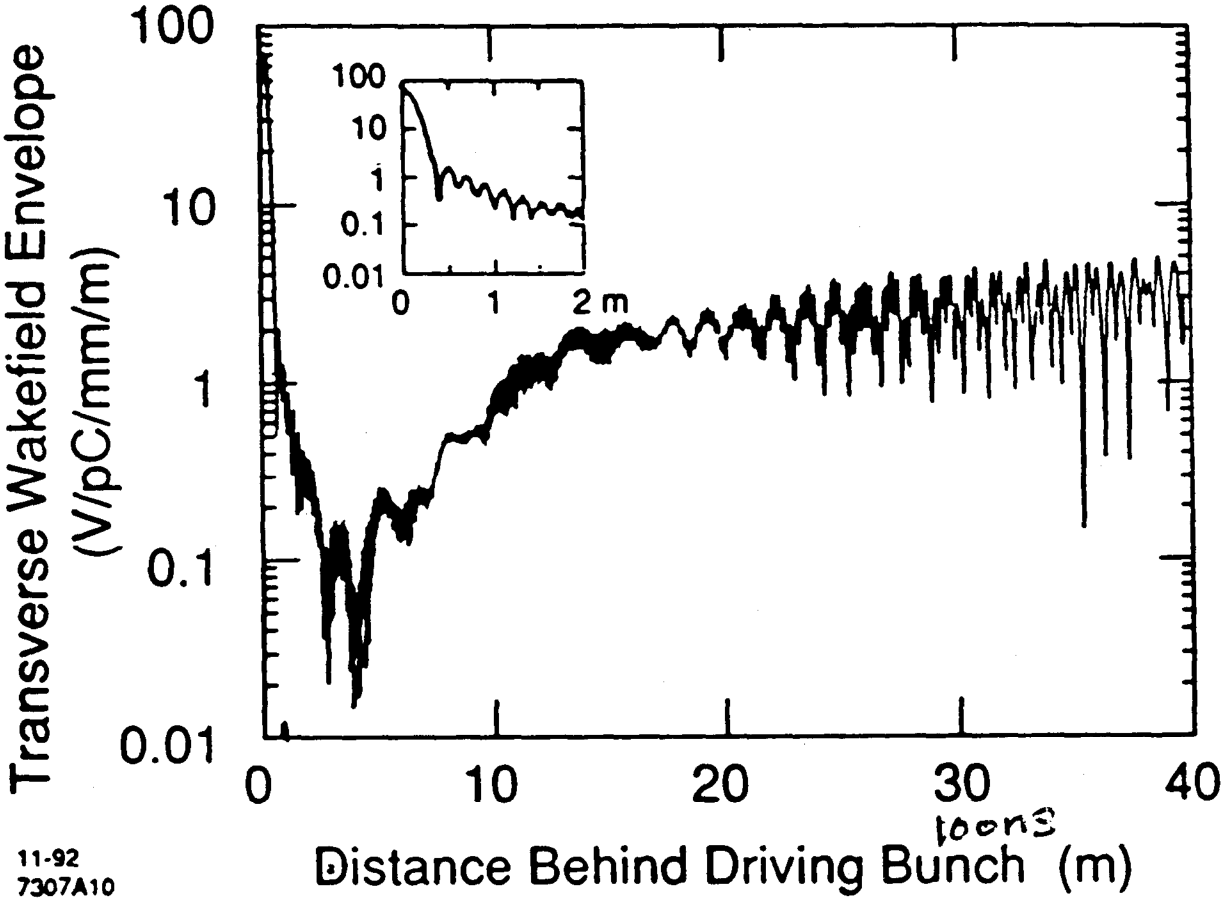

bunch spacing
0.42 m
1.4 ns

ACCELERING GRADIENT AT 100 MW INPUT POWER

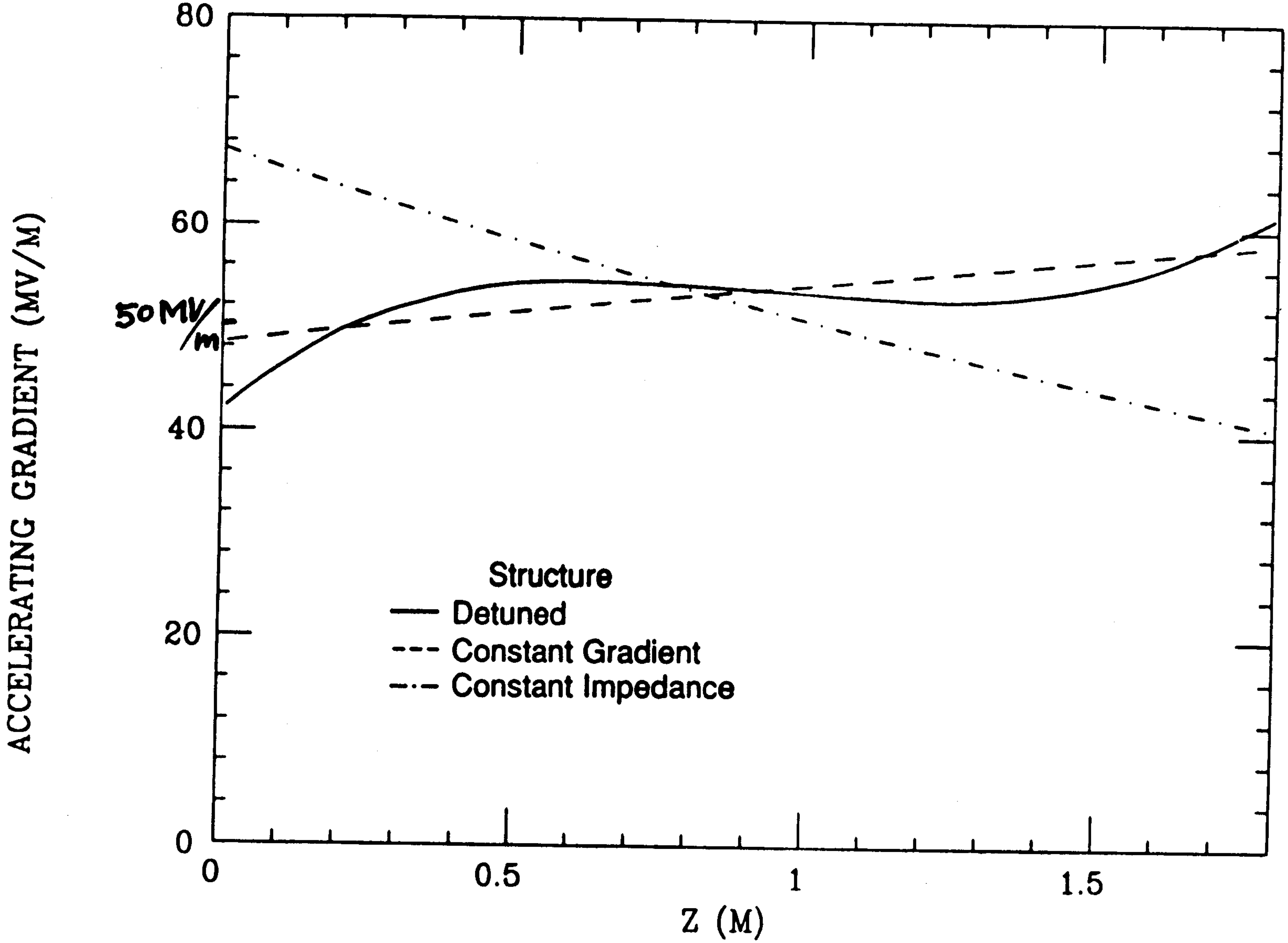

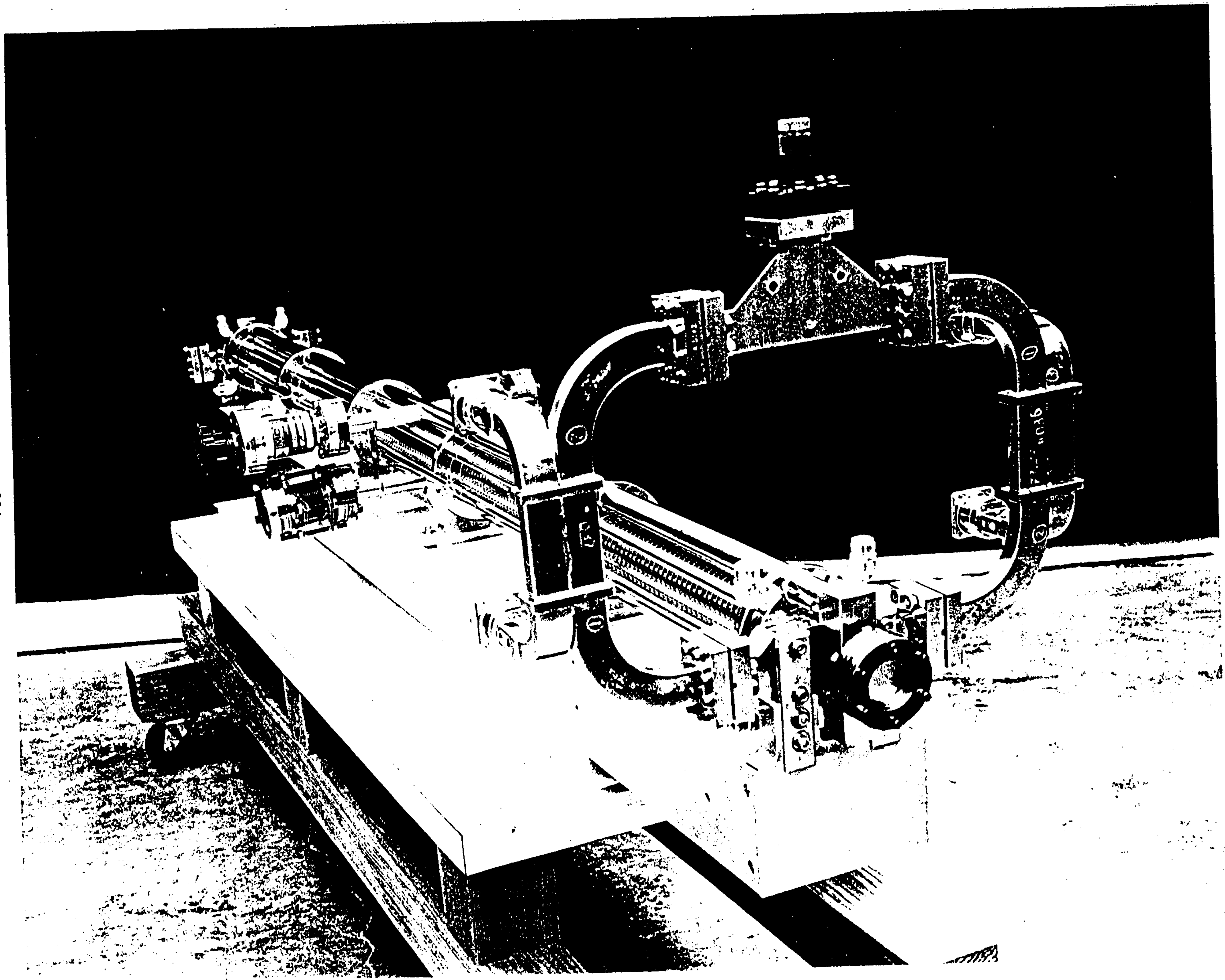

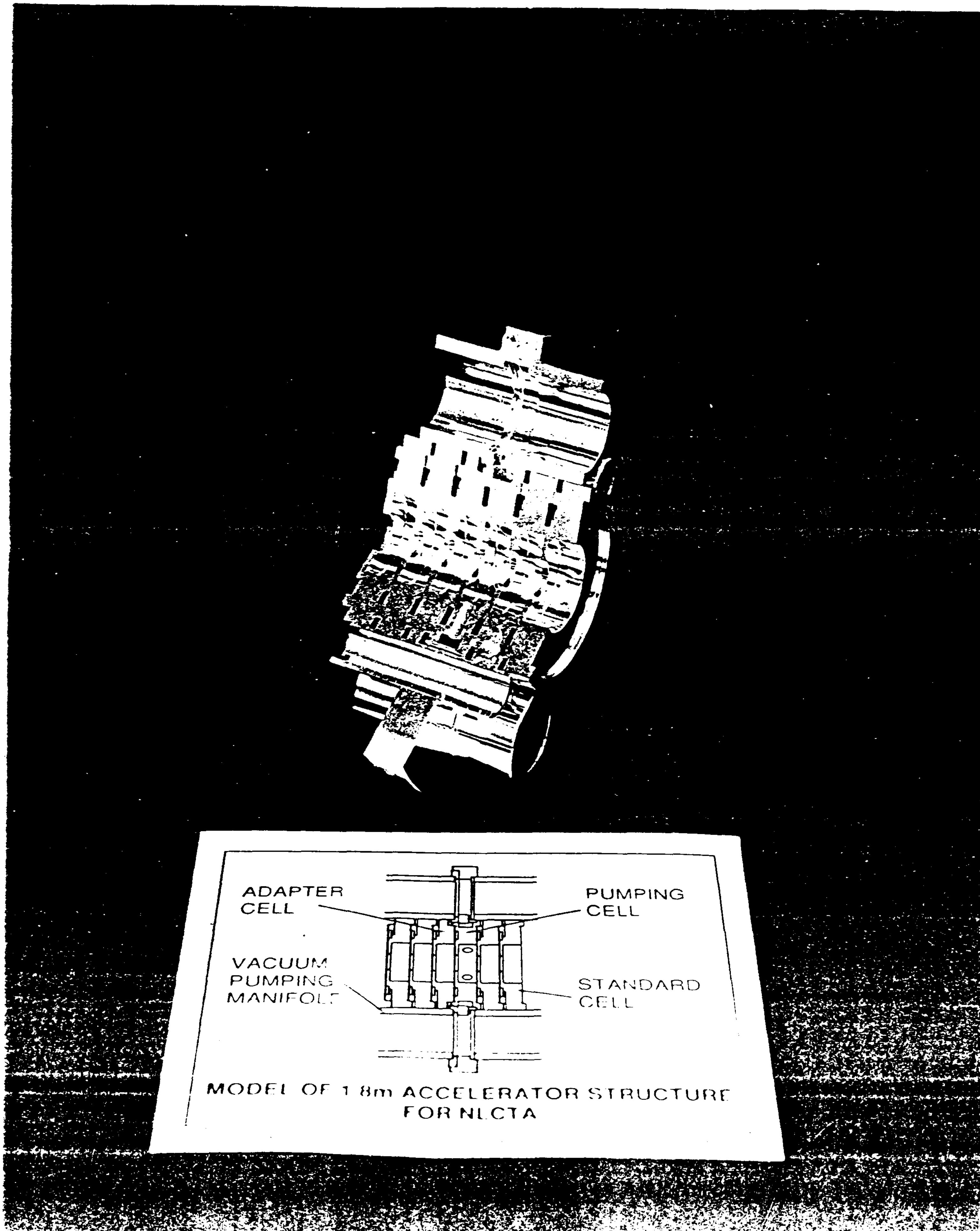
ADAPTER CELL
PUMPING CELL
VACUUM PUMPING MANIFOL
STANDARD CELL
MODEL OF 1.8m ACCELERATOR STRUCTURE
FOR NLCTA

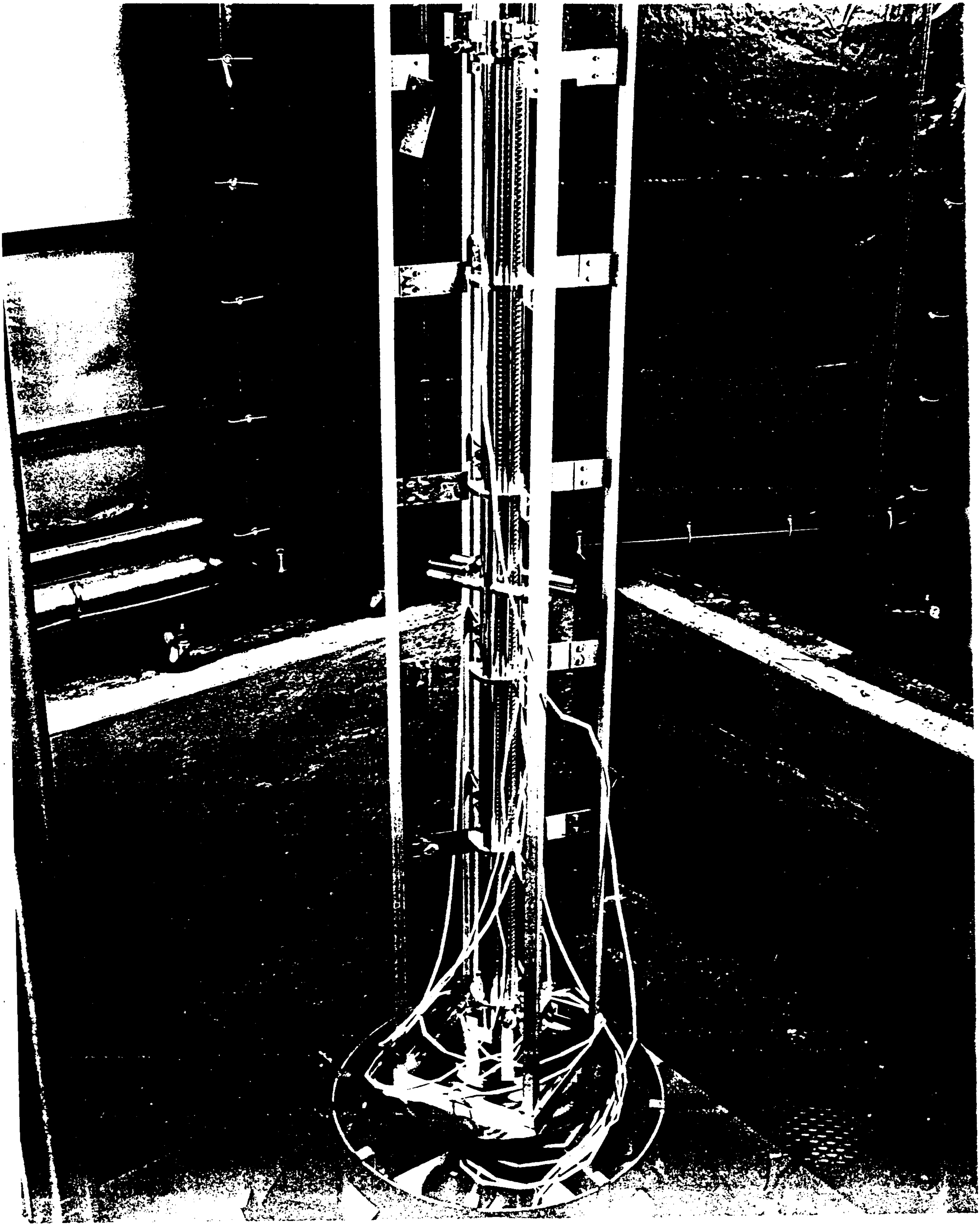

Beam Loading and Compensation for 1.8m Detuned Structure

F- 11424.0 MHz Ib-0.743 A SL- 1.802 m VG- 0.1186 VGL- 0.0297 TF- 0.101 us tau- 0.524

VO- 90.07 Vb- 23.20 VL- 66.88 MV EAGS-49.99 EABS-12.87 EALS-37.11 MV/m

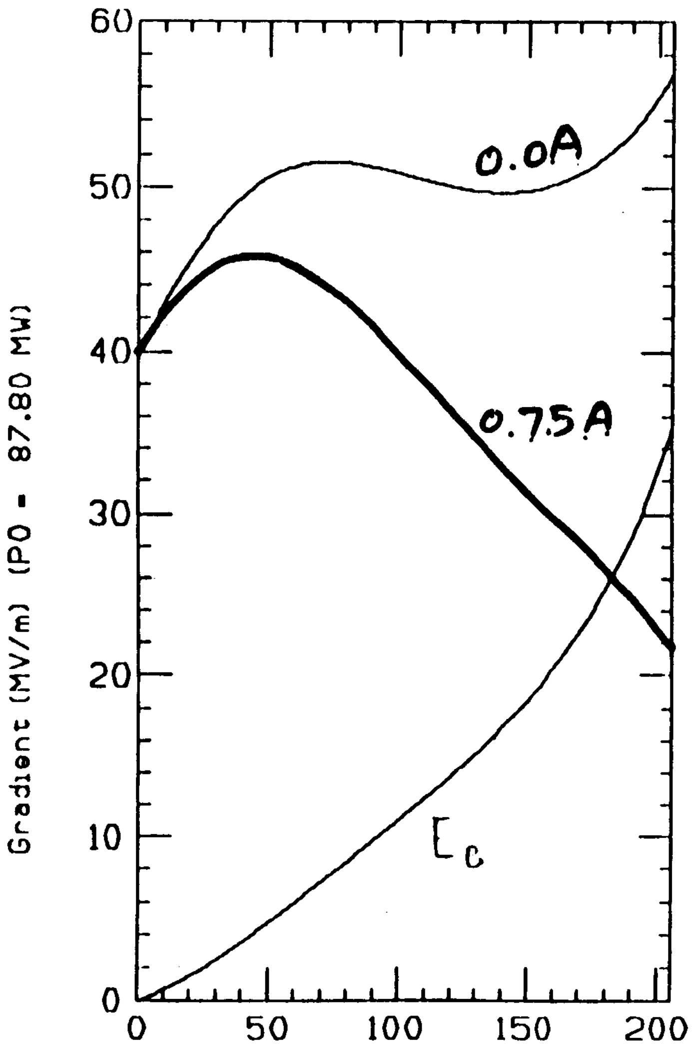

Pin = 87.8MW, Steady Case

Fig. 1. Generator, beam and loaded gradients as a function of cell number n.

Rsh1- 67.48 Rsh2- 87.96 Q1- 7416. Q2- 6674.

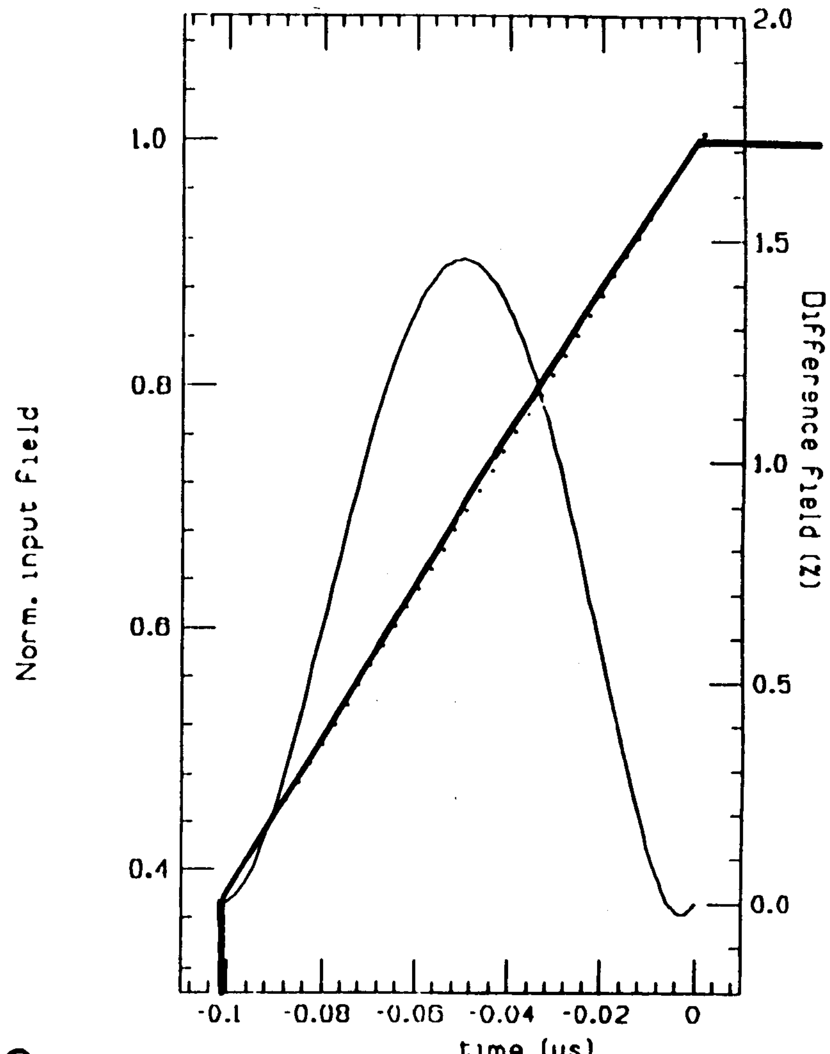

Fig. 2. Norm. input field and difference between it and a linear field (dots) vs time

Initial norm. power- 0.3758

Farkas / Wilson

Beam Loading and Compensation for 0.9m Detuned Structure

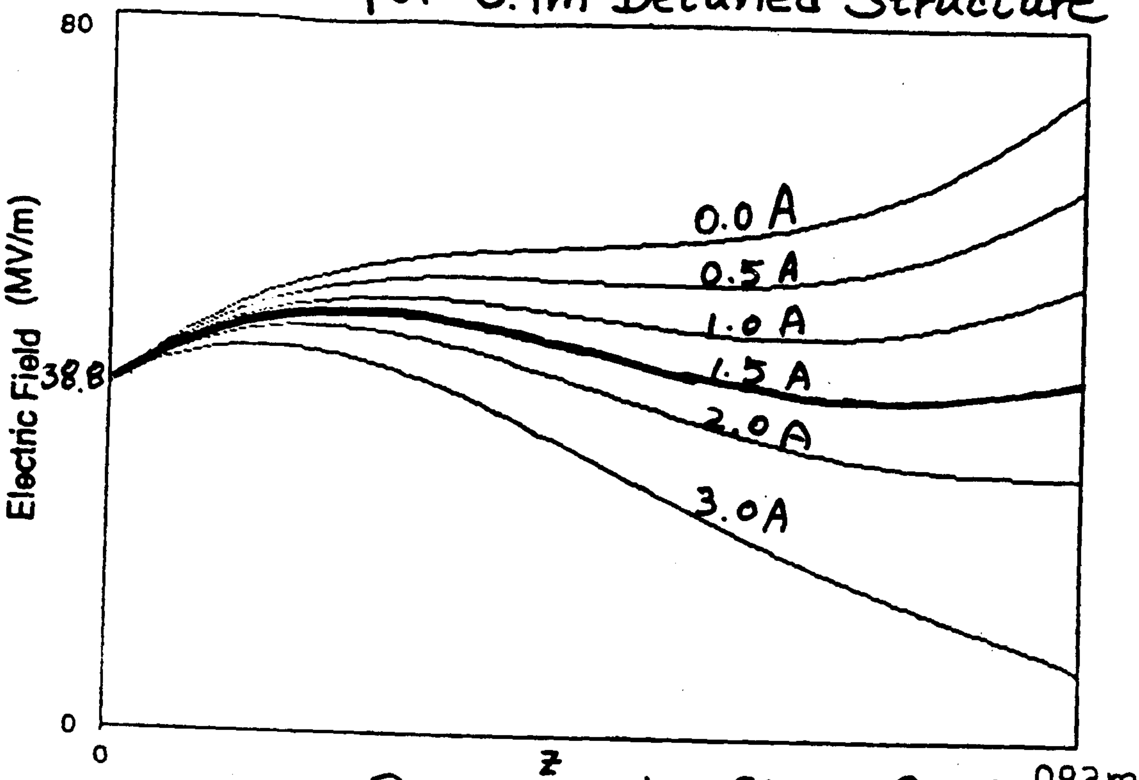

Pin=86.5MW Steady Case

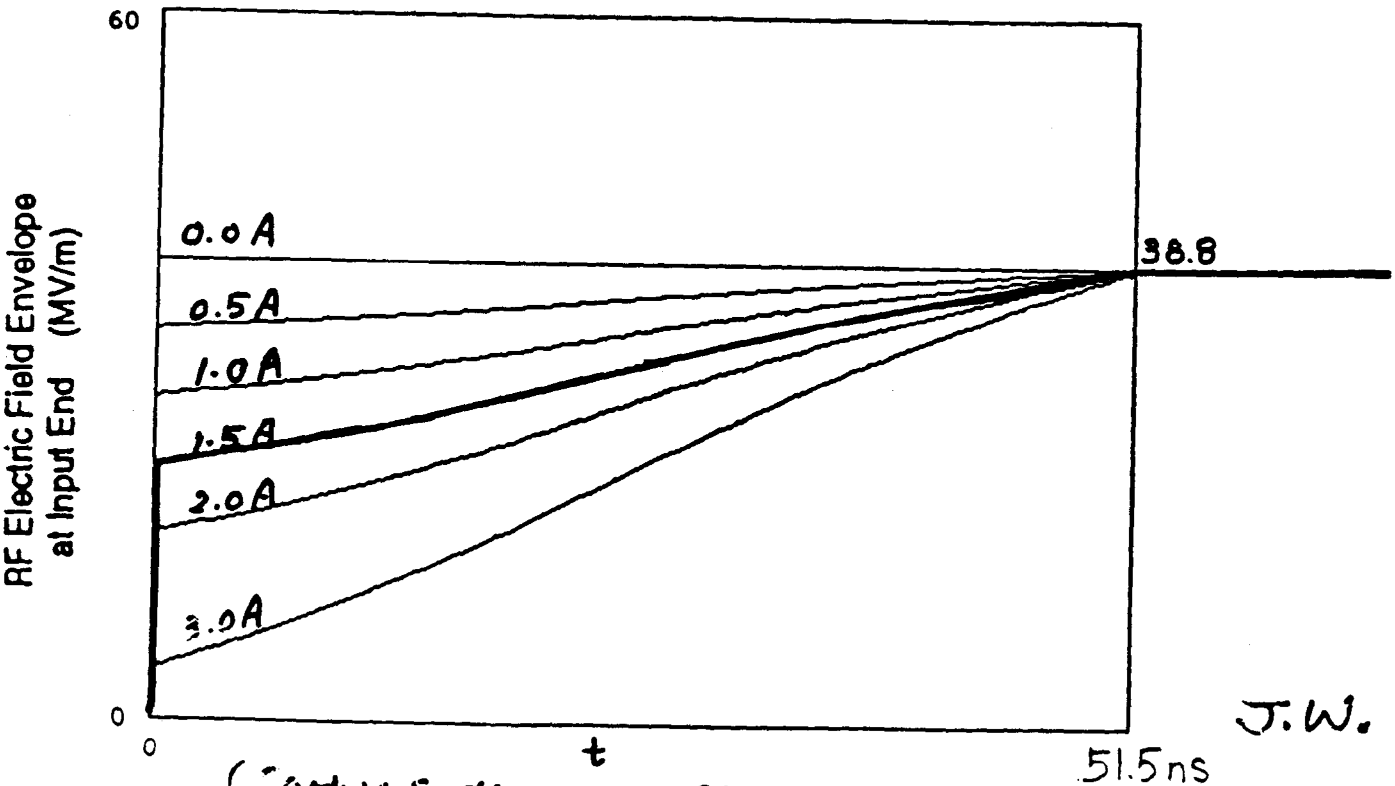

J.W.

(Capture Section needs Special consideration.)

High-Gradient Studies at SLAC

X-Band SW E_s =570MV/m

X-Band TW	E_{acc}(MV/m)	$E_{a,max}$ (MV/m)	Limited by
26cm CI	101	108	Power
75cm CI	79	90	Power
1.8m Detuned	55	65	Power
(CERN) 24cm CI	125	152	Time

Learned a Great Deal about

- RF Processing
- Dark Current Due to Field Emission
- RF Breakdown Phenomenon

Acceleration Test in ASTA

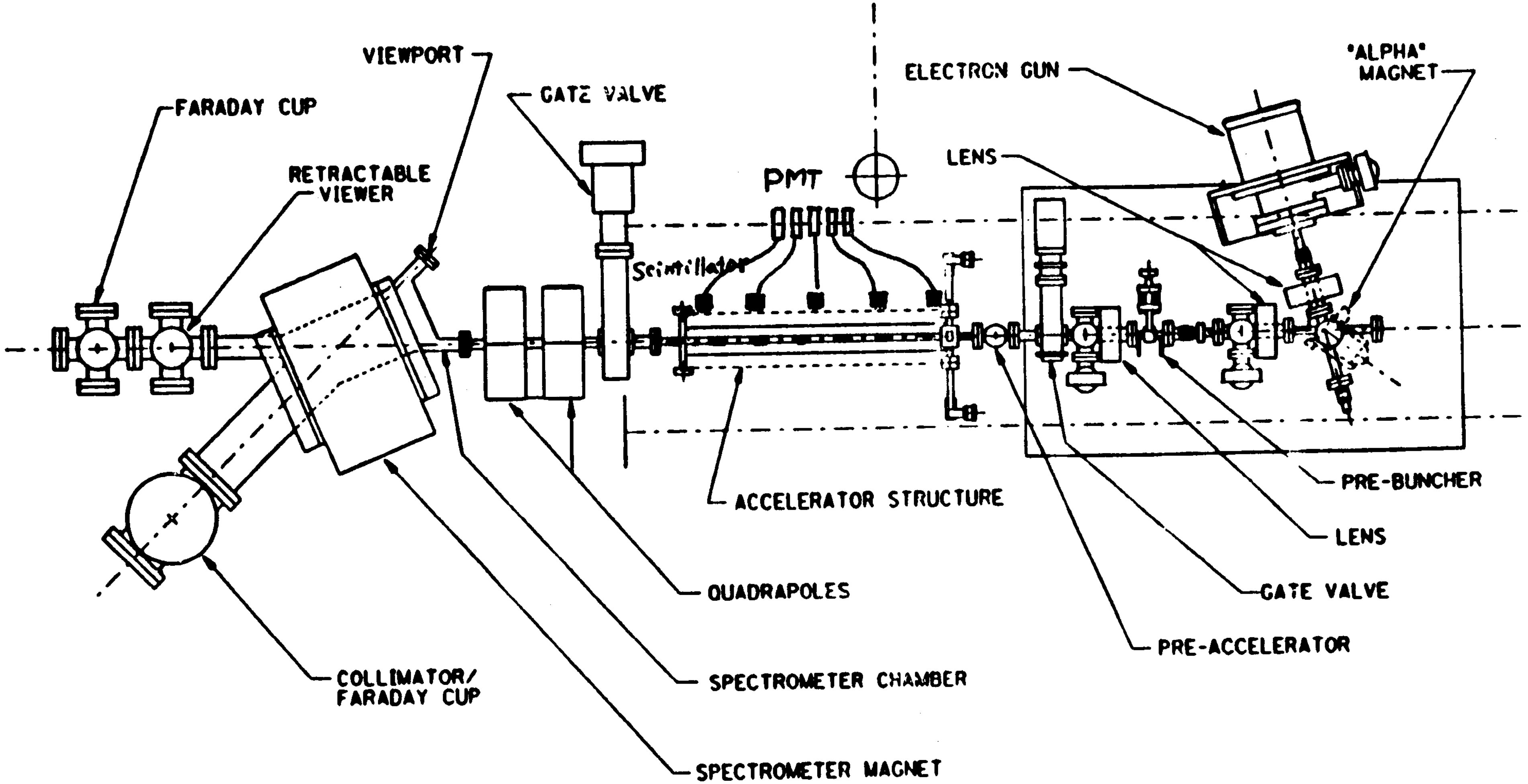

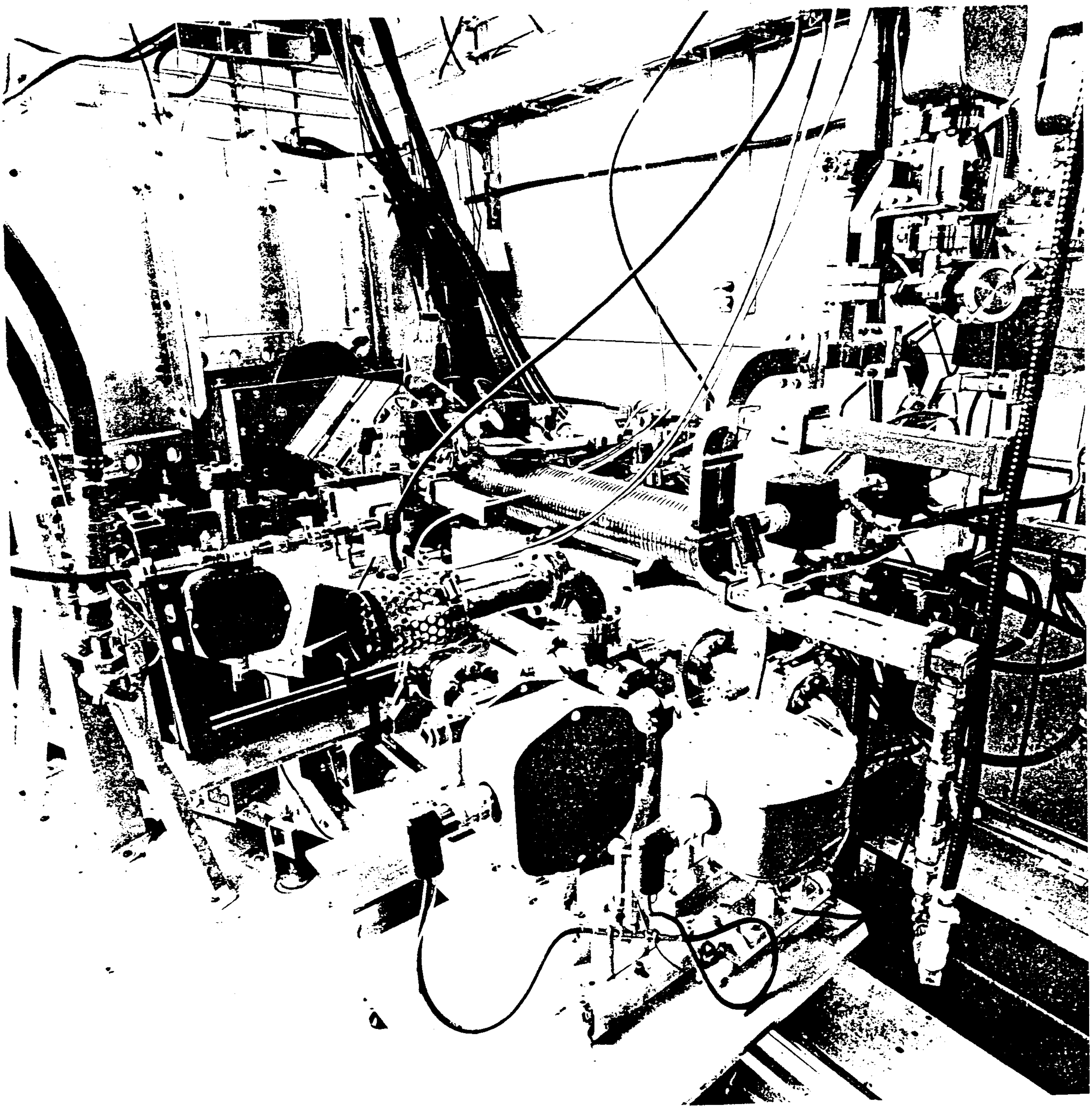

1.8m X-Band TW Section at $E_{acc} = 53 MV/m$

DSA 602 DIGITIZING SIGNAL ANALYZER
date: 4-MAR-94 time: 22:59:35

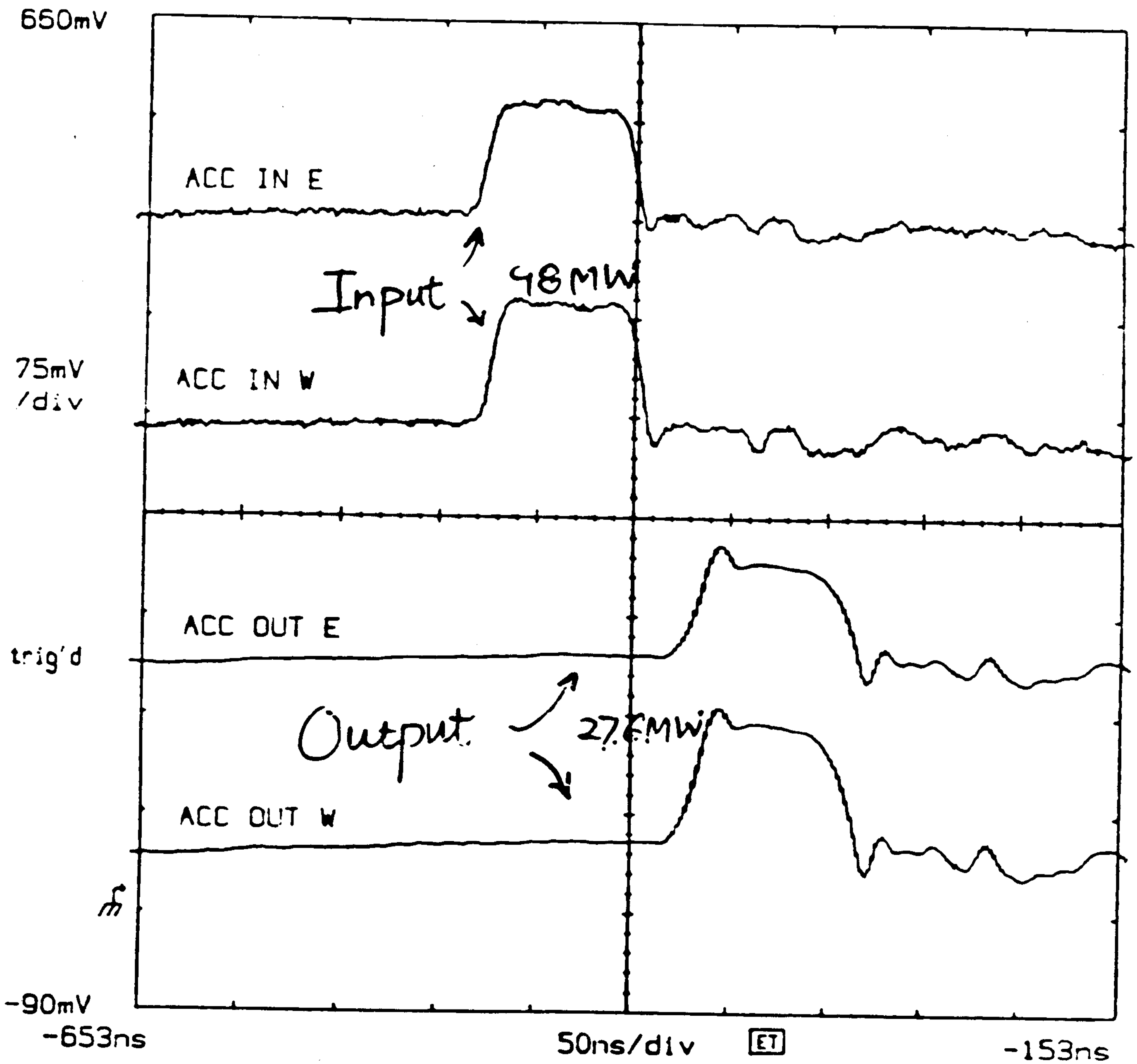

DARK CURRENT PRODUCED BY TW ACCELERATOR SECTIONS

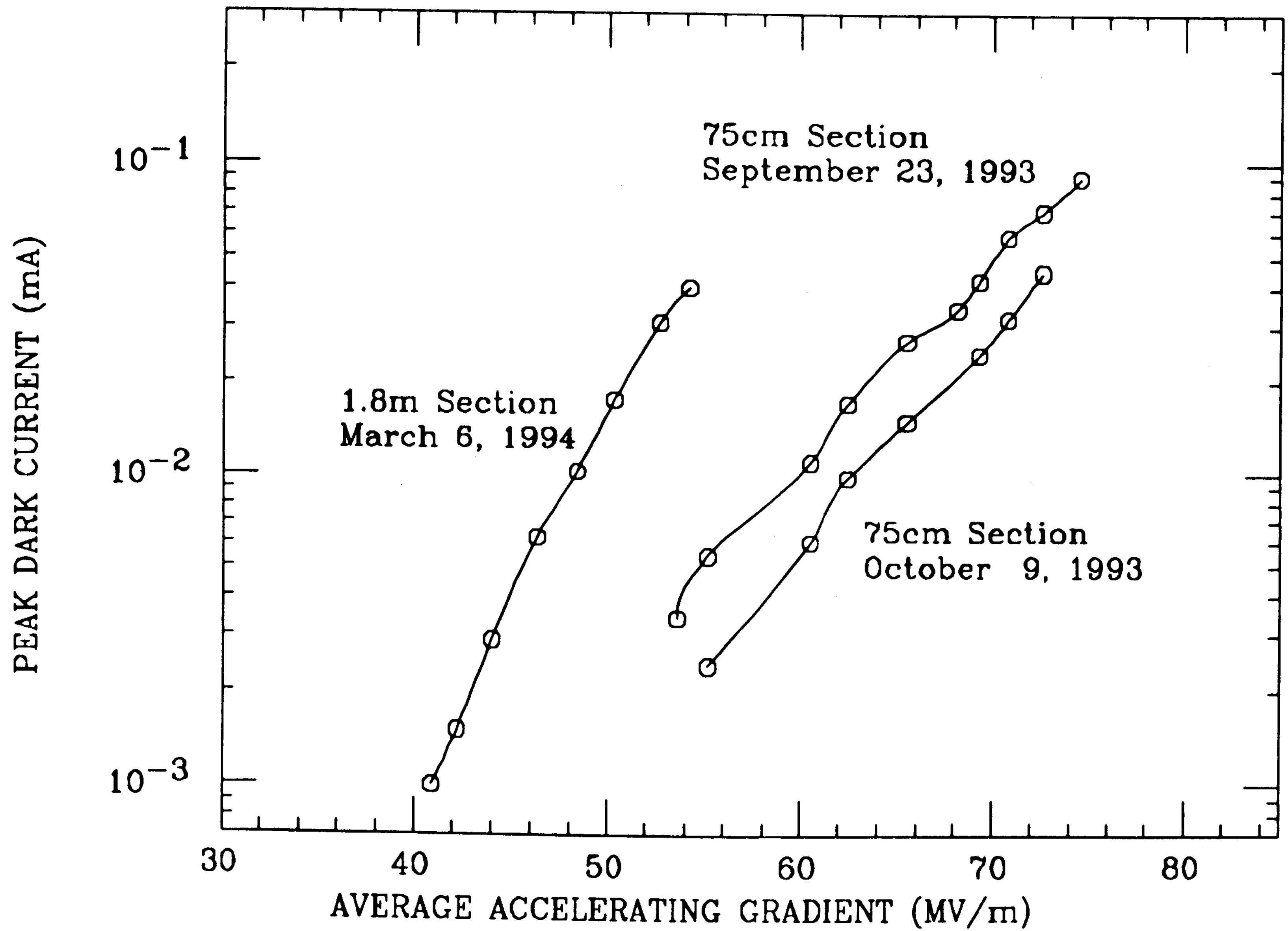

Adolphsen et. al.

Accelerator Structure SETup (ASSET) in the SLC

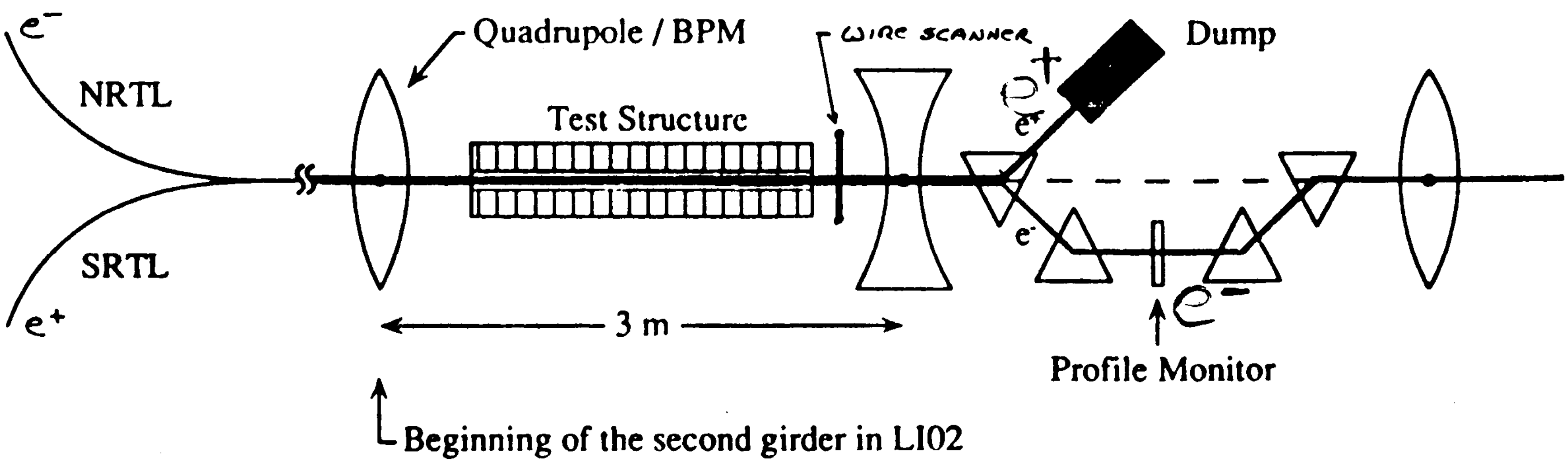

MEASUREMENT OF THE BUNCH-TO-BUNCH TRANSVERSE WAKEFIELD COUPLING IN THE TEST STRUCTURE

- Inject a positron bunch into the linac followed by an electron bunch - the positrons serve as the drive bunch and electrons as the witness bunch.
- Vary the vertical drive bunch amplitude and measure the betatron amplitude of the witness bunch in the linac after the drive bunch is dumped - the ratio of these amplitudes is proportional to the wakefield coupling.
- Repeat for different bunch-to-bunch time separations to measure the temporal dependence of the long-range transverse wakefield.

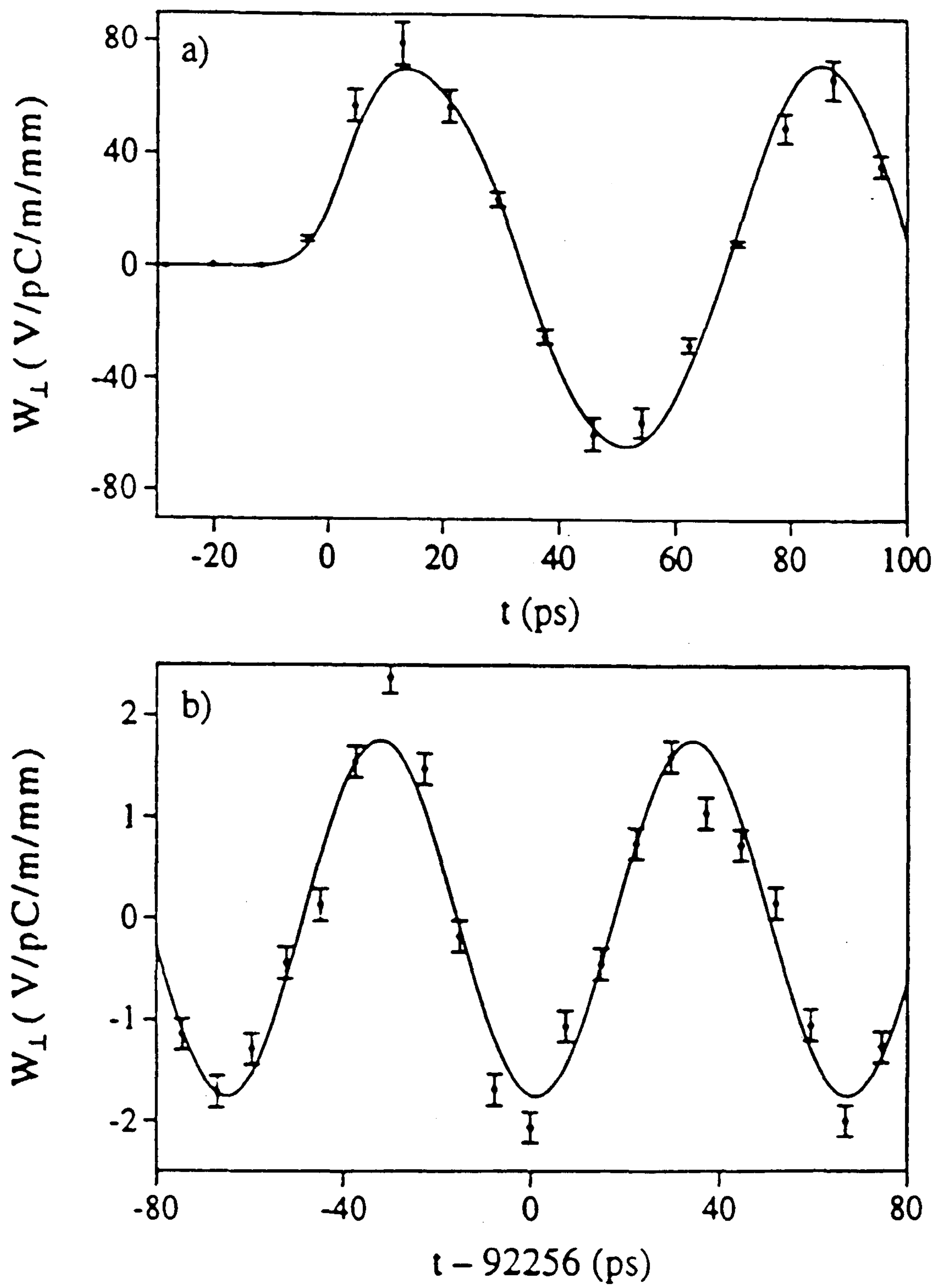

Dipole wakefield measured (a) near the bunch crossing and (b) at a bunch separation of about 92 ns. The solid lines are described in the text.

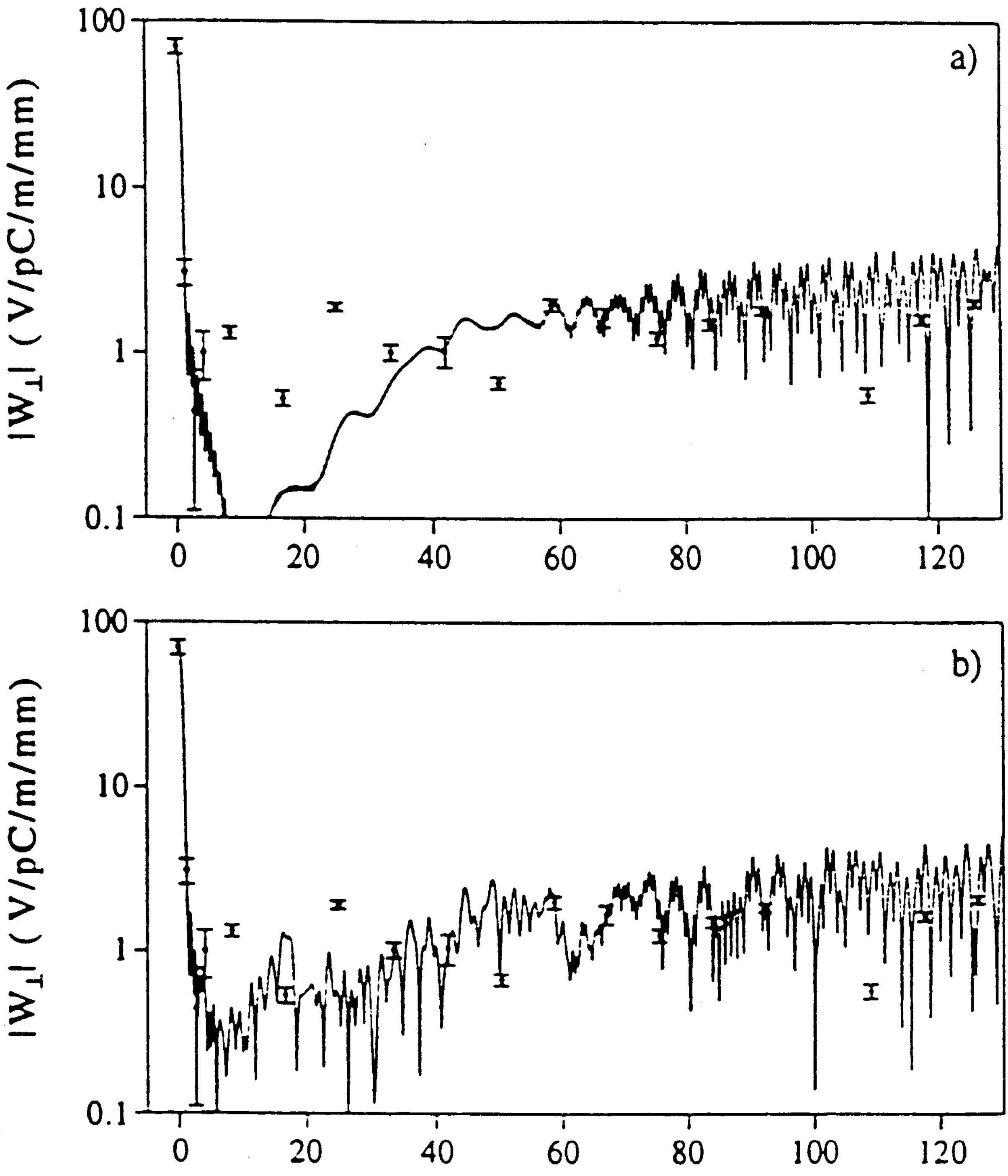

Dipole wakefield amplitude measurements and prediction a) without cell frequency errors and b) with 1.5×10^{-4} rms fractional frequency errors.

1.8 m NLCTA Structure: Short Stacks

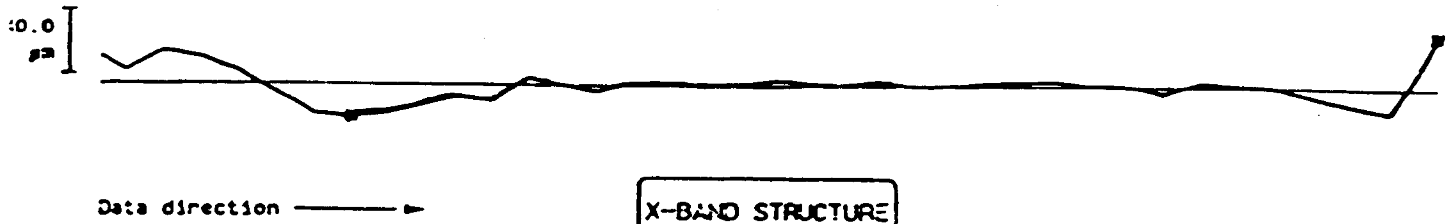

$\sigma_x = 10\mu m$

cells 163 - 200

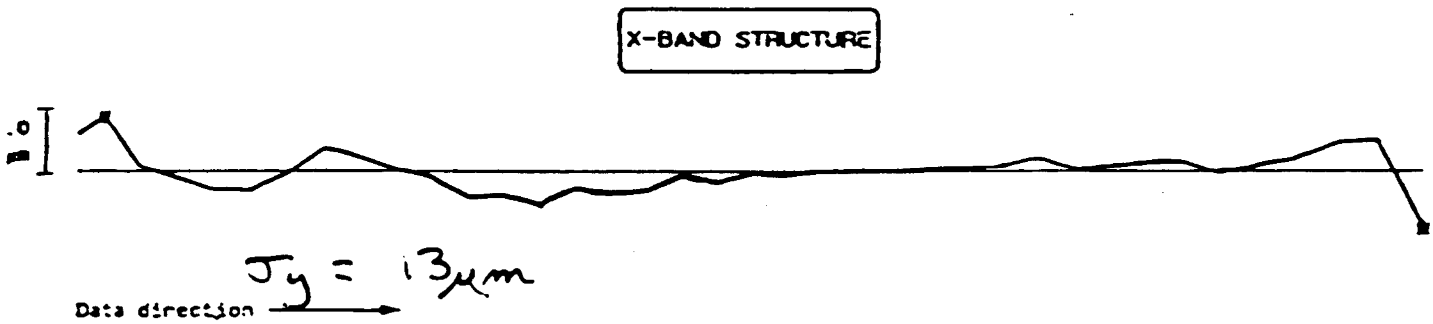

$\sigma_y = 13\mu m$

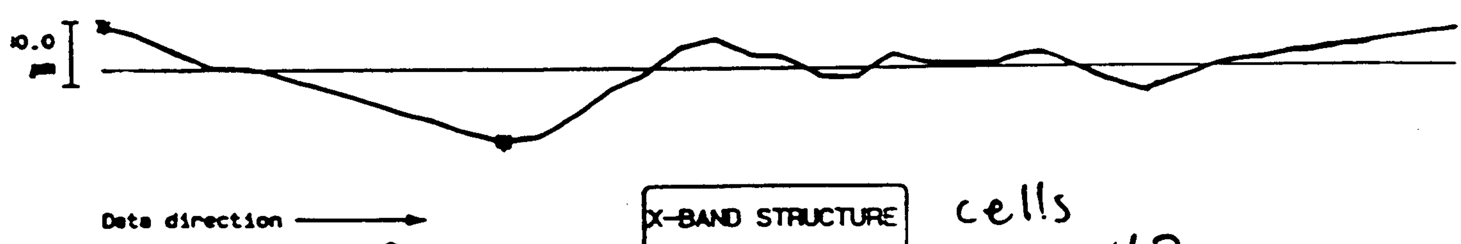

$\sigma_y = 18\mu m$

cells 44 - 82

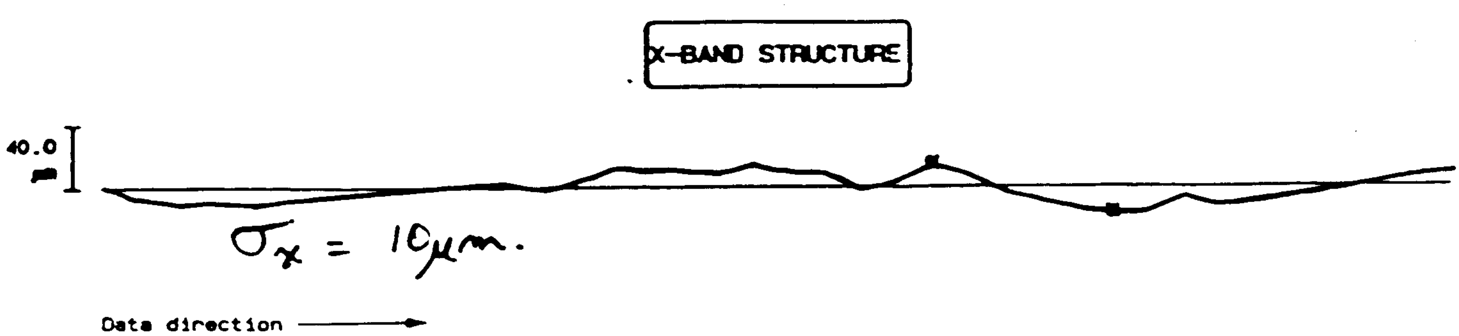

$\sigma_x = 10\mu m.$

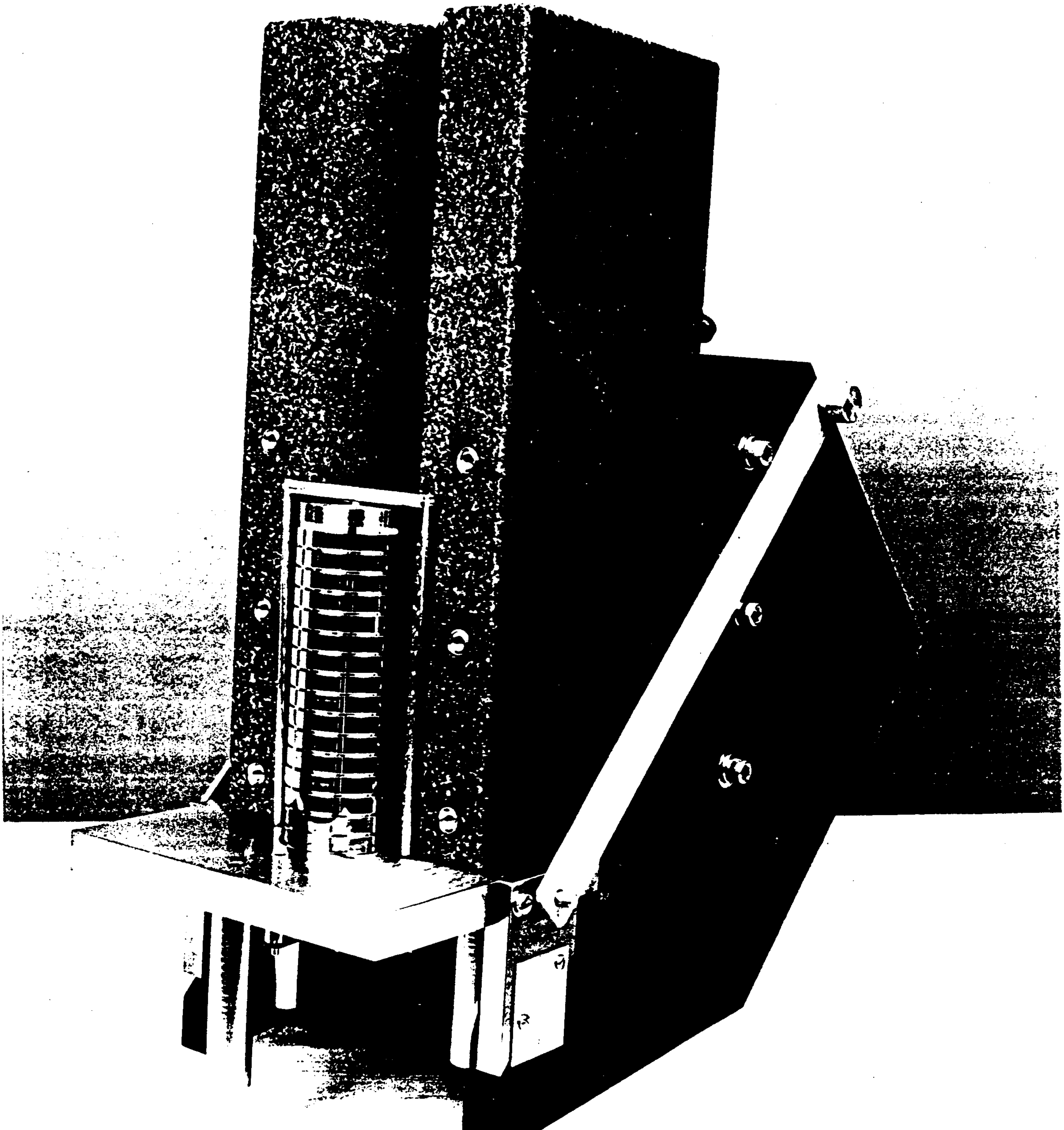

	Regular Machine	Diamond Machine
Dimension Tolerance	±7μm	$\Delta f_0 < 1.5$ MHz ±2μm $\frac{\Delta f_0}{f_0} < 1 \times 10^{-4}$
Surface Finishing	0.2μm	0.025μm

Alignment

Nesting (40-cavity stack) ±20μm

Vee-Block (16-cavity stack) ±4μm

MANIF FREQS, BG LFS, CONST Q = 6500.

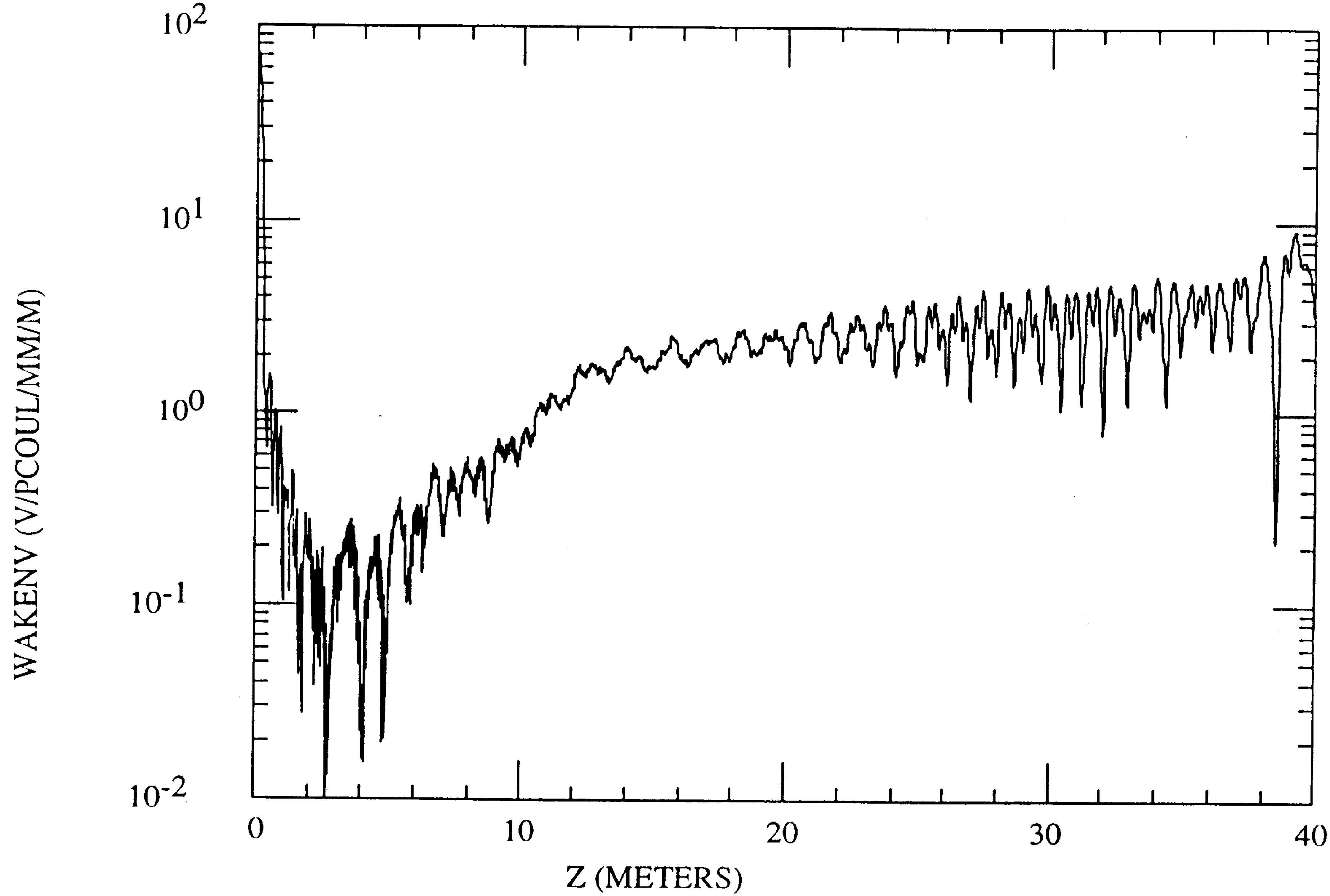

Thompson

Wake envelope for 4 interleaved structures

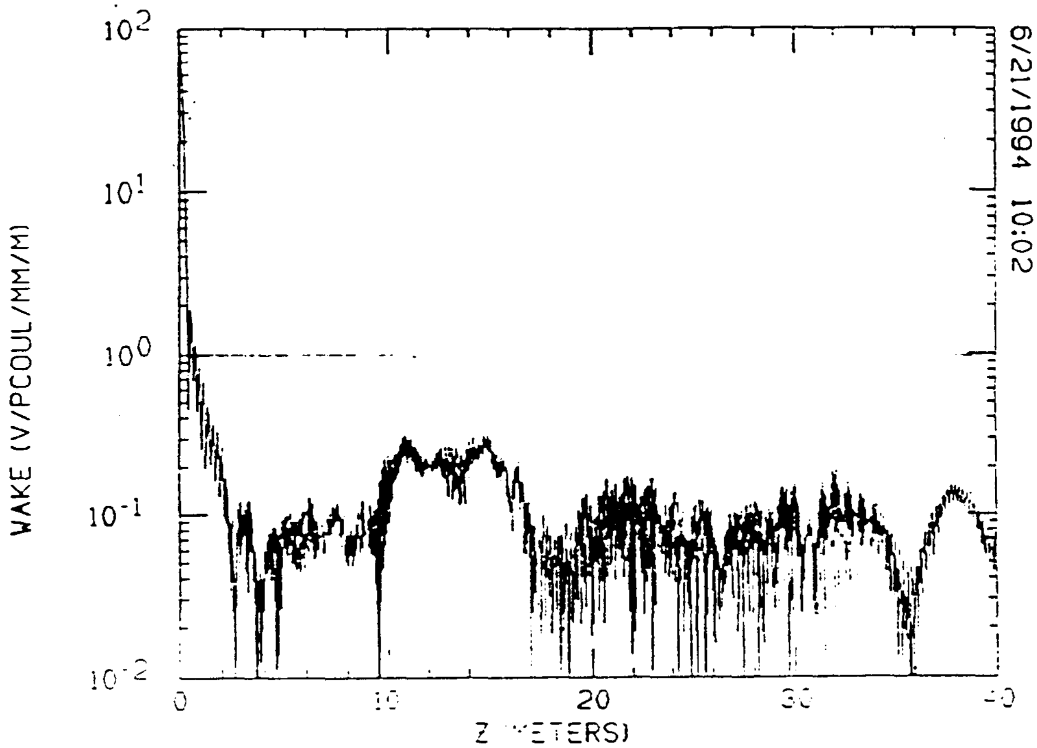

No freq. errors

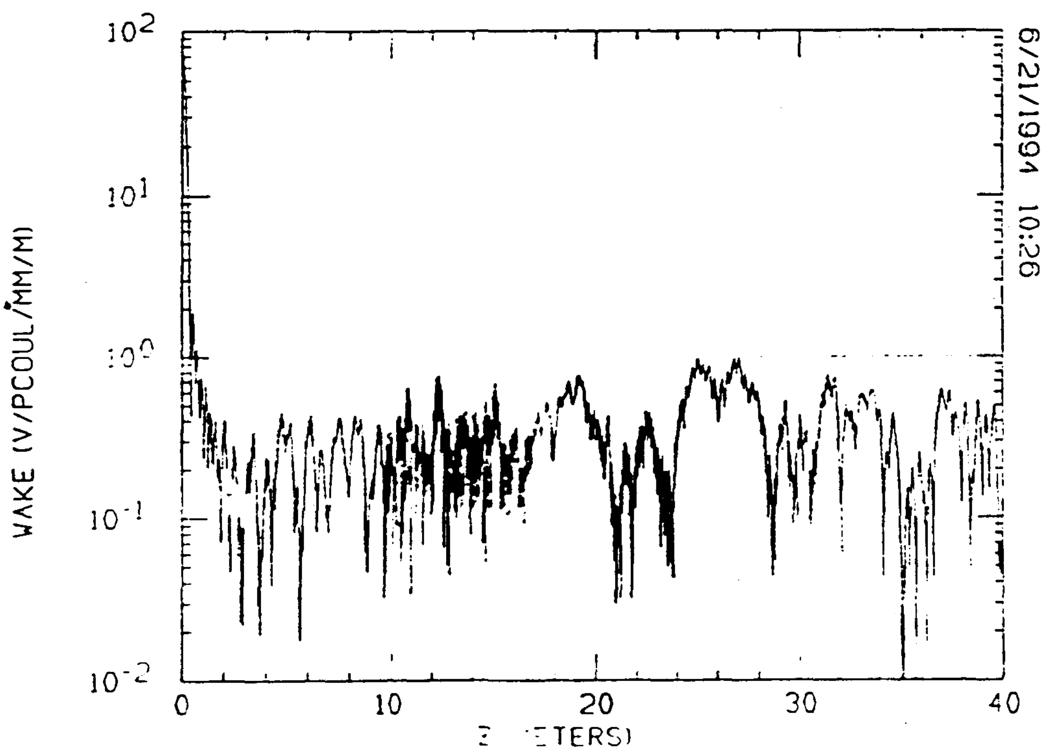

$\sigma_{\epsilon,sys} = 1\times10^{-4}$ freq errors (typical seed)

Considerable degradation of wake due to frequency errors

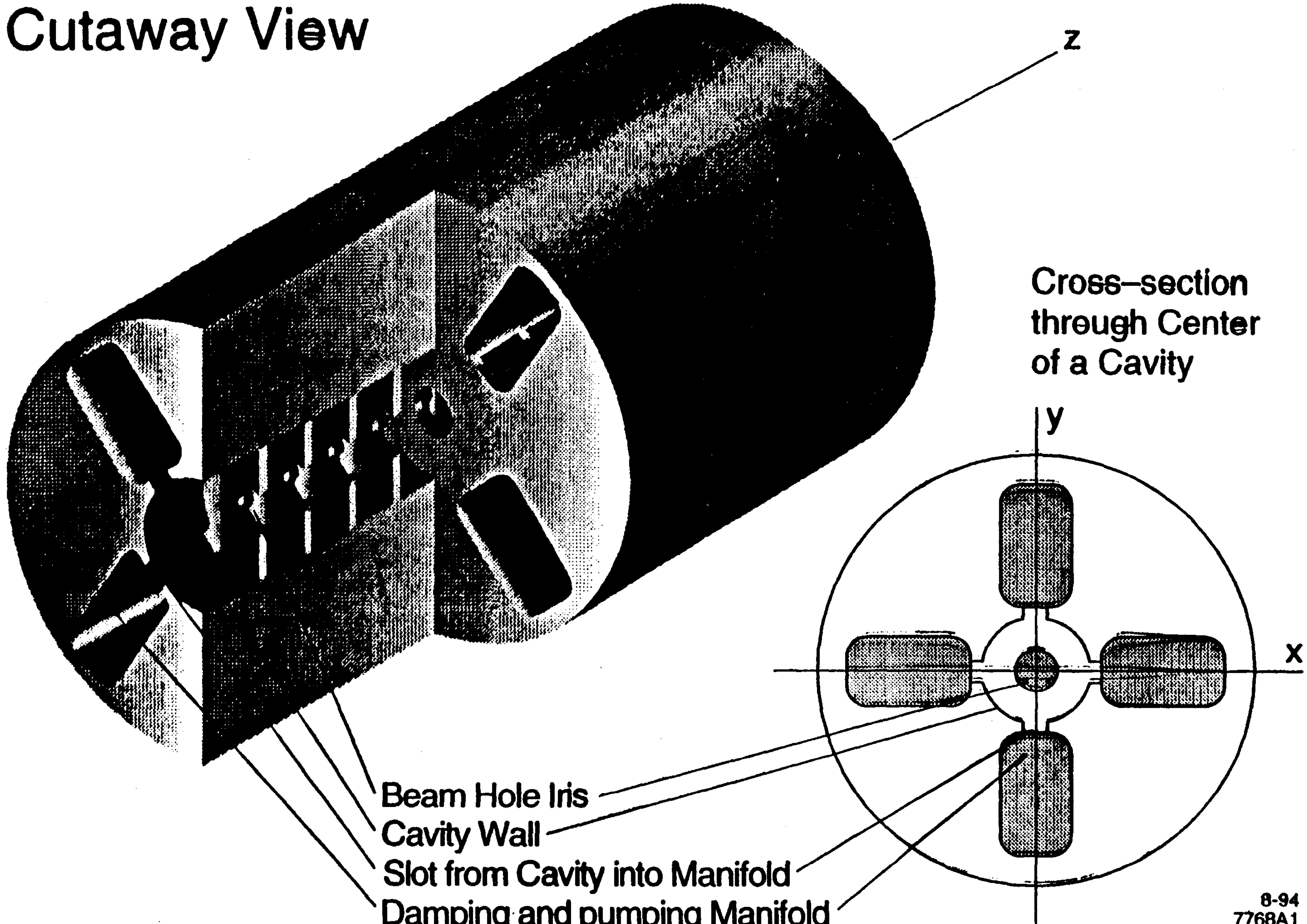
Cutaway View
z
Cross–section
through Center
of a Cavity
y
x
Beam Hole Iris
Cavity Wall
Slot from Cavity into Manifold
Damping and pumping Manifold
8-94
7768A1

① Single-mode (TE₁₀) manifold

② Double-mode

~~③ multi-mode~~

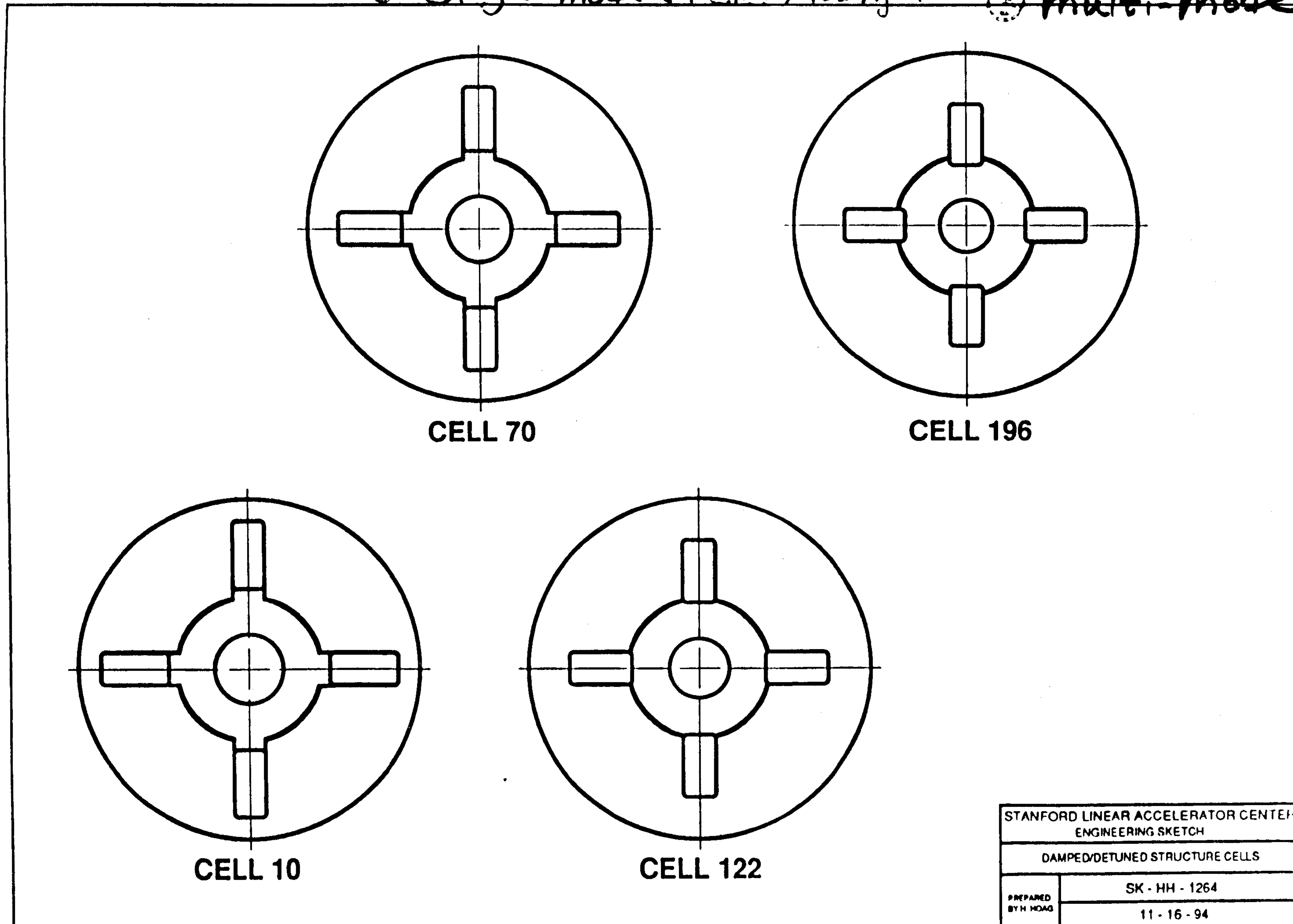

KWOK

< SINGLE-MODE MANIFOLD >

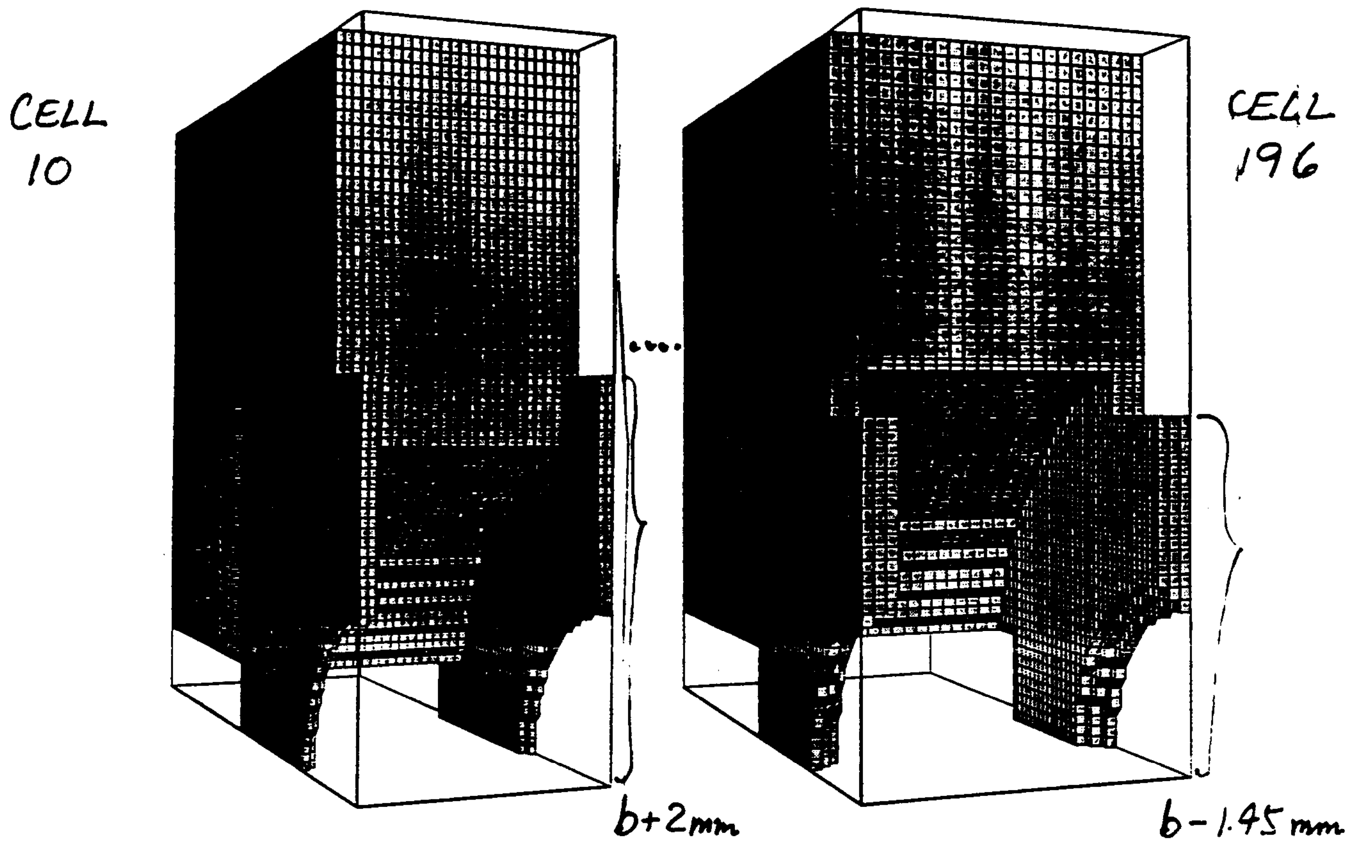

CELL		10	70	122	196
mm.	WG	5 × 10.8	5 × 10.2	5 × 9.7	5 × 9.4
	SLOT	5 × (+2.0)	5 × (+1.0)	5 × (-0.5)	5 × (-1.45)
$\hat{\eta}$		0.083	0.081	0.084	0.068
ϕ_{cr}		58°	67°	72°	83°
f_c (GHz)		12.208	12.910	13.315	13.706
$-\frac{\Delta R}{R} \times 100$		1.53%	1.38%	3.9%	5.0%

Thompson

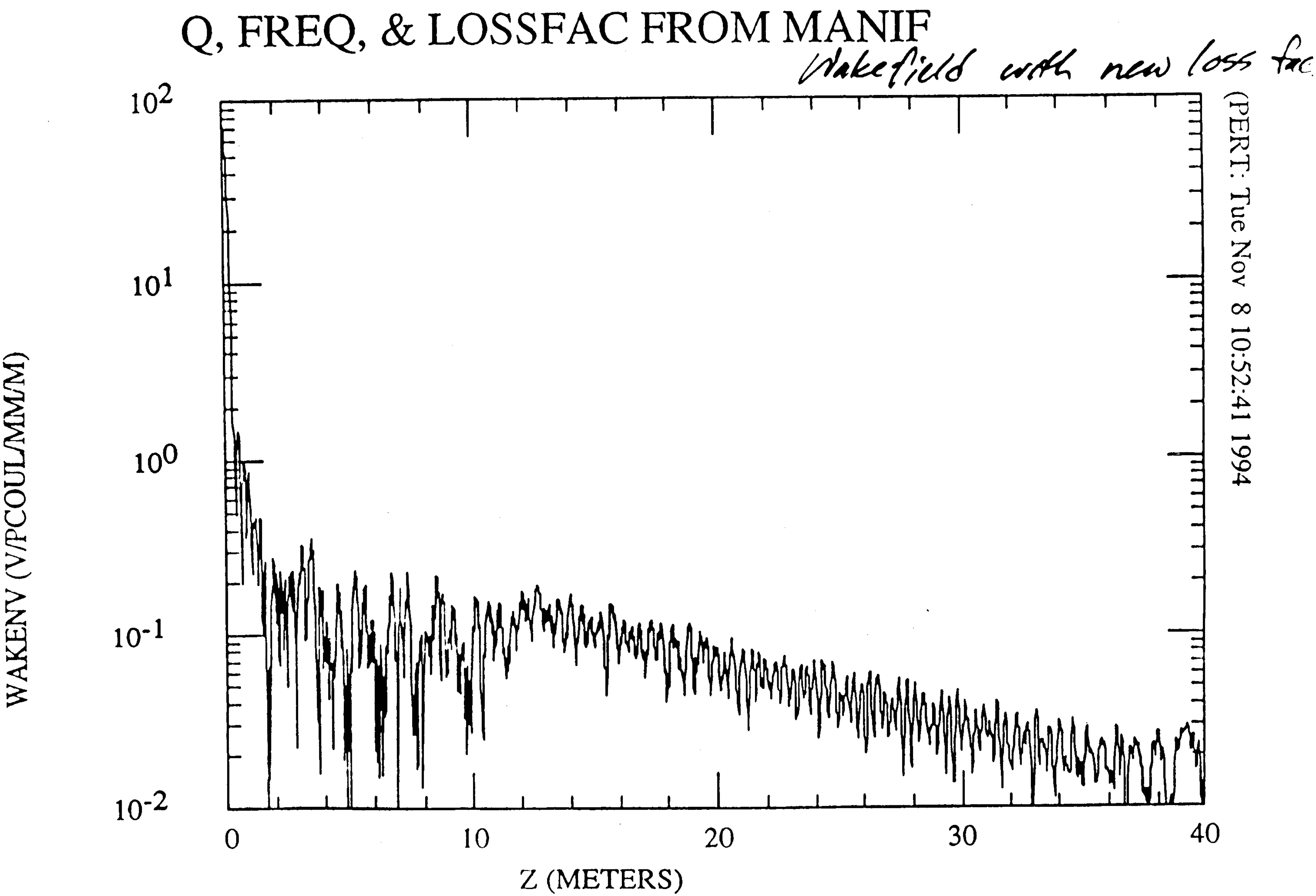

255

• NLC ACCELERATOR PARAMETERS
(Single Mode DDT)

Section length	1.8 m
Phase advance per cell	$2\pi/3$
Iris aperture diameter	1.134–0.786 cm
Cavity diameter	2.228–2.059 cm
Group velocity	$0.12c$–$0.03c$
Filling time	100 ns
Unloaded time constant	205–177 ns
Attenuation parameter	0.498 nepers
Shunt impedance	66.48–83.40 MΩ/m
Elastance ($\omega R/Q$ per unit length)	849–941 V/pC/m
Peak input power/(1.8 m) for 50 MV/m	49.9 MW/m
Peak power per feed for 50 MV/m	89.7 MW
Structure average power dissipation for 50 MV/m, 250-ns pulse length, 180 pps	1.45 kW/m

SUMMARY

1. **Several Short Sections Constructed**
   - Manufacture Studies
   - High Power Tested with E>100MV/m
2. **First 1.8 Detuned Section Constructed**
   - Design Studies
   - Cold Test Without Tuning
   - High Power Test with E>55 MV/m
   - ASSET Wakefield Measurement
3. **Second 1.8m Detuned Section**
   - Rough Machining at Local Company
   - Diamond Machining at KEK
4. **Two 0.9m Detuned Sections for NLCTA Injector**
   - Machining Started
5. **Third 1.8m Section**
   - Detuning with Weak Damping under Study

JLC-I 250 GeV + 250 GeV

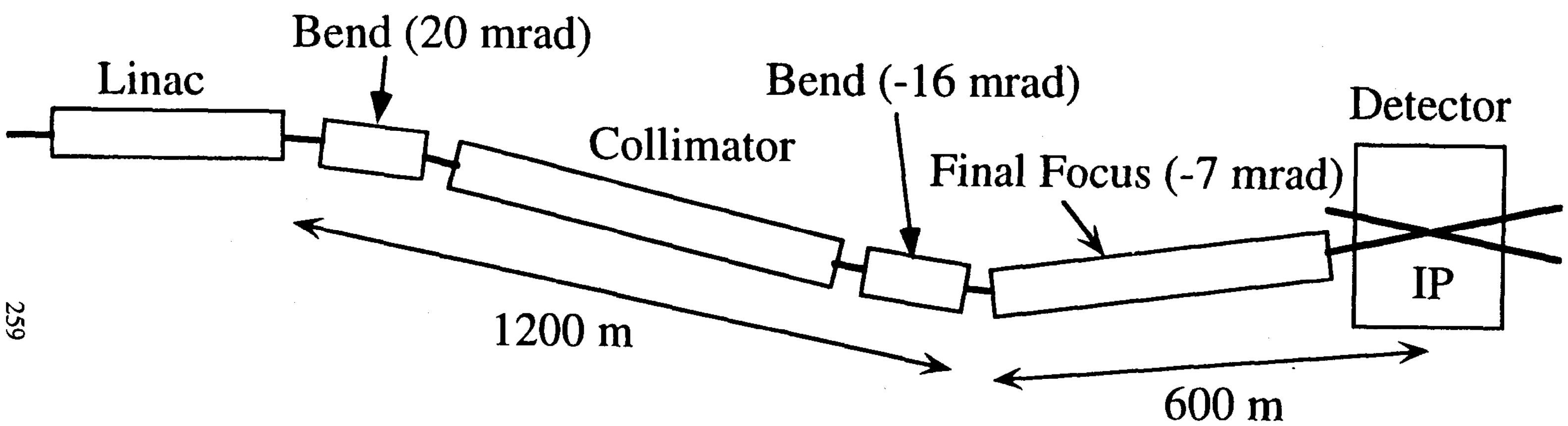

Table 3.5: Characteristics of JLC-I

E_{beam} (GeV)	150	150	150	250	250	250
Band	S	C	X	S	C	X
L (cm^{-2}sec^{-1}) $\times 10^{33}$	3.5	6.6	3.2	4.8	11.	6.3
L (cm^{-2}bunch^{-1}) $\times 10^{29}$	15.3	6.1	2.4	17.5	10.	4.7
rep. rate (Hz)	50	150	150	50	150	150
number of bunches	46	72	90	55	72	90
bunch separation	5.6ns	2.8ns	1.4ns	5.6ns	2.8ns	1.4ns
$N_{e^\pm}$/bunch $\times 10^{10}$	1.56	1.0	0.63	1.30	1.0	0.63
σ_x (nm)	335.	335.	335.	301.	260.	260.
σ_y (nm)	3.92	3.92	3.92	3.04	3.04	3.04
σ_z (μm)	80.	80.	85.	80.	80.	67.
β_x (mm)	10.	10.	10.	10.	10.	10.
β_y (μm)	100.	100.	100.	100.	100.	100.
D_x	0.21	0.13	0.090	0.13	0.13	0.071
D_y	18.0	11.5	7.7	13.0	11.5	6.1
disruption angle: θ_o (mrad)	0.88	0.57	0.35	0.49	0.44	0.27
crossing angle: ϕ_c (mrad)	11.0	10.4	9.0	7.3	8.0	7.2
$\langle\Upsilon\rangle$	0.14	0.093	0.059	0.23	0.19	0.15
Υ_{max}	0.47	0.32	0.19	0.78	0.70	0.51
energy loss $\langle\delta\rangle$ (%)	7.0	3.5	1.7	9.0	7.0	4.0
n_γ	1.7	1.1	0.74	1.6	1.4	0.91
A	1.3	0.95	0.74	1.0	0.93	0.66
$1.65 \times P_t^{max}$ (MeV)						
at θ =0.15	26.9	17.2	10.3	22.9	18.2	13.2
R_{mask} (cm)	9.0	5.7	3.5	7.7	6.1	4.4
L_{mask} (m)	0.60	0.38	0.23	0.51	0.41	0.29
$\eta_{mask}(L_Q = 2.5\text{m}) \times 10^{-4}$	6.0	1.9	0.60	3.9	2.2	1.0
total energy deposits(GeV)						
and e's/bunch						
ΣE_e(no θ_e cut) $\times 10^5$	1.8	0.60	0.17	5.8	3.0	0.91
ΣN_e(//) $\times 10^4$	6.2	2.0	0.62	7.0	3.9	1.3
$\Sigma E_e(\theta_e > .005) \times 10^4$	13.	4.0	0.55	11.	5.8	1.3
ΣN_e(//) $\times 10^4$	5.4	1.7	0.49	5.1	2.8	0.96
$\Sigma E_e(\theta_e > .050) \times 10^2$	5.4	4.9	0.94	21.	9.2	2.2
ΣN_e(//) $\times 10^3$	8.0	5.7	1.0	11.	9.4	3.2
number of hits(e's)/bunch						
in $\lvert\cos\theta_e\rvert < 0.9$						
$r = 2$ cm	429.4	117.8	63.1	350.2	100.4	81.6
	(188.5)	(21.1)	(5.8)	(69.8)	(34.4)	(11.1)
$r = 5$ cm	76.8	7.3	124.	51.7	21.7	23.3
	(14.6)	(4.7)	(2.8)	(10.9)	(6.8)	(2.9)
$r = 30$ cm	2.3	1.1	0.	1.4	0.3	0.3
	(1.0)	(0.5)	(0)	(0.75)	(0.2)	(0.2)

1 Design of Optics

The design concept of the JLC final focus system has its base on the non-interleaved two-family sextupole chromaticity correction scheme [?]. Table 1 lists the main parameters of the final focus system. The parameters are for the beam energy 250 GeV and we can use the same optics for a lower energy only with scaling of the strengths of magnets. In Table 1, the incoming emittances are somewhat larger than those at the damping ring. We design the focusing optics to accept a beam with a certain amount of blow-up and a emittance dilution. The emittances at the interaction point(IP) are larger than the incoming, since they suffer from optical aberrations including the synchrotron radiation. The beta functions at IP are determined considering the chromaticities and the effects of the synchrotron radiation in the final lenses on their focusing. The focusing components including the final lenses are all conventional and possible to be built under existing technologies.

Table 1: Parameters of the JLC final focus system

Beam energy	E_0	250	GeV
Incoming invariant emittances	$\varepsilon_x/\varepsilon_y$	$3.6\times10^{-6}/5.0\times10^{-8}$	m
Invariant emittances at IP	$\varepsilon_x/\varepsilon_y$	$3.8\times10^{-6}/6.0\times10^{-8}$	m
β functions at the IP	β_x^*/β_y^*	10/0.1	mm
Spot sizes at the IP	σ_x^*/σ_y^*	280/3.5	nm
Free area length	ℓ^*	2.5	m
Half aperture of the final quad	a	6.8	mm
Pole-tip field	B_0	1.3	T
Length of the final quad	L_1	2.2	m
Chromaticities of final lenses	ξ_x/ξ_y	3200/43000	
Momentum bandwidth	χ_m	±0.8	%
Total bend angle	θ	7.1	mrad
Length/beam	L_0	590	m

This optical scheme is essentially same as the FFTB optics[?]. The magnet lattice and the optical functions are show in Fig. 1. We have installed several new characteristics on top of the FFTB design. The first one is the long length of the free area for the detector. We set this length ℓ^* to 2.5 m, which is a sufficient length to place the masks for the background,

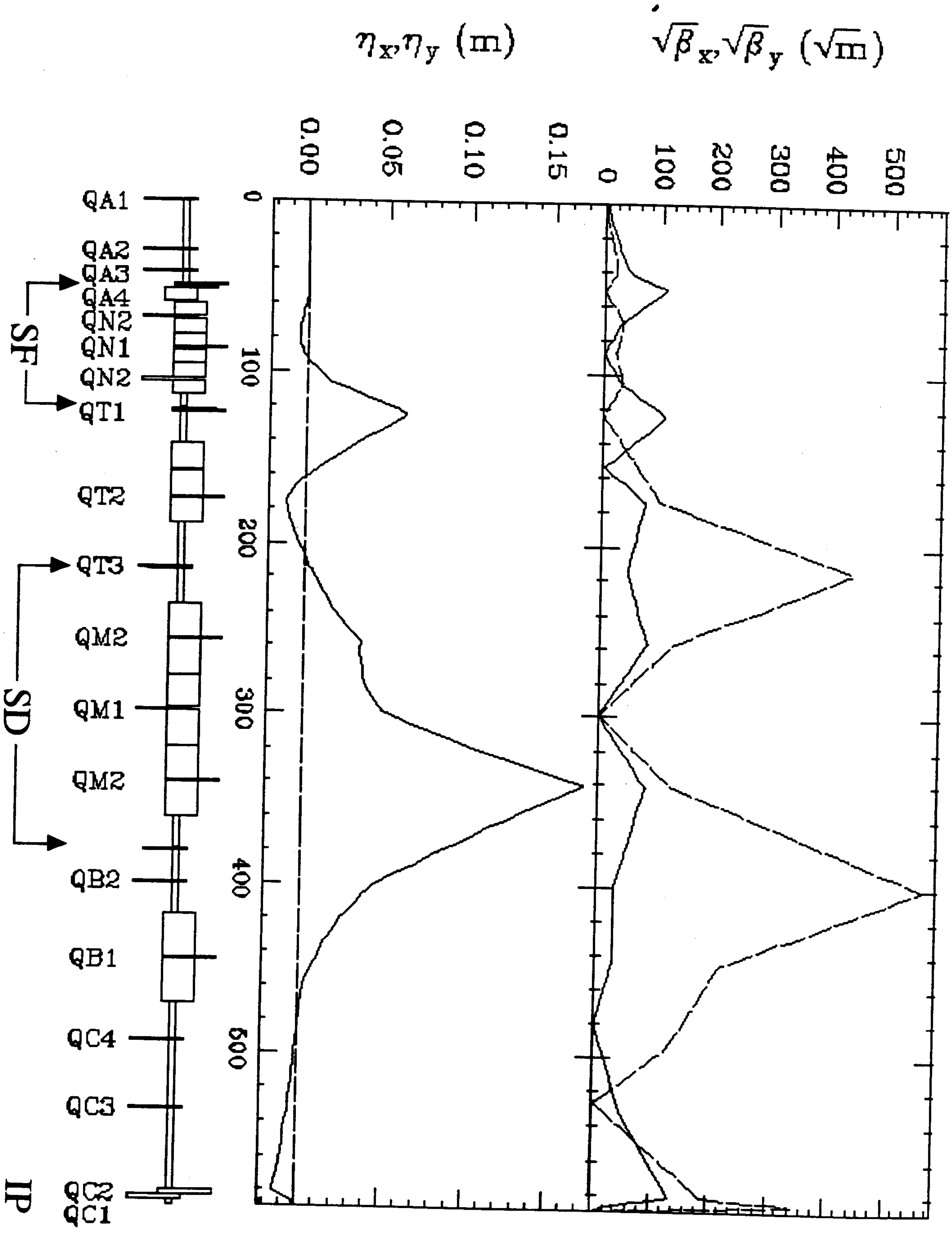

ηx,ηy (m)
√βx,√βy (√m)
0.00
0.05
0.10
0.15
0
100
200
300
400
500
0
100
200
300
400
500
QA1
QA2
QA3
QA4
QN2
QN1
QN2
QT1
QT2
QT3
QM2
QM1
QM2
QB2
QB1
QC4
QC3
QC2
QC1
SF
SD
IP

Beam size at the IP in JLC-FF with and without orbit correction

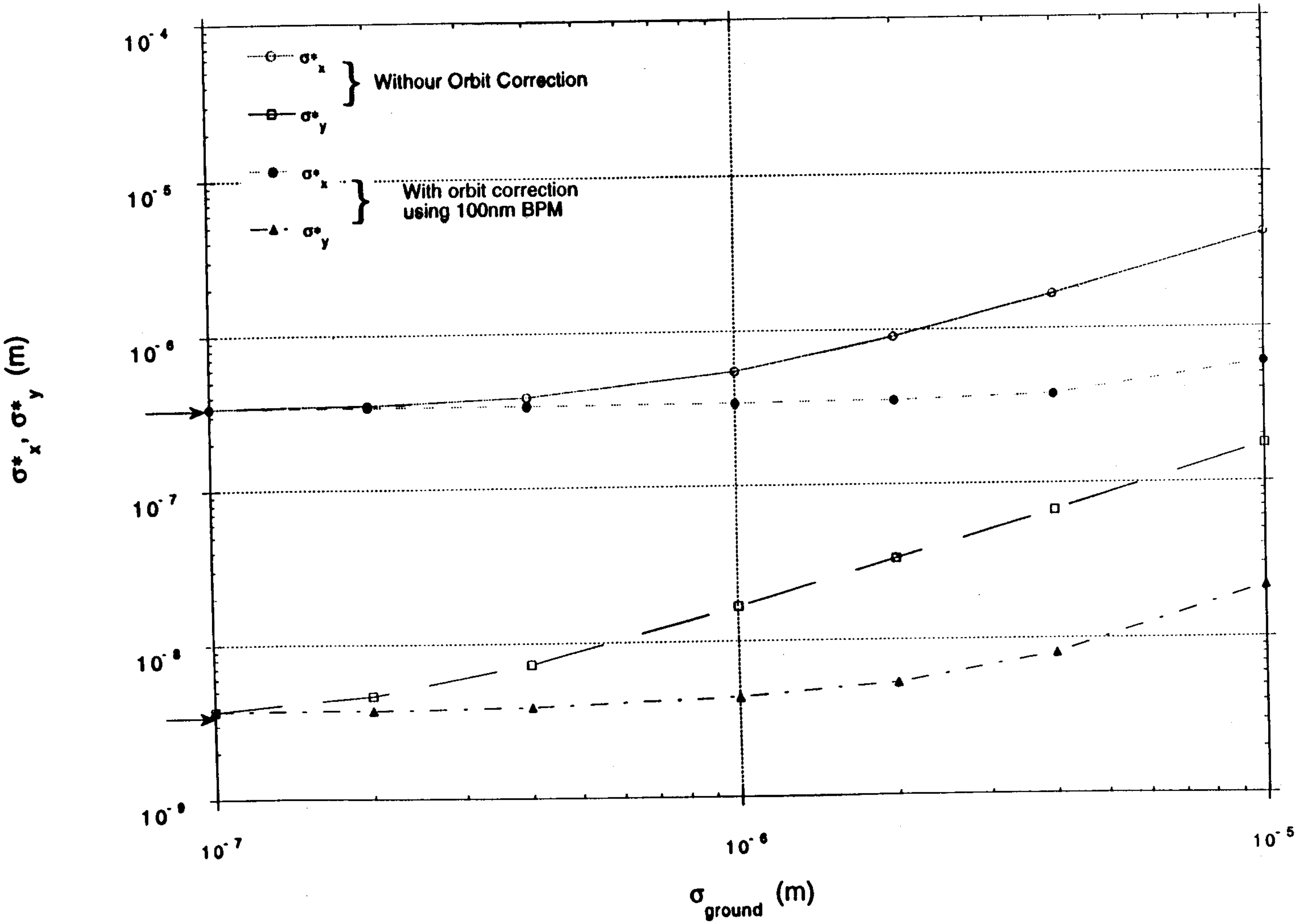

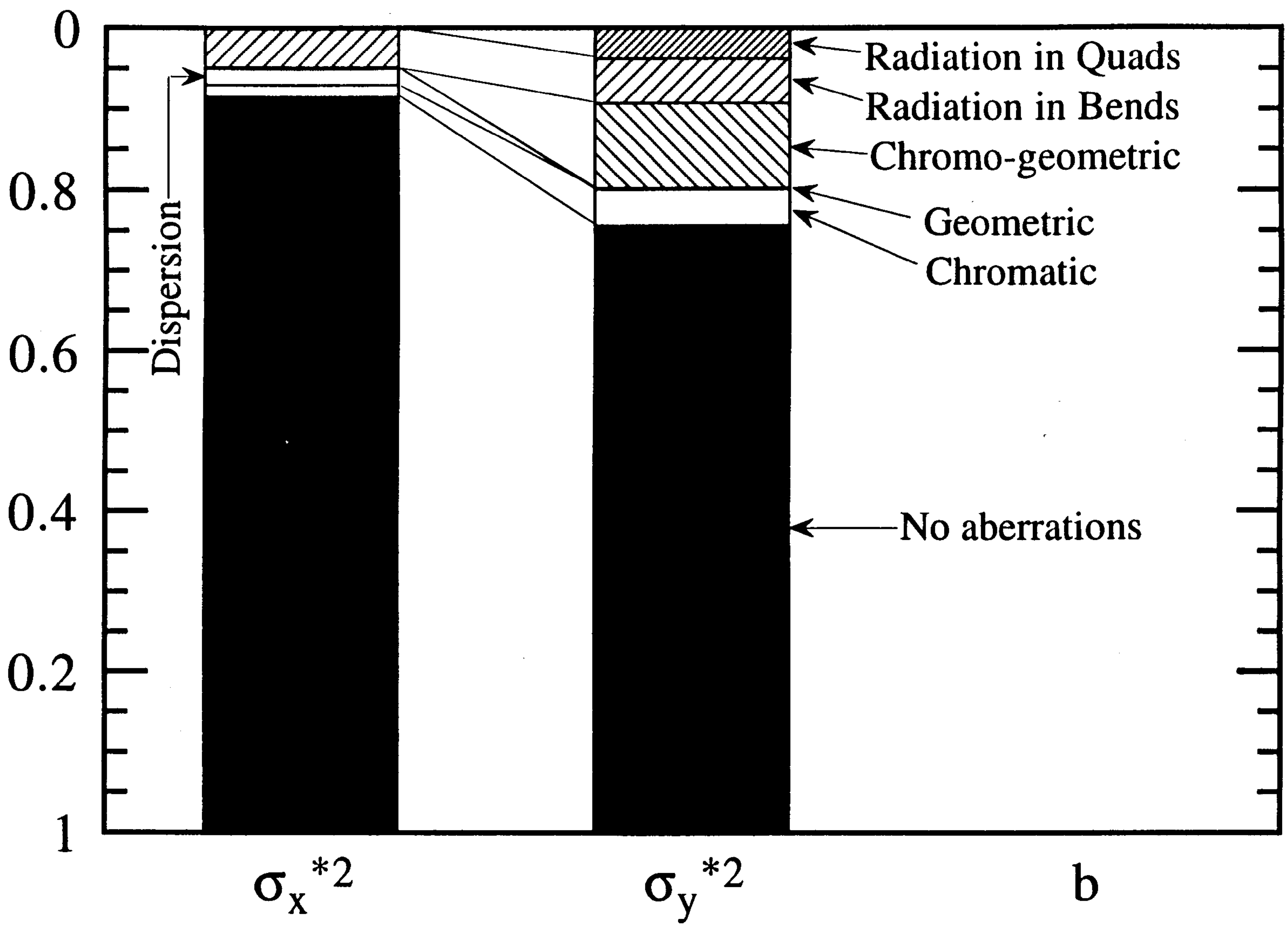
Radiation in Quads
Radiation in Bends
Chromo-geometric
Geometric
Chromatic
No aberrations
Dispersion
0
0.8
0.6
0.4
0.2
1
$\sigma_x{}^{*2}$
$\sigma_y{}^{*2}$
b

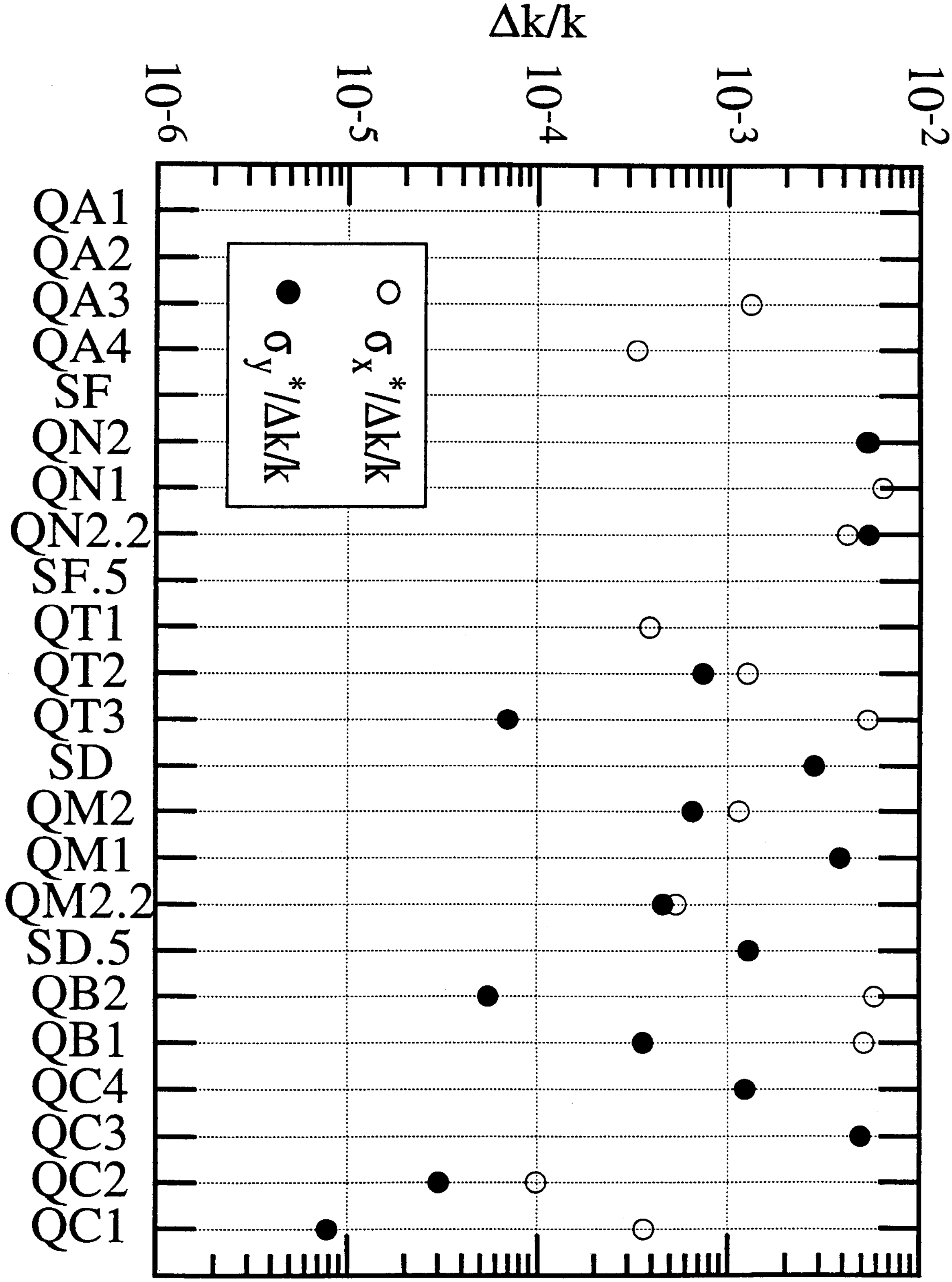
Δk/k
10-6
10-5
10-4
10-3
10-2
σx*/Δk/k
σy*/Δk/k
QA1
QA2
QA3
QA4
SF
QN2
QN1
QN2.2
SF.5
QT1
QT2
QT3
SD
QM2
QM1
QM2.2
SD.5
QB2
QB1
QC4
QC3
QC2
QC1

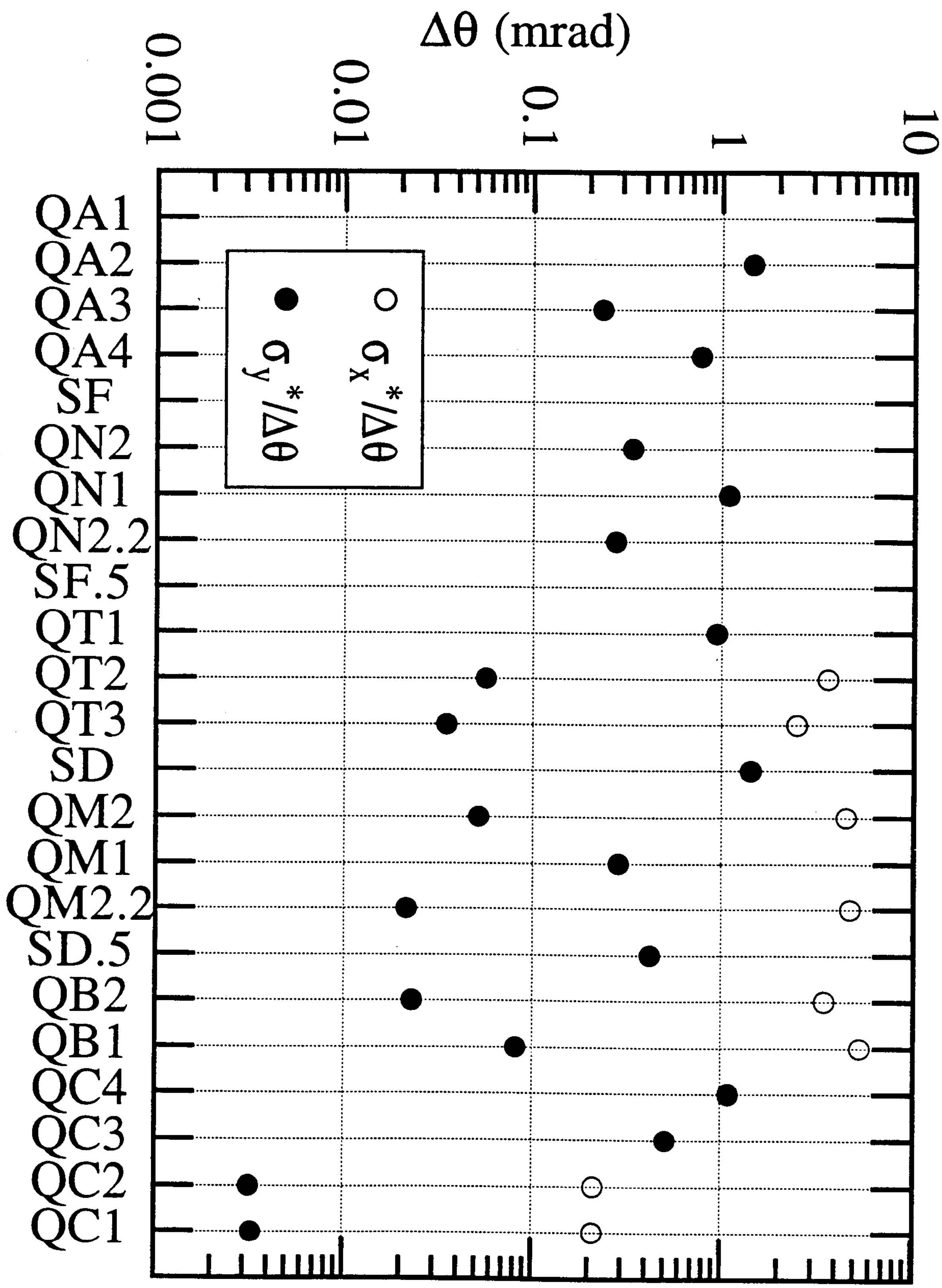
Δθ (mrad)
0.001
0.01
0.1
1
10
σx*/Δθ
σy*/Δθ
QA1
QA2
QA3
QA4
SF
QN2
QN1
QN2.2
SF.5
QT1
QT2
QT3
SD
QM2
QM1
QM2.2
SD.5
QB2
QB1
QC4
QC3
QC2
QC1

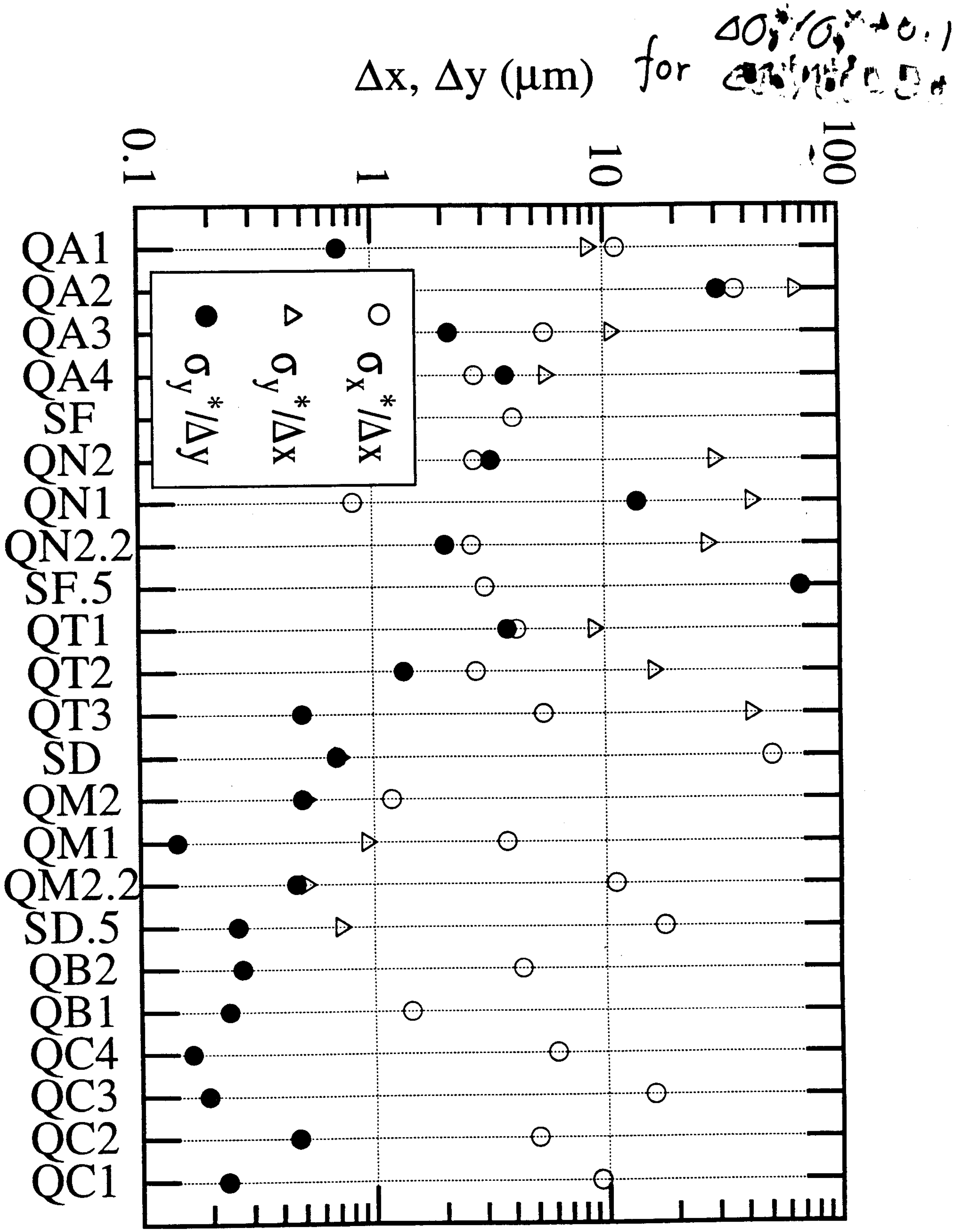
Δx, Δy (μm)
0.1
1
10
100
QA1
QA2
QA3
QA4
SF
QN2
QN1
QN2.2
SF.5
QT1
QT2
QT3
SD
QM2
QM1
QM2.2
SD.5
QB2
QB1
QC4
QC3
QC2
QC1
σx*/Δx
σy*/Δx
σy*/Δy

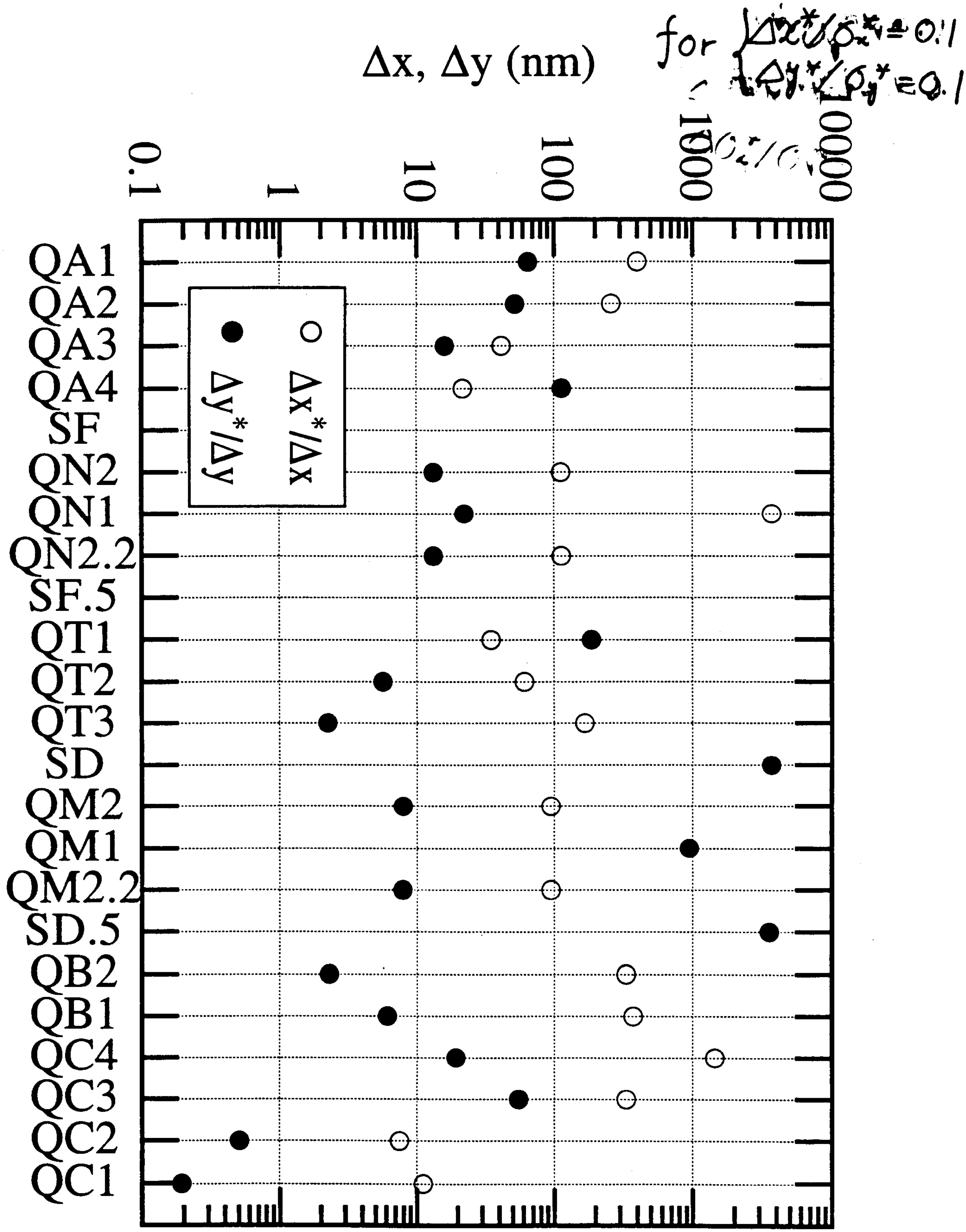
Δx, Δy (nm)
0.1
1
10
100
1000
10000
QA1
QA2
QA3
QA4
SF
QN2
QN1
QN2.2
SF.5
QT1
QT2
QT3
SD
QM2
QM1
QM2.2
SD.5
QB2
QB1
QC4
QC3
QC2
QC1
Δx*/Δx
Δy*/Δy

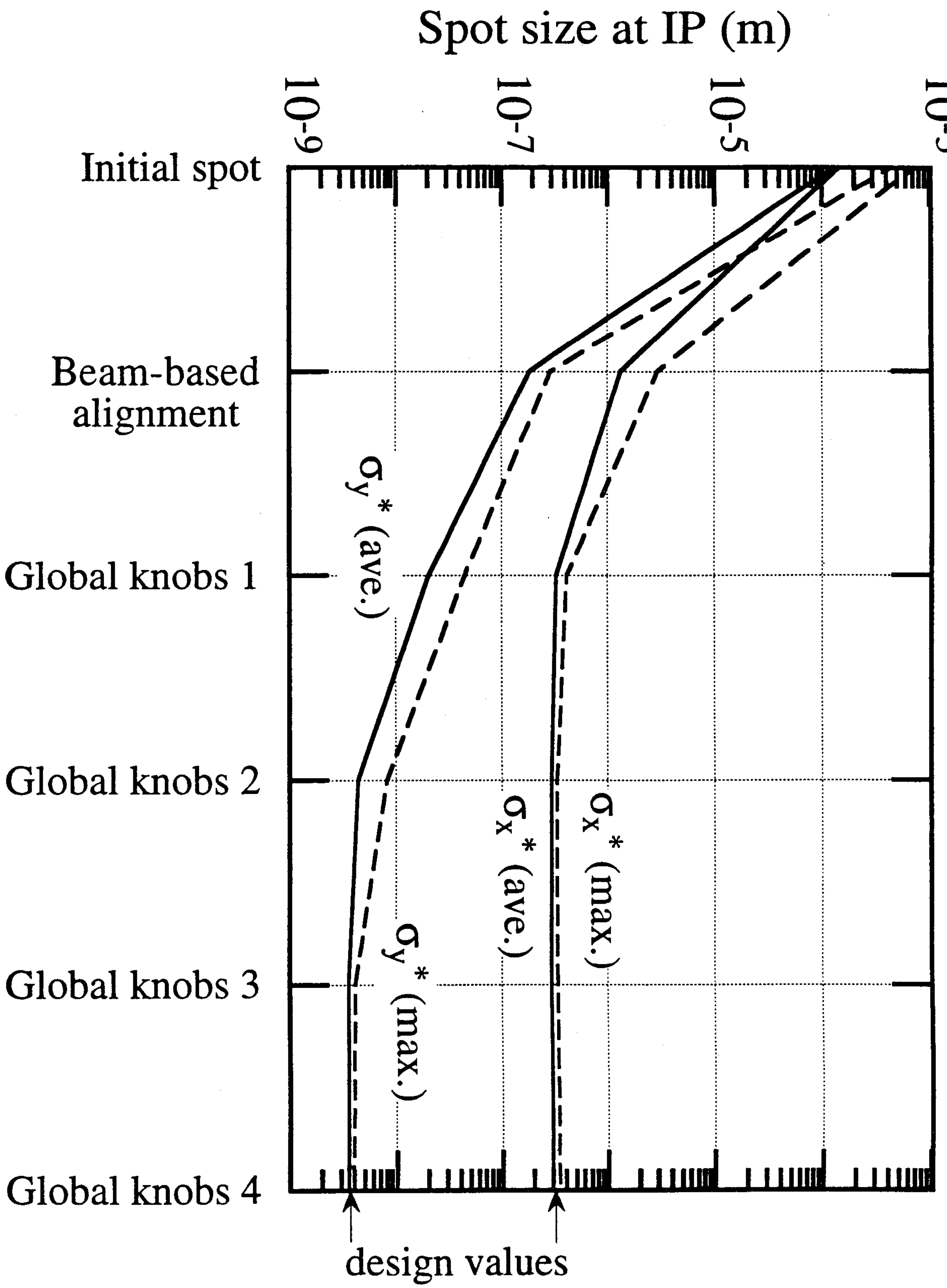

Spot size at IP (m)
10-9
10-7
10-5
10-3
Initial spot
Beam-based alignment
Global knobs 1
Global knobs 2
Global knobs 3
Global knobs 4
σy* (ave.)
σy* (max.)
σx* (ave.)
σx* (max.)
design values

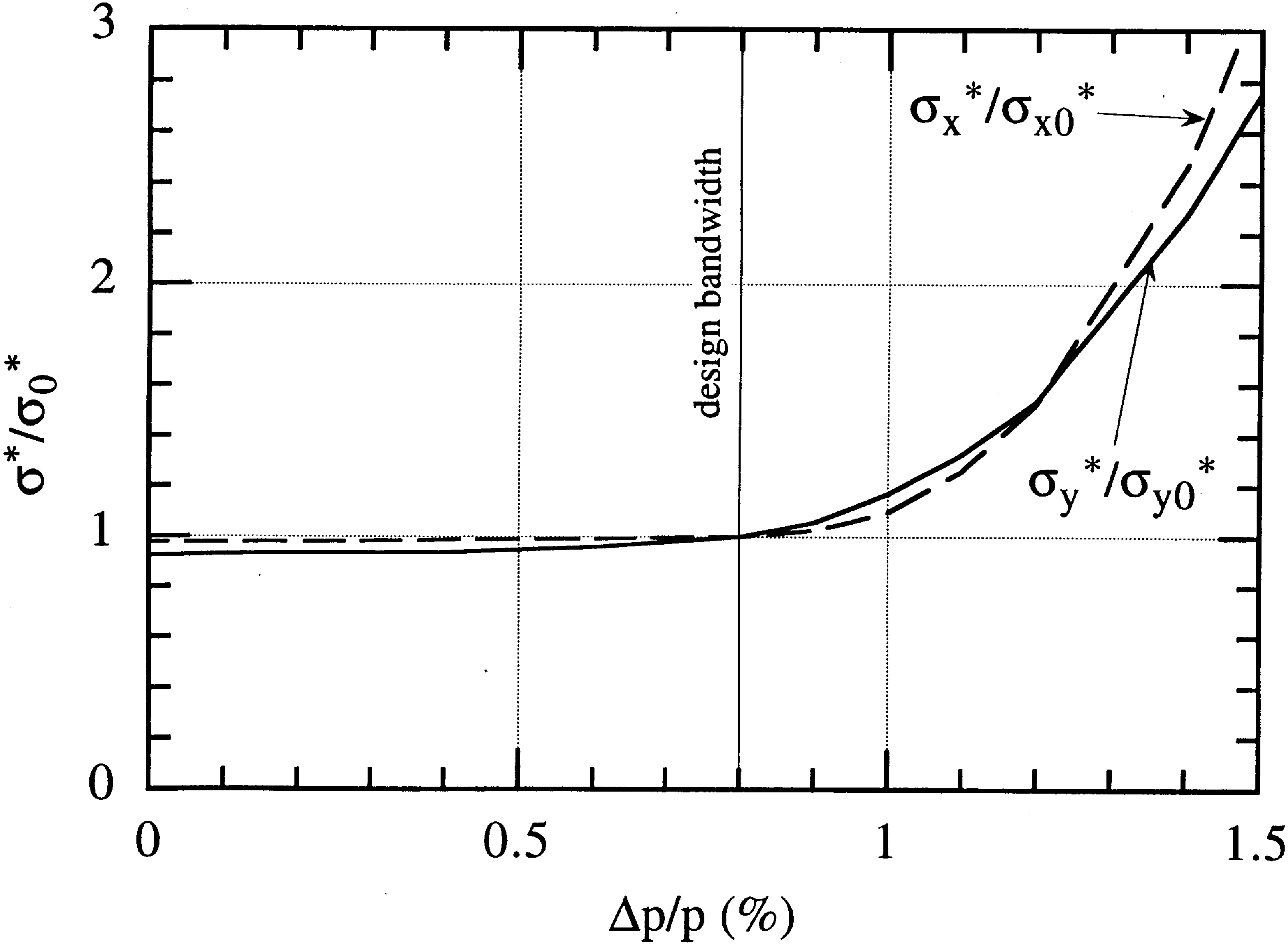

3
2
1
0
0
0.5
1
1.5
$\Delta p/p$ (%)
σ^*/σ_0^*
design bandwidth
σ_x^*/σ_{x0}^*
σ_y^*/σ_{y0}^*

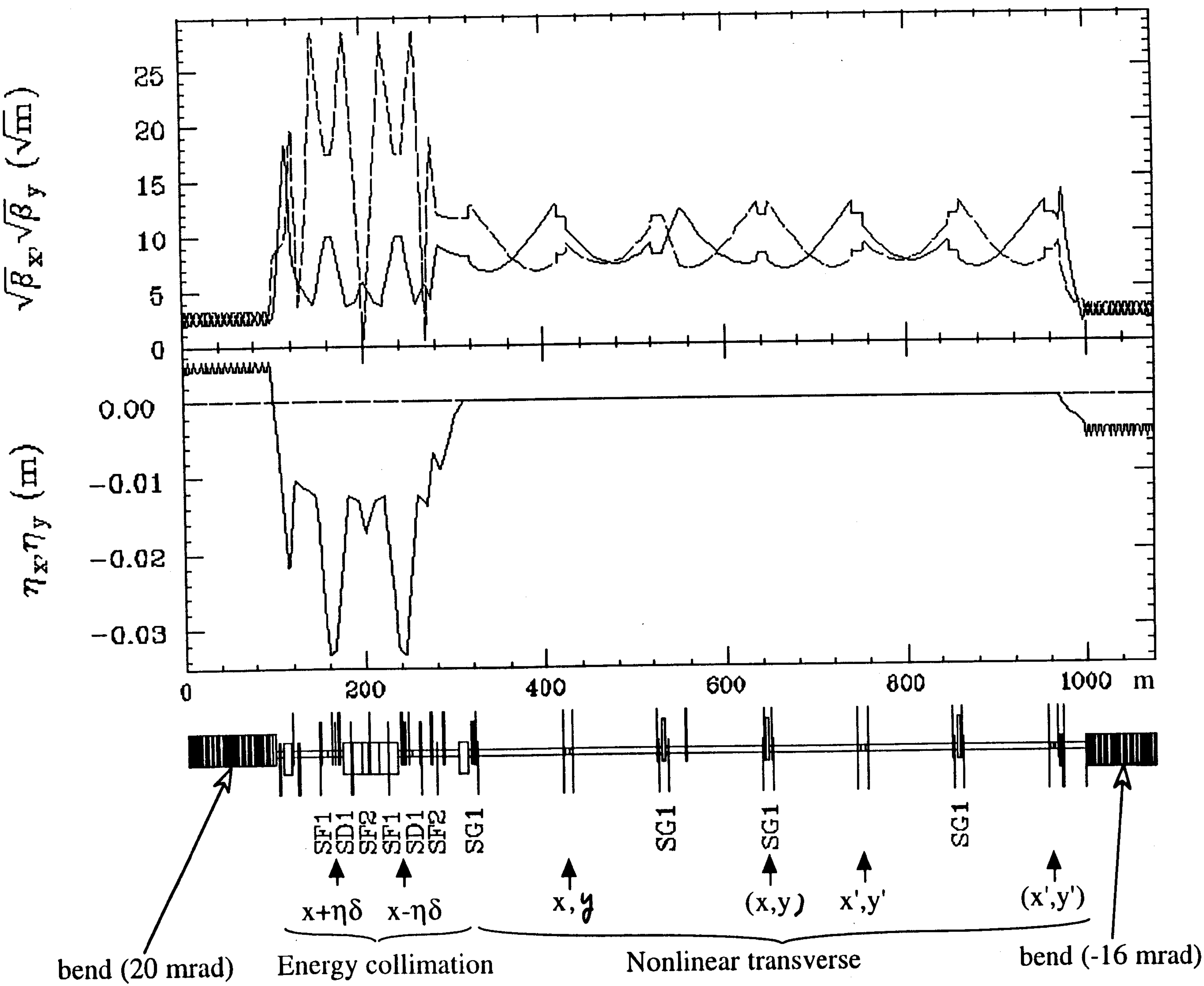

$\sqrt{\beta_x}, \sqrt{\beta_y}$ ($\sqrt{m}$)
η_x, η_y (m)
0
200
400
600
800
1000
m
25
20
15
10
5
0
0.00
-0.01
-0.02
-0.03
SF1
SD1
SF2
SF1
SD1
SF2
SG1
SG1
SG1
SG1
x+ηδ
x-ηδ
x, y
(x,y)
x',y'
(x',y')
bend (20 mrad)
Energy collimation
Nonlinear transverse
bend (-16 mrad)

Table 3: Parameters of the JLC collimation section

Bending section 1 & 2		
Bending angle	20 & -16	mrad
Bending radius	4200	m
Tune $\nu_x = \nu_y$	3.5 & 2.75	
Energy collimator		
Acceptance $\Delta p/p$	±1.5	%
Collimator half aperture	0.5	mm
Beta at col. β_x/β_y	100/300	m
Nonlinear transverse collimator		
Acceptance $x/y = x'/y'$	$\pm6\sigma_x/\pm35\sigma_y$	
Collimator half aperture	0.3	mm
Beta at sextupoles β_x/β_y	67/134	m
Sextupole pole tip field	1	T
Sextupole aperture	5	mm
Sextupole length	4	m

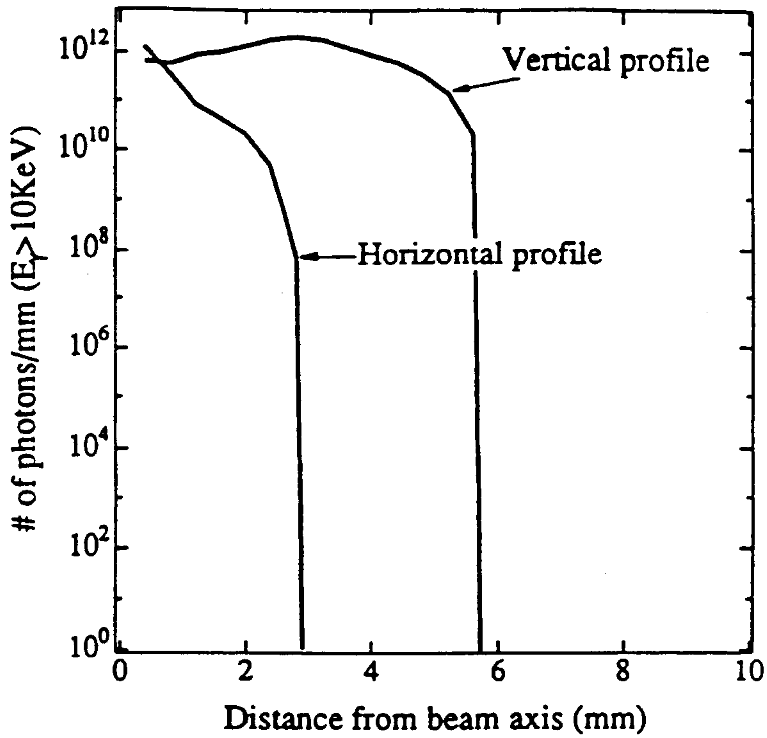

gure 3.20: Profile of synchrotron radiation per train crossing from QC4-QC1 at the front face QC1 seen from IP,*i.e.* 2.5m upstream from IP for E_{beam} =250GeV.

orizontal and vertical directions, which correspond to $22\sigma_x$ and $264\sigma_y$, respectively, there emittance growth due to a wake field by the mask. There is no secondary particles ($e^{\pm}$'s $\mu^{\pm}$'s) created at the mask because no beam tail can hit it. With this mask the synchrotron tion is well collimated to 1 cm at IP.

adrupole Magnets

ere are only 4 quadrupole magnets, QC1 - QC4, in a straight section between the last g magnet and IP. Among them QC2 is the largest radiation source. Here we do not r any mask since a doublet of final quadrupole magnets (QC1 and QC2) is so near IP ere is no way to stop back-scattered synchrotron radiations from the mask. The control rotron radiations from the quadrupole magnets is uniquely provided by the optics of focus system. The optics is carefully determined in order to have a large bore (1.34 cm 1, which is enough for the synchrotron radiations to go through without scattering for collimated at $\pm 6\sigma_x$, $\pm 35\sigma_y$. The tail of the synchrotron radiations is also produced il of beam. Figure 3.20 shows the lateral spread of radiations from QC3,QC4,QC2 itself in front face of QC1, *i.e.* 2.5 m upstream of IP. Tolerable number of photons is x,y > 0.67cm in this figure, which may hit the "iron" pole of QC1 and back-scatter discussed in the previous section there must be tails up to 10^4 photons beyond sharp lateral spreads in Fig.3.20. We show Fig.3.21 to see how the radiations go through g.3.21 cross sectional views of radiations are shown at the entrance and the exit of wo off-axis profiles are those of the radiations with exit beam (after collision) since ngle is 8 mrad at E_{beam} =250GeV and QC1 is 2.4 m long, whereas the profile at that of focusing beam (before collision). Therefore there is no serious background e synchrotron radiations.

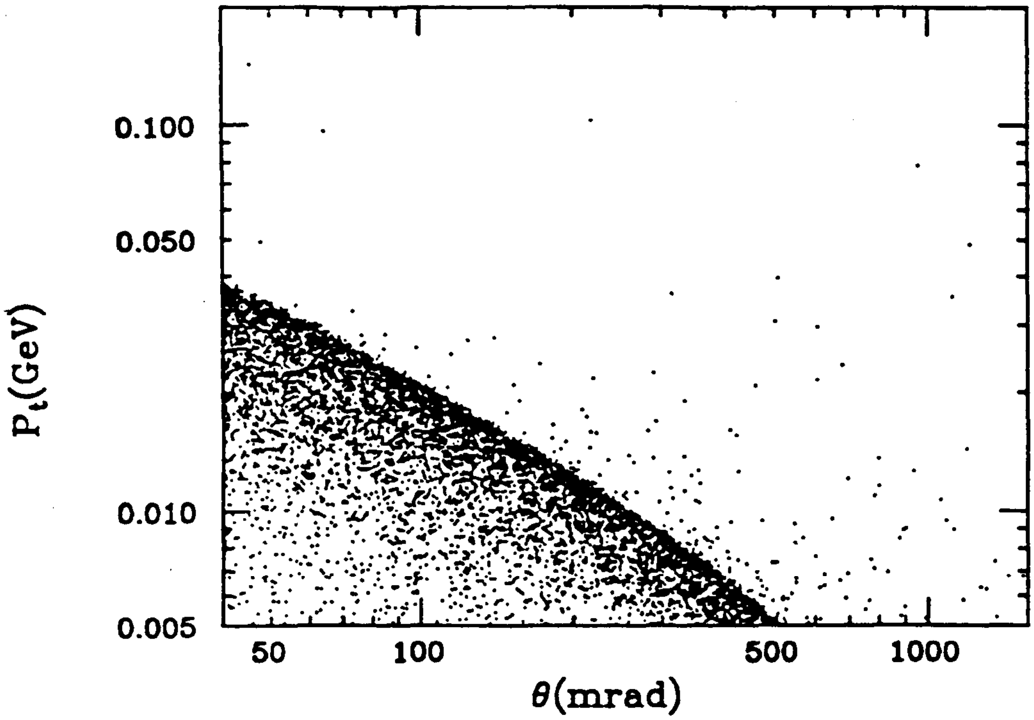

Figure 3.22: Pairs simulated by ABEL on a plane of p_t and θ_e at E_{beam}=250GeV for JLC-I(c-band).

3.7.5 Masking System

Our masking system is schematically shown in Fig.3.24. A mask is employed in order to shield against the large amount of the secondary photons. The probability for the O(10^7) photons/train (see Tab.3.5) to escape from the mask, η_{mask}, should be less than 10^{-3}, which is geometrically determined by the front aperture of the mask. Most of the escaped photons hit the mask surface on the opposite side, then they enter the detector region. In addition the mask must have enough thickness to absorb the photons, that is, its attenuation coefficient should be less than 10^{-5} for 0.5MeV photons which corresponds to a 5cm thick tungsten. We require that the acceptable number of photons in the detector region is O(10^2) per train crossing. As we fix the angular region of the mask as $0.15 < \theta_{mask} < 0.2$, it remains to determine only one parameter to fully specify the geometry of the mask. We take the half aperture of the mask, R_{mask} in Fig.3.24, for this parameter. R_{mask} can be linearly related to a diameter of circular trajectory of a charged track in a solenoidal magnetic field(B), *i.e.* $R_{mask} = p_t^{max}/0.15B$ and B=2Tesla. We determine R_{mask} for the pairs, which comprise a shoulder in Fig.3.23, to loop inside the mask. There is another important constraint from the solid angle seen by the photons back-scattered at QC1, *i.e.* $\eta_{mask} = R^2_{mask}/4(L_Q - L_{mask})^2 < 1 \times 10^{-3}$, where L_{mask} and L_Q are the distances of the mask and the final focus quadrupole magnet from the interaction point(IP), respectively(Fig.3.24). The location of the final focus quadrupole magnet has been set to be 2.5 m from IP for the synchrotron radiations to go through QC1 without scattering as mentioned in the previous section. The optimized values of R_{mask}, L_{mask} and η_{mask} are also listed in Tab.3.5. With this masking system, the total number of charged particles hitting the outer surface of the mask is less than 10^3/train(72 bunches) as shown in Fig.3.23.

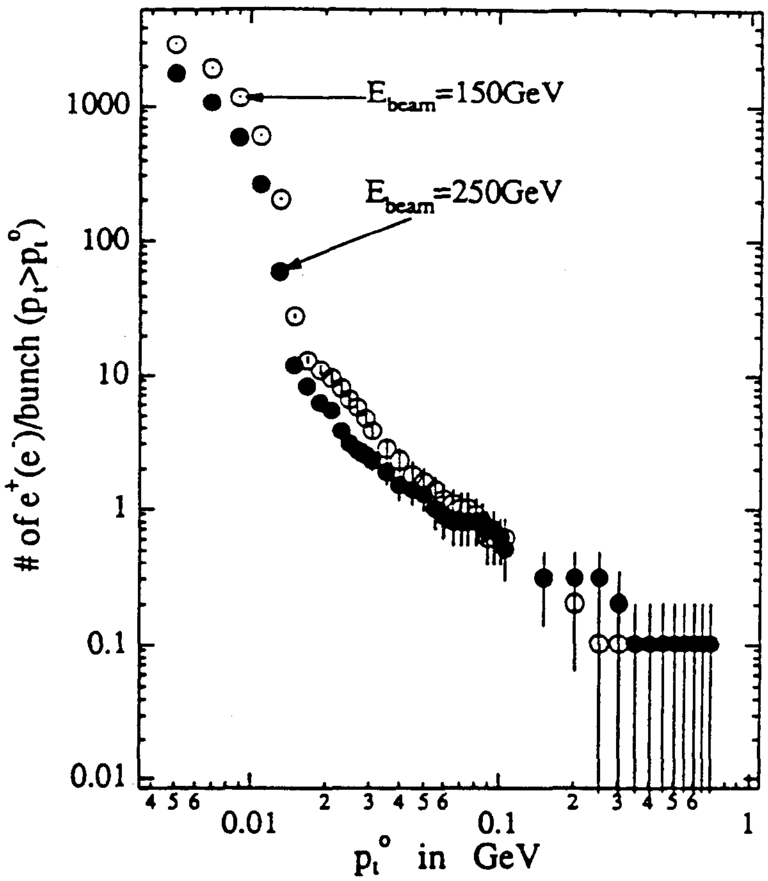

Figure 3.23: Pair yield/bunch crossing as a function of P_t° for $\theta_e > 0.15$ at JLC-I(c-band).

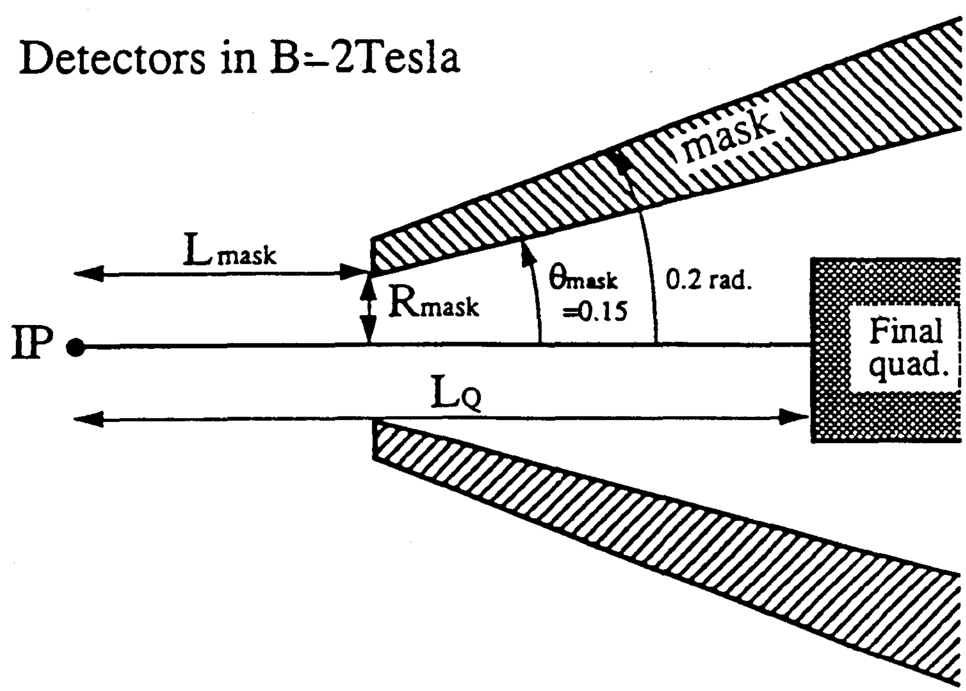

Figure 3.24: A masking system at the interaction region

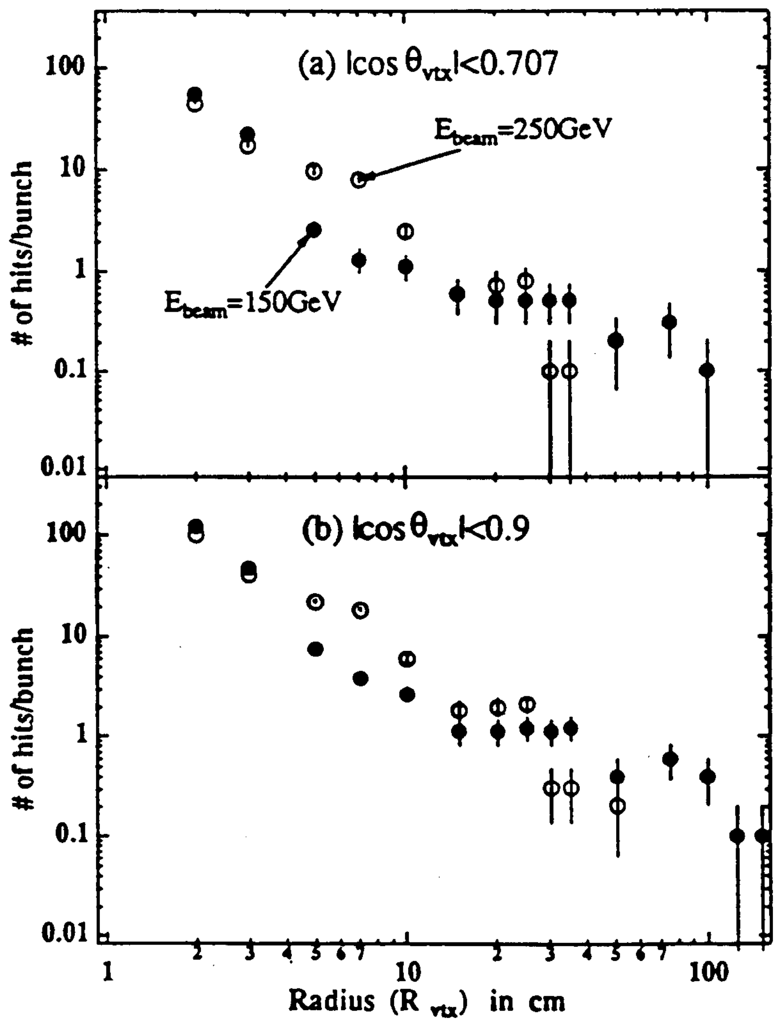

Figure 3.25: background hits by the pairs in B=2Tesla as a function of radius(R_{vtx}.

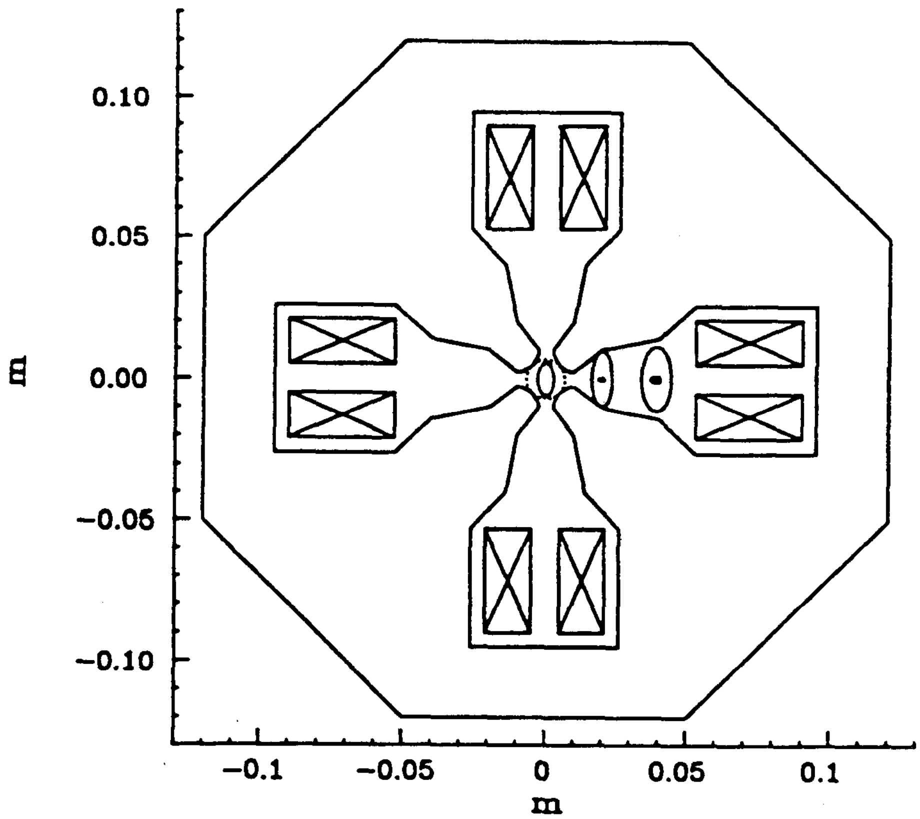

Figure 3.21: Cross sectional views of incoming and outgoing synchrotron radiations, which are shown as ellipses, at the entrance and exit of QC1, for E_{beam}=250GeV, where the crossing angle of two beams is 8 mrad. QC1 is located at 2.5m upstream from IP, and its half aperture and length are 6.7mm and 2.4m, respectively. Its coils are indicated by crosses boxes. Disrupted beams after collision are also plotted by dots.